TABLE OF CONTENTS

LIST OF TABLES

LIST OF FIGURES

CHAPTER 1

1 INTRODUCTION

1.1 General

Recently, there is an increase in trend of using fiber reinforced polymers (FRP) as external confining medium for the retrofitting and strengthening of concrete structures. Damaged reinforced concrete structures have been successfully rehabilitated and strengthened using these polymers. The most employed method of strengthening a structure using FRP is by providing confinement by wrapping glass fiber reinforced polymer (GFRP) and carbon fiber reinforced polymer (CFRP) wraps to enhance axial compressive strength and ductility. The structural members especially columns are wrapped with FRP sheets keeping the orientation of fibers in hoop direction. A triaxial stress condition is achieved by the confinement of concrete. The effectiveness of FRP confinement depends on the unconfined concrete strength, wrap thickness, number of FRP confining layers and the angle of orientation of the fibers (Nanni et al. 1993; Parretti and Nanni 2002).

1.2 Background

Structures in service are being subjected to increased service loads and severe environmental conditions. Rehabilitation and retrofitting of existing structures is traditionally done using steel or reinforced concrete jacketing. To ensure safety of structurally deficient reinforced concrete structures, there is a need for better methods and techniques to strengthen and rehabilitate these structures. Reinforced concrete columns are the main members that resist the lateral and vertical loads and hence are more vulnerable to failures during earthquakes and a need to retrofit them seismically was highlighted after the collapse and damage of several structures during earthquakes. During an earthquake, good energy dissipation is

facilitated by well-confined concrete core resulting in structural safety. External wrapping of concrete structures using FRP composite wraps provides significant amount of lateral confinement leading to increased axial strength and energy absorption (Seible et al. 1997).

Structural fire is another hazard resulting in deterioration in strength of concrete (Khaliq 2012) that can be retrofitted by FRP. Both normal strength concrete (NSC) and high strength concrete (HSC) have different behavior under fire conditions (Khaliq and Kodur 2011) and appropriate retrofit system should be carefully selected to meet the strength requirements in such structures. This can be accomplished by selection of suitable fiber reinforced polymer (FRP) confinement to fire damaged concrete structural members.

This research evaluates confinement related strength, stiffness and ductility increases in FRP wrapped concrete cylinders. Strength and stiffness increases of a wrapped cylinder depend on the properties of FRP material and concrete. Constituents and properties of the FRP material like type of resin, fiber orientation, fillers and additives, processing techniques and concrete properties like f'_c (compressive strength of concrete) etc. influence behavior of FRP wrapped concrete members.

From the past studies it has been observed that the following questions need to be answered more accurately:

a) How the FRP confined concrete will behave under axial loading and what pattern of stress-strain response will it follow?
b) How will GFRP and CFRP behave when wrapped on normal and high strength concrete?
c) If GFRP costs almost half to that of CFRP then are two layers of GFRP comparable to single layer of CFRP with respect with to strength and ductility enhancement?
d) Do the FRP design guidelines predict the exact behavior of CFRP at different strengths?

e) Can the same guidelines used for CFRP be used to predict the behavior GFRP?

The present study is an experimental investigation on concrete cylinders confined with GFRP and CFRP composites under axial loading. For response to the above questions, a number of unreinforced concrete cylinders were prepared and wrapped with GFRP and CFRP composites.

1.3 Research Objectives

The objectives are as under:

1. Experimental work to investigate effectiveness of confinement provided by FRP to normal and high strength concrete.
2. Comparison of two different types of FRP wraps i.e CFRP and GFRP on normal and high strength concrete.
3. Comparison of existing design guidelines for normal and high strength concrete confined with CFRP and GFRP wraps.

1.4 Thesis Outline

This research is organized in 6 chapters. In chapter 1 there is basic introduction about FRP and its types CFRP and GFRP. Then the objectives of present research are discussed.

Chapter 2 includes the detailed literature review of FRP, its types and advantages. It also reveals different researches for effectiveness of CFRP and GFRP wraps on concrete. Past research in the related topic will be studied along with different confinement and strength models.

Chapter 3 includes the experimental work adopted for present research, properties of materials used and test performed on CFRP and GFRP wrapped cylinder specimens. Chapter

4 consists of the results obtained from the experimental work regarding the compressive strength, load carrying capacity and ductility of the unconfined and FRP confined specimens.

Chapter 5 discusses the final results of research program, results of different tests performed on unconfined and FRP confined concrete cylinders, their strength comparison with different updated codes and also plotting of graphs and tables for evaluation of effectiveness of different codes in predicting confined strength.

Chapter 6 consists of final conclusions made on the basis of results from chapter 4 and overall recommendations for future research.

CHAPTER 2

2 LITERATURE REVIEW

2.1 Fiber Reinforced Polymers (FRP)

Fiber reinforced polymer (FRP) is a composite material made of a polymer matrix reinforced with fibers. Fibers are available in three major forms like glass, carbon and aramid. FRP is combined with an epoxy to form a laminate that can be used in a structure to increase its strength and ductility.

2.2 Types of FRP

Three major types of FRP are carbon, glass and aramid based on the fiber and material composition. These are discussed one by one in coming sections.

2.2.1 Carbon Fiber Reinforced Polymer (CFRP)

Carbon fibers are formed when polyacrylonitrile fibers, rayon or pitch resins are carbonized at high temperatures. When the fibers are stretched, strength as well as ductility can be increased. The diameter of fibers is 9 to 17 micrometer. It is same in the case of glass fibers. A later step includes transportation of these fibers and then they are further treated as they are intertwined or laced into some cloth for ease of installation in structural purposes. CFRP is an economical material for strengthening structures such as bridges, residential areas as it is available in high achievable strengths. CFRP has been reported to enhance the strength of the structures more than two times. This mainly depends on tensile modulus of elasticity of the material. CFRP can be available in strengths of more than 420 GPa. CFRP is better in many properties than GFRP (Glass Fiber Reinforced Polymer) and AFRP (Aramid Fiber Reinforced Polymer) but it is more costly than the other two materials.

2.2.2 Glass Fiber Reinforced Polymer (GFRP)

GFRP is strong, light in weight and vigorous material. The properties are generally lesser than that of carbon fibers and the stiffness is also low as compared to CFRP but the material itself is not as much brittle. The product is cheap as its raw material is not costly. Its bulk strength and other properties relating to weight are also better and can be formed easily with processes such as molding. It is successfully used in structural applications although it is relatively inferior in properties than CFRP.

2.2.3 Aramid Fiber Reinforced Polymer (AFRP)

These fibers are generally prepared using carboxylic acid halide group and amine group. Effective elastic modulus, high strength and good resistance to abrasion make this material compatible for use in strengthening and other structural applications. They are much better than GFRP in alkaline resistance which ensures the durability of the retrofitting of concrete members. Their bulk strength and other properties relating to weight are also better and can be formed easily with processes such as molding.

2.3 Methods of Wrapping and Types of FRP Wraps

Different methods of wrapping are used for strengthening specimens based on the type of force to be resisted. Type of strengthening for beams, slabs, columns and piers to resist the necessary force within a structural system is tabulated in Table 2-1.

Among various techniques used to repair and rehabilitate the existing structures, usage of FRP sheet wrapping is the most common technique. The advantages of using FRP sheets are flexibility in coping with different shapes of structures, ease in site handling and cost effectiveness while the disadvantages are least quality control and demand on labor.

Table 2-1 Rehabilitation techniques

Type of Specimens	Force Resisted	Rehabilitation/Strengthening Technique
Beams	Flexure	Bonding of FRP plates, wet lay-up of fiber sheets or strips, prepreg winding
	Shear	U jacketing plates, FRP sheet wrapping
Slabs	Flexure	FRP sheet or strip bonding
Columns	Axial	FRP sheet or strip wrapping, filament winding, bonding prefabricated shells
	Eccentric	FRP sheet wrapping, prefabricated shells
Piers	Flexure	Jacketing using FRP plates, FRP rods
	Shear	FRP sheet wrapping

Different types of fibers used in FRP composites are glass, carbon and aramid. The qualitative comparison between glass, carbon and aramid fibers is given in Table 2-2. Carbon wraps show high tensile and compressive strength and also shows good long-term behavior in terms of creep and fatigue.

Table 2-2 Qualitative comparison between fibers

Criterion	FRP Composites		
	E- Glass	Carbon	Aramid
Tensile Strength	Very Good	Very Good	Very Good
Compressive Strength	Good	Very Good	Inadequate
Young's Modulus	Adequate	Very Good	Good
Ductility	Very Good	Adequate	Good
Long Term Behavior	Adequate	Very Good	Good
Fatigue Behavior	Adequate	Excellent	Good
Bulk Density	Adequate	Good	Excellent
Alkaline Resistance	Inadequate	Very Good	Good
Price	Very Good	Adequate	Adequate

2.4 Past Researches

Confinement due to external wrapping of FRP has been reported to increase confined compressive strength, load carrying capacity, stiffness and strain.

(Nanni et al. 1993) studied the effects of lateral confinement of concrete members by using FRP reinforcement by spirally wrapping the FRP onto the concrete surface. The specimens of size 150 mm x 300 mm with diameter to height ratio 1:2 were used for axial compression

tests. Twenty such specimens were tested in uniaxial compression. Tape wrapping was done using braided aramid FRP impregnated with epoxy (Dow Chemical Der 330). When the pitch was high about 50 mm the wrapped specimens showed no increase in strength and strain. At 25 mm pitch the ductility of the columns was increased with no increase in strength and with 0 mm pitch the increase in both strength and stiffness was observed.

(Picher et al. 1996) studied the effects of confinement of concrete cylinders with CFRP wraps. Fifteen circular cylinders 150 mm diameter and 300 mm height (1:2 ratio) wrapped with unidirectional carbon composite sheet using epoxy resin were tested. Wrap was applied in hoop direction in continuous manner in one or three layers. An angle ply configuration [±θ/0] was applied in helicoidal shape. Stress-strain response was plotted and the results were compared to unconfined concrete specimens. The curves clearly showed a plastic zone in the confined concrete cylinders. Even though the curves indicate an increase in the ductile behavior, failure of confined concrete cylinders occurred without warning. Failure was usually caused by a sudden breakage of the composite wrap due to brittle behavior of CFRP. When the wrap failed, the concrete core was unable to withstand the load and triggered immediate failure. Location of initial failure was difficult and the failure was characterized by a combination of fiber breakage and separation between parallel fibers. Confinement enhanced both the stress at the initiation of the plastic zone and mean slope of the plastic zone in the stress-strain curve thus indicating enhancement in stiffness.

(Mirmiran and Shahawy 1997) studied the behavior of axially loaded 152.5×305 mm concrete cylinders by confining them with E-glass FRP tubes with winding angle of 15º. Different jacket thicknesses were employed with 6, 10, and 14 layers of FRP, while the angle of winding was kept fixed. As a result, the axial strength and ductility increased with increasing jacket thickness

(Matthys et al. 1999) carried out an experimental study on columns and cylinders confined with FRP sheet wrapping by conducting axial loading tests on them. Standardized cylinders (6”x12”) were wrapped with one layer of CFRP (carbon). Strength increase of about 1.17 and 1.32 was obtained for wrapped cylinders. Once the cylinder was loaded above the strength of the unconfined concrete, stiffness decreased considerably. A combination of increase in load capacity and increase in ductility was noted. In addition to compression testing of confined cylinders, large scale testing of confined columns was also performed. Three columns were tested and one of these was non-wrapped while the other two were wrapped with CFRP. From the tests it was concluded that both strength and ductility were increased for wrapped columns with higher FRP stiffness, lower ductility. Compared to wrapped cylinders, lower ultimate hoop stresses were observed.

(Rochette and Labossiere 2000) conducted experiments on circular, rectangular and square shaped concrete columns wrapped with variable thicknesses of FRP wraps to observe the behavior of shape and wrap thickness on axial strength of the specimens. The FRP composites were wrapped in hoop direction. with the exception of one square column which was wrapped with the $\pm 15^{o}/0^{o}$ (angle-hoop) configuration. The strength of the specimens was found to be dependent on the shape of the specimens and it increased with increasing wrap thickness.

Similarly, (Pessiki et al. 2001) conducted experiments on square and circular plain concrete specimens subjected to axial load. The specimens were confined with GFRP wrapped in hoop direction and $\pm 45^{o}$ to hoop direction along with CFRP wrapped in hoop direction only. The enhancement in compressive strength was found to be 128% for circular specimens confined with one ply of GFRP jacket at $0^{o}/\pm 45^{o}$ with respect to hoop direction and 244% for CFRP confined specimens with two layers of CFRP jackets in hoop direction. Moreover, axial

strains at peak stress were found to be enhanced approximately seven times as compared to that of unconfined specimens.

(Karabinis and Rousakis 2002) studied the behavior of concrete confined with high modulus carbon FRP sheets subjected to monotonic and cyclic loading. Concrete cylinders 6"x 12" were wrapped with 1, 2, 3 and 5 layers of carbon FRP sheets and the confining effect was evaluated in terms of concrete strength, ductility and expansion. Increasing the volumetric ratio of the carbon sheet enhanced the axial rigidity of the carbon jacket. The results showed an increase of strength of 1.64 and 2.7 times for 1 and 3 wraps respectively. The ductility increased 4.48 to 7.85 times correspondingly. Similarly, the behavior of CFRP confined specimens have been studied regarding the axial compressive strength, ductility and amount of energy absorbed (Rahai et al. 2008).

(Parretti and Nanni 2002) conducted axial tests on confined concrete columns with different fiber orientations of the carbon FRP. The performance of the ± 45° FRP laminate was compared to the unidirectional 0° FRP laminates of different materials from different manufacturers. Five circular columns and three rectangular columns were tested under pure axial load. Three circular columns were tested using ± 45° wrap and three columns using 0° unidirectional CFRP laminates. The columns had internal longitudinal and lateral reinforcement. Specimens strengthened with 0° unidirectional fibers had explosive failures. A gentler and less sudden failure was observed for the specimens wrapped with ± 45-degree wrap. The failure was progressively reached and warnings of collapse were noted.

In an analytical study, (Parvin and Jamwal 2005) employed non-linear finite element analysis to investigate the effect of angle of orientation of fibers with respect to hoop direction and the thickness of confining FRP layer. In another study, same approach of non-linear finite element analysis was employed to investigate the behavior of FRP confined columns with varying parameters of unconfined concrete strengths, angle of winding of ply, number of

confining layers and fiber orientation of each layer. The strength of FRP confined concrete was found to be predictable and dependent on thickness of confining layer and angle of orientation of fibers with respect to hoop direction (Parvin and Jamwal 2006).

(Li et al. 2006) carried out an experimental study on on 27 concrete cylinders wrapped with 6 fiber orientations. It was found that the failure modes strength and ductility of FRP wrapped specimens depend on thickness of confinement and orientation of fibers. It was also concluded that the orientation of fibers other than axial and hoop direction may give lesser strength than obtained from orientation in axial and hoop direction.

2.5 Uses of FRP in Structural Strengthening

FRPs are used to strengthen, repair or retrofit a structure. They can be used even if a structure is highly damaged. The open spaces or voids are covered with resin and then sheets are wrapped on the damaged member with the help of FRP sheets with adhesive/epoxy for increasing load carrying capacity. FRP can also be used for flexural and shear strengthening. There can be some reduction ductility of the member while increasing its flexural strength. The properties and compatibility of epoxy is equally important in enhancing the strength of the member. FRP and resin mixed together is called a laminate. The retrofitting technique is also very common in these days. The older structures that were designed to take lesser loads can be retrofitted if the new demand loads are higher. Also replacing the structure can be more disastrous sometimes. In this case, FRP can be applied to strengthen or retrofit a structure. CFRP is very useful material for strengthen columns, piers, bridges and other structures (Nanni et al. 2004). Axial capacity in strength can be increased in a column by wrapping sheets of FRP.

FRP has a lot of advantages that include high strength, low weight to strength ratio and good corrosion resistance. In past steel and concrete jacketing were the most common techniques that were used to increase the strength of members and for retrofitting. Nowadays, these

conventional methods have been replaced by new techniques and smart materials like FRP etc. FRP has been used as an internal and external reinforcement. Internal reinforcement is used preferably for slabs, beams etc and external reinforcement for outer covering in retrofitting of structures. Steel corrosion is the main problem in concrete reinforced structures. So FRP is used as an alternative in these structural members. FRP is used to provide lateral confinement in concrete. For example a load is applied to a column, the concrete expands in the lateral direction. FRP provides confinement laterally. As FRP can also take the load itself and also provides confinement so the load carrying capacity of concrete can be increased significantly (Wu et al. 2006).

FRP with their fibers oriented in the hoop direction can be used extensively for strengthening the structures. In order to predict their behavior when wrapped with the FRP system complete material properties should be known. They may be taken from the supplier/manufacturer or can be tested. Determination of Elastic modulus and other strength properties is difficult if not provided by the manufacturer. Usually the manufacturers provide properties like thickness of FRP sheets, elastic modulus, tensile strength and orientation of fibers that are used in the system. Based on these material properties, their confined strength can be predicted by several models that have been proposed preferably from the design codes that are in practice like CSA and ACI. Confinement models and stress-strain response can provide a better understanding on the behavior of FRP systems of different types (Parretti and Nanni 2004).

Because of the above mentioned uses, FRP are becoming increasingly popular in practical applications such as bridges, residential buildings and other structures for repairing, strengthening and rehabilitation. FRPs are very easy to handle and versatile in nature. Good corrosion behavior makes these materials an asset for civil engineering structures in repairing and strengthening. Another great advantage is the ease of installation of FRP system and the

faster application. It can be done rapidly and cost effectively. The confining mechanism of FRP is shown in Figure 2-1.

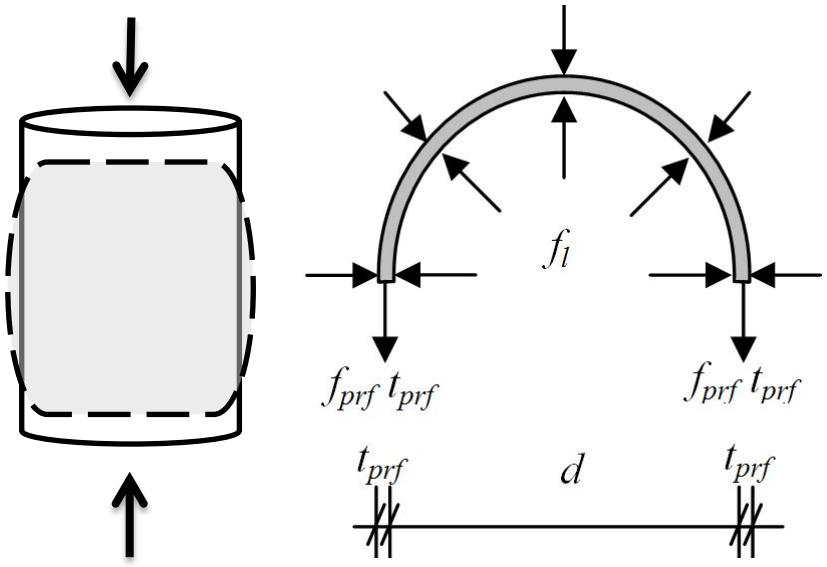

Figure 2-1 Schematic confinement mechanism for axial strengthening of circular cylinders using externally bonded FRP wraps (Benzaid and Mesbah 2013).

Here f_l = Confining pressure

f_{prf} = Hoop stress in polymer fibers

t_{prf} = thickness of confining FRP

D = Diameter of specimen

2.6 Analysis of FRP Confined Structures

In the recent years numerous models of confinement have been developed. (Lam and Teng 2003; Samaan et al. 1998; Teng et al. 2007; Teng and Lam 2004) The contribution of these models helped the research teams to develop international design codes. A number of guidelines and different authentic codes have been presented like American Concrete Institute (ACI 440.2R-08), Canadian Standards Association (CSA S806-02), Intelligent

Sensing for Innovative Structures (ISIS M04-01) and European CEB/FIP Model Code 2010. The European CEB/FIP Model Code uses the guidelines provided in *Technical Report by the Fédération Internationale du Béton, fib Bulletin 14,* 2001. Increased database helps updating design codes. These guidelines are used as design equations to strengthen any structure where FRP can be used effectively (ACI 440.2 2002; CSA S806-02 2002; fib 2001; ISIS M04-01 2001).

A lot of research has been conducted for strengthening and repairing of concrete structures. Extensive research has been published on FRP confinement strength models to investigate the behavior of FRP confined concrete. Most of the published research available on FRP confinement strength models and design guidelines that predict the confined compressive strength and ultimate loads were developed based on normal strength concrete. Very little research work is available for prediction of the confinement on high strength concrete.

To develop better understanding in this area, the experimental results were correlated with the predictions of the FRP design guidelines ACI, CSA, ISIS and *fib* in order to investigate the relative effectiveness for predictions of confined concrete strengths by these design guidelines.

Figure 2-2 illustrates the stress-strain response of few of FRP confined concrete specimens presented here. It can be seen that the stress-strain response presented by Rahai et al (2000) is significantly stiff compared to others and this can attributed to Carbon Fiber Reinforced Polymer (CFRP) confined high strength concrete having strength of 45 MPa. Pessiki et al (2001) used cylindrical specimens with 610 mm height and 152 mm diameter having internal reinforcement and FRP confinement with fiber oriented at 45° to hoop direction which increased the ductility in the specimens. This behavior closely matches the square unreinforced specimens tested by Rochette and Labossiere (2000) wrapped with confining carbon fibers 15° oriented with respect to hoop direction. This indicates that the behavior of

FRP confined concrete depends on the presence of internal reinforcement as well as on the shape of the specimen.

The confinement of circular concrete specimens 912 mm tall by 152 mm diameter tested by Li et al (2006) show quite different response compared to Mirmiran and Shahaway (1997), this is attributed to number of layers used for confinement as well as type of confining material and shape of specimens. It can be seen that with 6 layers of Glass Fiber Reinforced Polymer (GFRP) by Li et al (2006) show stiff stress-strain response compared to highly ductile response by 6, 10, and 14 plies of GFRP confinement used by Mirmiran and Shahaway (1997).

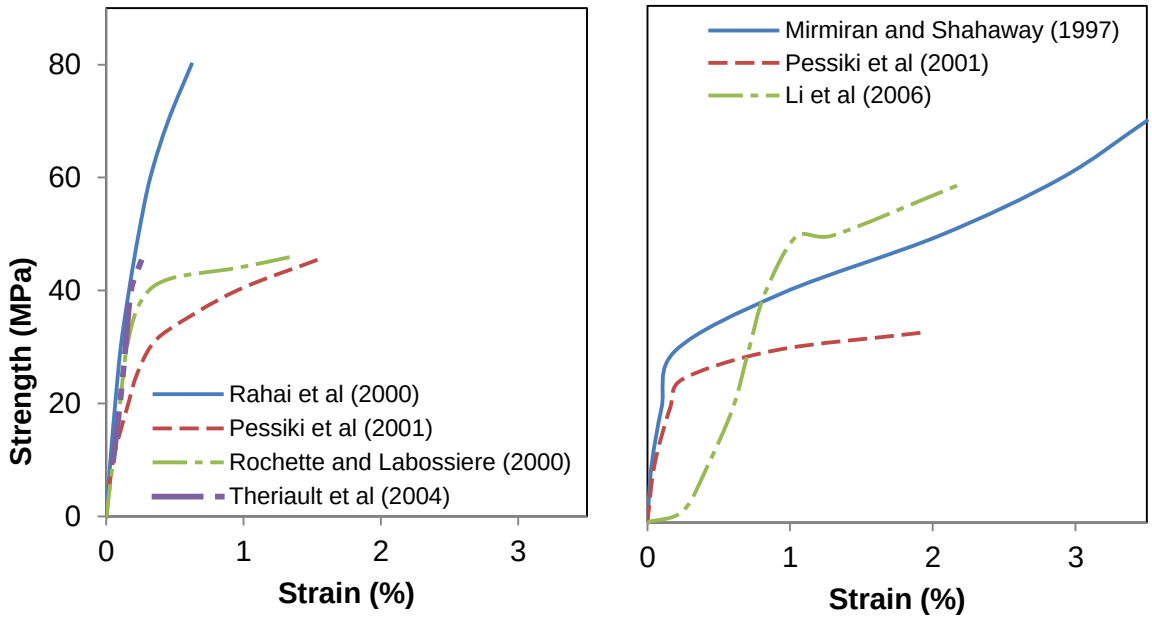

(a) CFRP confined (b) GFRP confined

Figure 2-2 Stress-strain responses of different confined specimens.

The difference in the stress-strain response of FRP confined concrete can be attributed to unconfined concrete strength, internal reinforcement, FRP (fiber) orientation of confinement, type of FRP used for confinement, and shape of the specimen. With such variation in parameters affecting the behavior of confined concrete, accurate prediction of stress-strain response becomes difficult. Moreover, a single design model or code cannot be used for

design being number of variable parameters mentioned above. It is therefore desired to recognize and quantify more effective and economical confinement by studying the stress-strain response of two types of FRP confinements namely CFRP and GRRP.

2.7 Summary

CFRP and GFRP are used to enhance the strength and ductility of concrete. The enhancement in strength and ductility depends upon the type of FRP used and also on the unconfined strength of the concrete. There is a need to quantify the strength and ductility enhancement provided by GFRP and CFRP confinement. Since these polymers are quite expensive, so a comparison is needed to identify an optimum and economical FRP for confinement, strengthening, repair and rehabilitation of structures.

A lot of research has been carried out to study the behavior of these polymers and many design guidelines have been derived in order to predict the behavior of confinement provided by these FRPs to concrete but these design guidelines usually underestimate or overestimate the effectiveness of these polymers. Therefore, a comparative parametric study is required in which the predictions of FRP design guidelines are compared with experimental results in order to validate the effectiveness and limitations of these guidelines.

This research will help in identifying the most suitable FRP to induce specified increase in strength and enhancement in ductility for different concrete strengths. This will help in more predictable and cost efficient retrofitting of the concrete sections.

CHAPTER 3

3 MATERIAL PROPERTIES AND EXPERIMENTAL PROGRAM

3.1 General

This chapter focuses on the material properties and the experimental work that was performed on the specimens. A total of 27 specimens were cast using three batches of concrete and cured for 28 days. 9 of these specimens were wrapped with GFRP, 9 with CFRP and the remaining 9 were kept unwrapped. The specimens were then capped using sulfur and then subjected to axial compression loading. Strain gauges and rosettes were used to record strains induced in these specimens during compression testing.

3.2 Materials

The following materials are used which are described as follows:

3.2.1 Cement

Type I ordinary Portland cement was used in all three batches of concrete. One of the most popular brand of ordinary Portland cement (OPC) in Pakistan is "BESTWAY CEMENT" which has been used in this work. The chemical composition and some physical properties of the OPC are shown in Table 3-1.

Table 3-1 Physical properties of OPC

Compound	Value (%)
SiO_2	22.0
Al_2O_3	5.50
Fe_2O_3	3.50
CaO	64.25
MgO	2.50
SO_3	2.90
Na_2O	0.20
K_2O	1.00

3.2.2 Carbon Fiber Reinforced Polymer

CFRP employed was Sika wrap Hex 230 C. It is a woven carbon fiber fabric and is shown in figure 3-1. It is mainly used for repairing in cracks and strengthening of the structures. It can also be used in retrofitting of structures. Its advantage include that the fabric is made up of weft fibers due to which fibers keep the system or fabric stable. It can be used for a variety of purposes for strengthening and retrofit. This fiber can be used in a wide variety of shapes or it has a better geometric configuration. Fibers used were of high strength. The orientation of fibers was 0 degree or uni-directional. The overlap of 4 inches was provided in the experiment according to the design requirements. The values given in the table 3-2 and 3-3 are the dry fiber properties but the properties of the fiber wrap with epoxy are given in the table 3-4.

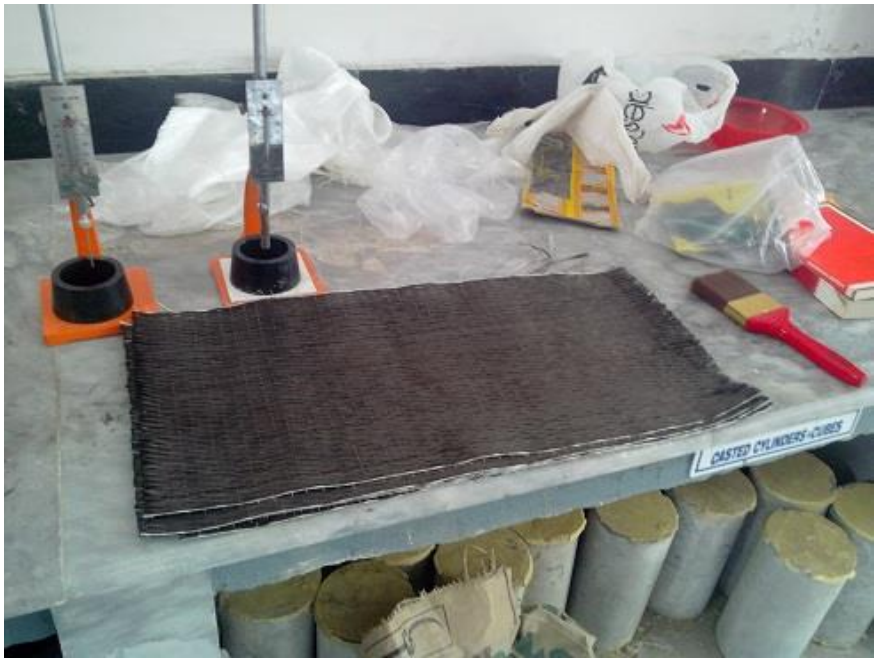

Figure 3-1 Sika wrap Hex 230 C

Table 3-2 Dry fiber wrap properties of Sika wrap Hex 230 C

Fiber Type	High strength carbon fibers
Fiber orientation	0°unidirectional
Areal weight	220 $g/m^2 \pm 10g/m^2$
Fiber Density	1.78 g/cm^3
Fiber design thickness	0.12mm (based on total Carbon content)

Compatibility of the system must not be changed. It can be done by strictly sticking to the proposed epoxy that is given in the table named Sikadur 330. This fiber wrap can be applied both in wet as well as dry application. In the datasheet the thicknesses and weight per unit area of the epoxy to be applied is mentioned. It is written that the fiber should not be fold and the fiber should be splitted into pieces with sharp instrument. This wrap is to be coated with epoxy named Sikadur 330 for ensuring proper bonding with the Sikawrap 230 C. The following Table 3-3 shows the properties of laminate.

Table 3-3 Dry fiber wrap properties of Sika wrap Hex 230 C

Tensile strength of fibers	4100 N/mm^2
Strain at break of fibers	1.7%
Tensile E-modulus of fibers	231000 N/mm^2
Fabric width	300/600 mm

The overlapping should be minimum 10 cm or according to the requirements of the system where it is to be installed. The properties given in the table are dependent on the type of resin used with the system. 30 percent change in the values can be observed for actual testing. The wrap was wrapped with Sikadur 330 at the rate of 50 ft^2/ Gallon (fifty square feet per gallon). The epoxy was applied with gloves in hand and voids and other irregular surface profile was adjusted with cutting so that the resin can be applied on the smooth surface. Other additional properties Sika wrap Hex 230 C laminated with Sikadur 330 epoxy are shown in Table 3-4.

Table 3-4 Properties of Sika wrap Hex 230 C laminated with (Sikadur 330)

Properties	Design value (units in MPa)	ASTM Test Method
Tensile Strength	715	D-3039
Tensile Elongation %	1.09	D-3039
Tensile Modulus	59896	D-3039
Compressive Strength	668	D-695
Ply thickness	0.381 mm	

3.2.3 Glass Fiber Reinforced Polymer

The employed GFRP SikaWrap Hex 106G is a bi-directional E-glass fiber fabric. Material is field laminated using Sikadur 330 epoxy to form a glass fiber reinforced polymer (GFRP) used to strengthen structural elements. The wrapping of Sika Wrap Hex 106G is shown in figure 3-2. Its uses include Seismic strengthening of columns, masonry walls, damaged structural parts and temporary strengthening. It is also employed for change in structural system and also to cater for construction defects. As approved by ICBO/ICC ER-5558, it is used for shear, confinement or flexural strengthening. Its advantages include:

- Flexibility so it can be wrapped around complex shapes.
- Light weight.
- Non-corrosive behavior.
- Acid resistance.
- Low aesthetic impact.
- Economics.

The dry fiber properties of SikaWrap Hex 106G are given in the Table 3-5.

Table 3-5 Dry fiber wrap properties of Sika wrap Hex 106G

Tensile strength of fibers	2276 N/mm^2
Strain at break of fibers	4%
Tensile E-modulus of fibers	72390 N/mm^2
Density	2.54 g/cm^3

The overlapping should be minimum 10cm or according to the requirements of the system where it is to be installed. The epoxy was applied with gloves in hand and voids and other irregular surface profile was adjusted with cutting so that the resin can be applied on the smooth surface. Other additional laminate properties are given in Table 3-6.

Figure 3-2 Sika wrap Hex 106 G

Table 3-6 Cured laminate properties with (Sikadur 330) Epoxy

Property	Design value (units in MPa)
Tensile Strength	244
Tensile Elongation %	1.43
Tensile Modulus	16215
Strength per inch width	2.53 kN
Ply thickness	0.33

3.2.4 Epoxy

Sikadur 330 has been used as an epoxy that is fully compatible with Sika wrap Hex 230 C and is shown in figure 3-3. Its advantages include great pot life of approximately 1 hour and 2 years in a sealed container. Sikadur 330 is easy to handle. It is tolerant to moisture and has great strength and modulus. It has great sticking properties with concrete and other materials like timber. It has great compatibility for Sika Wrap Hex 230 C which is available in the literature. It has great resistance to temperature and good resistance to abrasion. Table 3-7 shows some typical data for Sikadur 330 C like color, consistency etc.

Figure 3-3 Sikadur 330

Table 3-7 Typical data for Sikadur 330

Color	Light Grey
Mixing Ratio	Component A to B 4:1 by weight
Consistency	Non-sag paste
Pot Life	57 minutes
Tack Free Time	4-5 Hours

The first applied coat on the cylinders was 50 ft^2 / gallon. The final coat was 160 ft^2/ gallon. The surface was checked thoroughly and was made smooth before the application of epoxy. Dust was removed with the help of a common brush and other disturbing particles were also removed at the time of application of epoxy. The two components of epoxies were mixed with recommended ratio of 4:1 i.e four parts of component A and one part of component B. The epoxy fully hardened after 4-5 hours. The epoxy was applied with the help of gloves.

The technical data for Sikadur 33 is given in table 3-8.

Table 3-8 Technical data for Sikadur 330

Tensile strength (ASTM D-638)	33.8 MPa
Elongation @ Break (ASTM D-638)	1.2%
Flexural Strength (ASTM D-790)	60.6 MPa
Flexural Modulus (ASTM D-790)	3489 MPa

3.3 Preparation of Specimens

3.3.1 Mixing of Concrete

The motor operated drum mixer was used for mixing of concrete. The maximum capacity of the mixer was 2.5 cft.

3.3.2 Mix Proportions

Table 3-9 Mix proportions

Sr. No	Strength (MPa)	Cement (kg/m^3)	Sand (kg/m^3)	Aggregate (kg/m^3)	w/c	Aggregate size
1	30	475	617	1236	0.4	20 mm
2	42	572	550	1144	0.4	20 mm (80%) and <15 mm (20%)
3	64	1071	535	1060	0.35	15 mm and smaller

Table 3-10 shows admixtures used in the following samples.

Table 3-10 Type of admixture for mixes

Sr.No	Strength (MPa)	Admixture type
1	29	BASF 850 171 gram
2	42	S.F (1.38 kg) and FOSPAK 430R (345 gm)
3	64	S.F (2.21 kg) and FOSPAK 430R (552 gm)

3.3.3 Test Specimens

A total of 27 cylinders were casted from three different batches of concrete. 9 cylinders were casted from each batch out of which 3 specimens were wrapped with 2 layers of GFRP, 3 with 1 layer of CFRP and the remaining 3 cylinders were kept unwrapped. The strengths of the concrete batches are given in table 3-11.

Table 3-11 Casting of cylinders

Batch	Target Strength (MPa)	No of Cylinders
1	30	09
2	42	09
3	64	09

3.3.4 Compressive Strength Test

The 27 cylindrical specimens of 6x12 inches were tested in compression testing machine. To find concrete compressive strength, the mixes were poured in properly oiled cylindrical molds. 3 layers were used for filling the molds, and compaction was done by 25 strokes of a square rod of 1 inch. With the help of the float, the top surface was made smooth. After completion of casting, the molds were stored for 24 hours at room temperature. After the required time i.e., 24 hours, samples were un-molded and the casted cylinders were placed into laboratory water tank for curing of 28 days. Cylinders were taken out and capped with sulfur and then they were tested in universal compression test machine with a capacity of 2000 kN.

In order to measure strains, Micro-Measurements P3 Strain Indicator and Recorder manufactured by Vishay Precision Group was used. This system is capable of recording strains through linear strain gauges using 4 input channels. Vishay Micro-Measurements C2A-Series 062LW strain gages with 350 ohm resistance were utilized for measurement of strains. The strain gauges were attached to the specimens in horizontal, vertical and diagonal (45°) arrangement in order to measure longitudinal and lateral strains. Dial type strain gauges were also used in every third test to cross check the accuracy in measurements of linear strain gauges. The whole assembly for testing of unconfined and confined specimens is shown in figure 3-4.

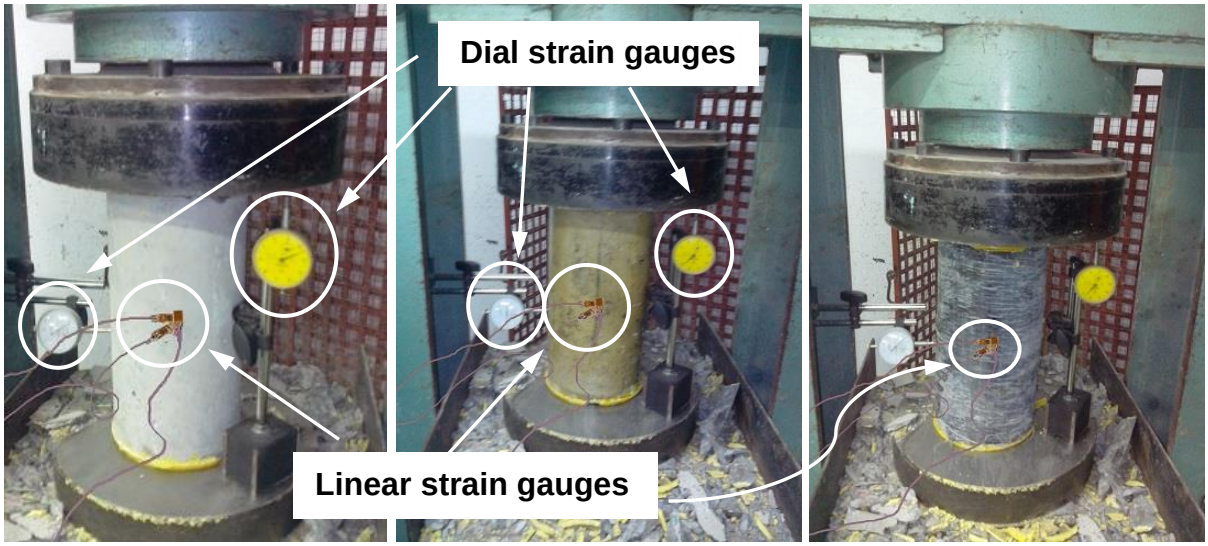

(a) Control specimen (b) GFRP confined (c) CFRP confined

Figure 3-4 Testing of specimens.

CHAPTER 4

4 RESULTS AND DISCUSSIONS

4.1 Introduction

In order to evaluate the effect of GFRP and CFRP on strength and ductility of concrete, compressive strength and stress-strain measurements were carried out. Based on the test results, comparison of axial compressive strengths, ultimate load carrying capacities, longitudinal strains, hoop strains and volumetric strains were carried out. Moreover, visual observations were also made to study the failure response of FRP strengthened specimens under load. The test data obtained in experimental program was also compared with the theoretical values predicted from three North American design guidelines which include American Concrete Institute (ACI), Canadian Standards Association (CSA), and Canadian Intelligent Sensing for Innovative Structures (ISIS), and European CEB/FIP Model Code 2010. The comparison was carried out in terms of axial strengths and axial load carrying capacities of confined specimens with that of unconfined specimens.

4.2 Mechanical Properties

Axial compression tests were conducted on the wrapped and non-wrapped specimens and the effect of confinement due to GFRP and CFRP wraps was determined in terms of maximum strength, strain and stiffness.

4.2.1 Ultimate Strength

Ultimate strength of the cylinder specimens was noted from the dial gauge when the specimens failed under compressive force. Values of load and displacement were also recorded continuously.

4.2.1.1 Control Specimens

Ultimate strength of the control specimens without wrapping is shown in Table 4-1. The average of 3 compression tests conducted on the specimens is given below. The tested specimens were 6" in diameter and 12" in height and three batches with compressive strength of 30, 42 and 64 MPa were tested.

Table 4-1 Test data for axial strength of control specimens.

Specimens Strength	Axial Load Carrying Capacity	Axial Compressive strength	Average Ultimate Load Carrying Capacity	Average Crushing Strength
	kN	Mpa	kN	Mpa
30 MPa	542.18	29.79	540.48	29.70
	550.91	30.27		
	528.35	29.03		
42 MPa	782.96	43.02	779.63	42.84
	774.23	42.54		
	781.69	42.95		
64 MPa	1180.82	64.88	1177.05	64.67
	1172.08	64.40		
	1178.27	64.74		

4.2.1.2 GFRP Wrapped Specimens

The specimens were wrapped with two layers of GFRP in hoop direction and were tested in axial compression. An overlap of 100 mm was provided for both wraps and wet laying method of wrapping was employed. The epoxy was spread uniformly for both wraps without any delay that might start setting of the epoxy. The ultimate strengths of the specimens are shown in Table 4-2.

Table 4-2 Test data for axial strength of GFRP wrapped specimens.

Unconfined Specimens Strength	Axial Load Carrying Capacity	Axial Compressive strength	Average Ultimate Load Carrying Capacity	Average Crushing Strength
	kN	Mpa	kN	Mpa
30 MPa	693.97	38.13	699.79	38.45
	711.44	39.09		
	693.97	38.13		
42 MPa	870.87	47.85	873.36	47.99
	872.14	47.92		
	877.06	48.19		
64 MPa	1253.43	68.87	1277.70	70.20
	1293.47	71.07		
	1286.19	70.67		

4.2.1.3 CFRP Wrapped Specimens

The specimens were wrapped with single layer of CFRP in hoop direction and were tested in axial compression. The ultimate strengths of the specimens are shown in Table 4-3.

Table 4-3 Test data for axial strength of CFRP wrapped specimens.

Unconfined Specimens Strength	Axial Load Carrying Capacity	Axial Compressive strength	Average Ultimate Load Carrying Capacity	Average Crushing Strength
	kN	Mpa	kN	Mpa
30 MPa	862.13	47.37	868.81	47.74
	892.16	49.02		
	852.12	46.82		
42 MPa	954.95	52.47	950.40	52.22
	960.05	52.75		
	936.21	51.44		
64 MPa	1355.17	74.46	1317.56	72.39
	1308.22	71.88		
	1289.29	70.84		

4.2.1.4 Effectiveness of GFRP Confinement on Concrete

This section shows the increase in compressive strength versus the unconfined concrete strength. The confined cylinders with the least unconfined strength (30 MPa) showed the maximum increase in confined strength. The confinement effectiveness provided by GFRP decreases as the unconfined strength increase from 30 to 64 MPa as shown in Table 4-4.

Table 4-4 Comparison of GFRP confined specimens with control specimens.

Unconfined Specimens Strength	**Confinement provided**	**Average Axial Compressive Strength**	**Increase in Axial Compressive Strength**	**% Increase in Strength**
		MPa	**MPa**	**%**
30 MPa	Unconfined	29.70	0.00	0.000
	GFRP	38.45	8.75	29.476
42 MPa	Unconfined	42.84	0.00	0.000
	GFRP	47.99	5.15	12.022
64 MPa	Unconfined	64.67	0.00	0.000
	GFRP	70.20	5.53	8.551

The results indicate an increase in confinement strength of about 29.47, 12.02 and 8.56 percent for 30, 42 and 64 MPa respectively when the confinement was provided by wrapping GFRP. Figure 4-1 shows the comparison of compressive strength of unconfined and GFRP confined concrete specimens while Figure 4-2 shows the strength increment for lower and higher strength concrete specimens. The increase in strength of 42 MPa concrete is 5.15 MPa while that observed by (Li et al. 2006) was found to be 3.8 MPa for GFRP confining a concrete of unconfined strength of 45.6 MPa. The difference in strength is due to the variation of strength and fiber density of GFRP wrap i.e tensile strength and density of GFRP was 3000 MPa and 200 g/cm^2 whereas in this study they were 2275 MPa and 254 g/cm^2 respectively.

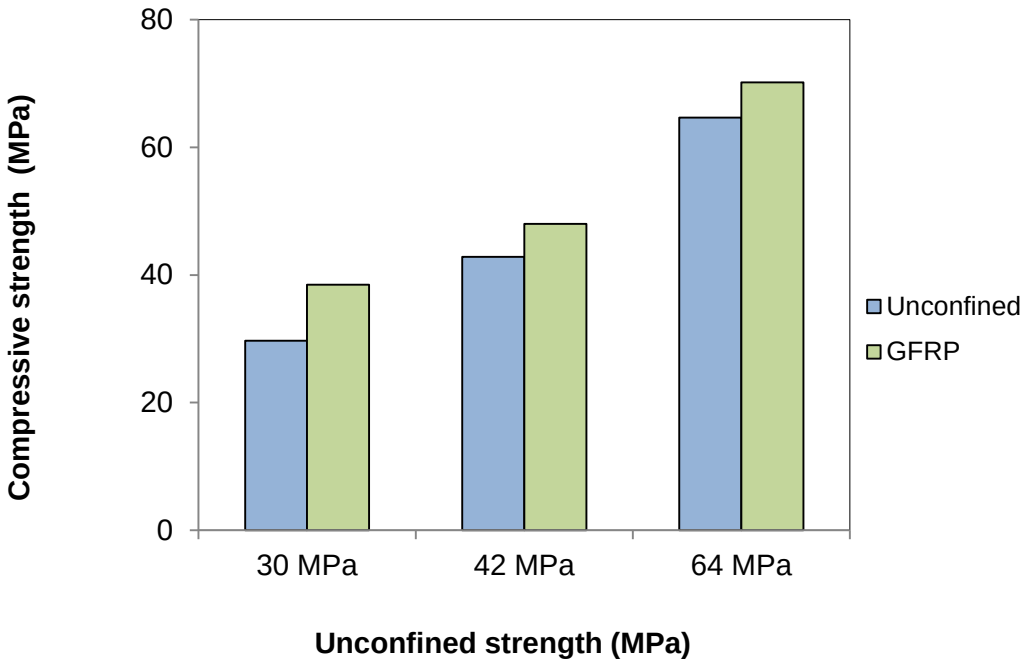

Figure 4-1 Comparison of the compressive strength of unconfined and GFRP confined specimens.

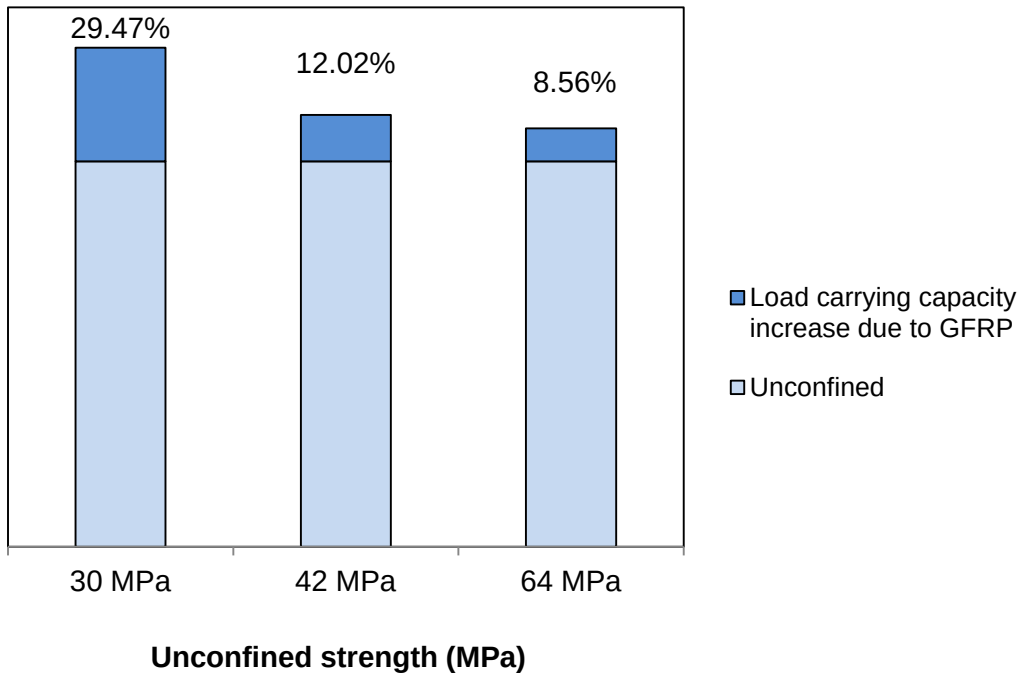

Figure 4-2 Strength increments in GFRP confined specimens.

The decrease in the strength increment can be justified by the fact that the GFRP wrap provides a specific confining pressure which is more prominent in normal strength concrete

but as the unconfined strength of concrete increases the confining pressure becomes less prominent as indicated in the figure 4-2.

4.2.1.5 Effectiveness of CFRP confinement on concrete

This section shows the increase in compressive strength versus the unconfined concrete strength. The research shows that the confinement becomes less effective as the unconfined strength increases. The confined cylinders with the least unconfined strength (30 MPa) show the maximum increase in confined strength. Confinement effectiveness of CFRP decreases as the unconfined strength increase from 30 to 64 MPa as shown in Table 4-5.

Table 4-5 Comparison of CFRP confined specimens with control specimens

Unconfined Specimens Strength	**Confinement provided**	**Average Axial Compressive Strength**	**Increase in Axial Compressive Strength**	**% Increase in Strength**
		Mpa	**Mpa**	**%**
30 MPa	Unconfined	29.70	0.00	0.000
	CFRP	47.74	18.04	60.75
42 MPa	Unconfined	42.84	0.00	0.000
	CFRP	52.22	9.38	21.90
64 MPa	Unconfined	64.67	0.00	0.000
	CFRP	72.39	7.72	11.94

The results indicate an increase in confinement strength of about 60.7, 22 and 12 percent for 30, 42 and 64 MPa respectively when the confinement was provided by wrapping CFRP. Less strength enhancement was observed for higher strength concrete wrapped with CFRP as compared to lower strength concrete. Figure 4-3 shows the comparison of the compressive strength of unconfined and CFRP confined specimens while Figure 4-4 shows that the strength increment was more significant for lower strength concrete and was less significant for higher strength concrete as confirmed by a previous study on the same CFRP wrap conducted by (Bisby et al. 2007) and his team in which Sika wrap Hex 230C was wrapped on plain concrete cylinders of 100 mm diameter and 200 mm height. The CFRP confined

strength values came out to be different as compared to this research but the pattern of strength increments was identical i.e the strength increments reduced with increase in unconfined strength of concrete.

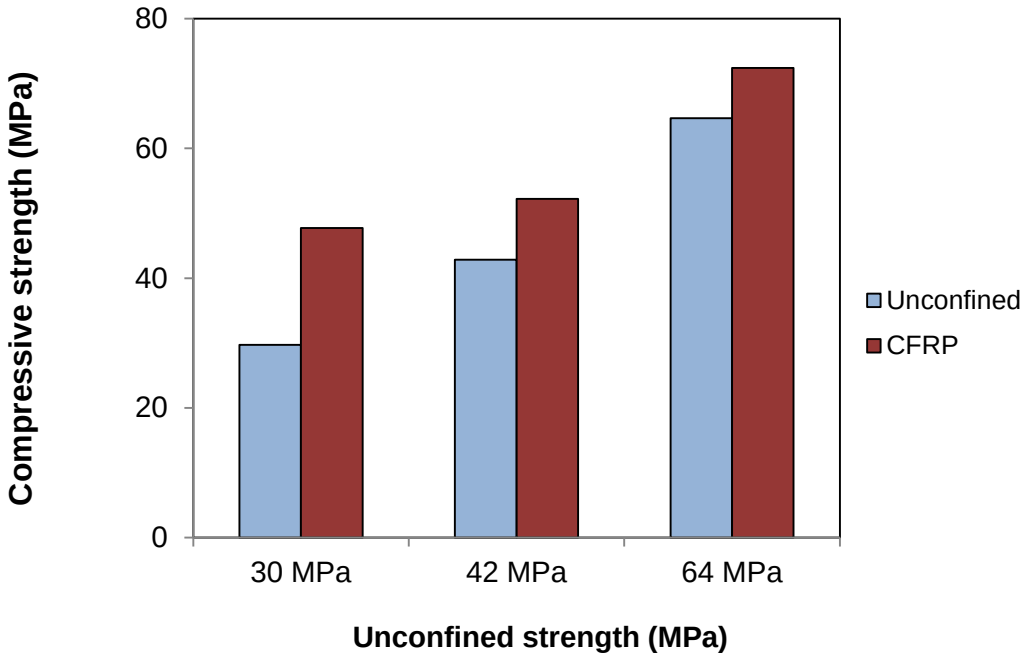

Figure 4-3 Comparison of the compressive strength of unconfined and CFRP confined specimens.

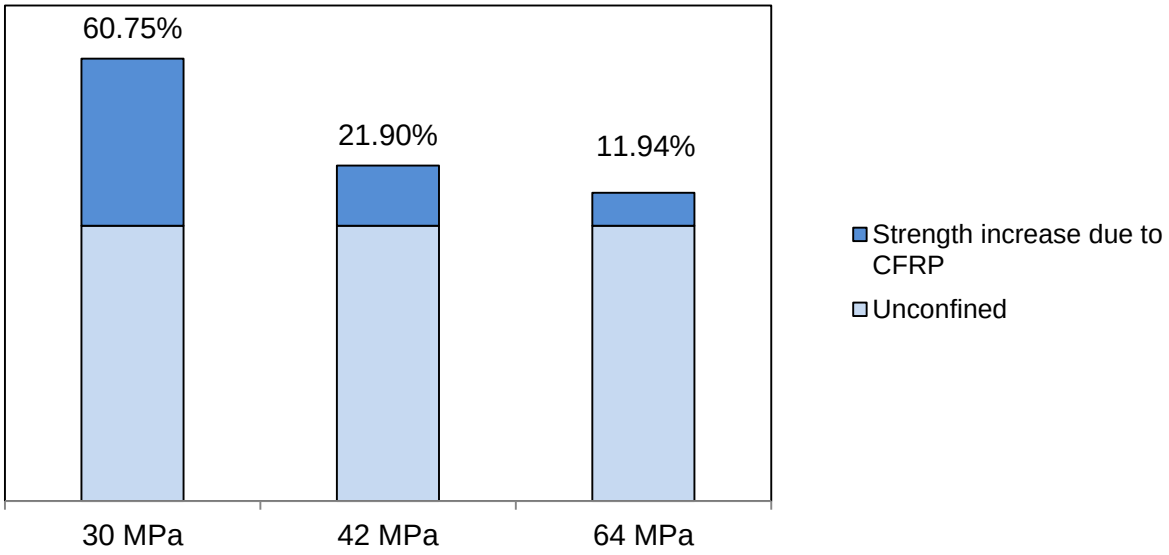

Figure 4-4 Strength increments in CFRP confined specimens.

The decrease in the strength increment can be justified by the fact that the total strength of confined concrete is equal to the sum of unconfined strength of concrete itself and the additional strength induced as a result of confinement provided by CFRP wrap. This additional strength remains almost same and comes out to be more significant for normal strength concrete but as the unconfined strength of concrete increases it gets less prominent in terms of percentage of the overall strength as shown in figure 4-4.

4.2.1.6 Comparison of effectiveness of CFRP and GFRP confined specimens with control specimens.

This section compares the results obtained by testing the unconfined control specimens with both CFRP and GFRP confined concrete specimens. The research has shown that when a concrete specimen was confined with GFRP it showed an increment both in axial load carrying capacity and ultimate compressive strength however this increment was lesser than that provided by CFRP confinement as shown in Table 4-6.

Table 4-6 Comparison of GFRP and CFRP confined specimens with control specimens.

Unconfined Specimens Strength	**Confinement provided**	**Average Axial Compressive Strength**	**Increase in Axial Compressive Strength**	**% Increase in Strength**
		Mpa	**Mpa**	**%**
30 MPa	Unconfined	29.7	-	-
	GFRP	38.45	8.75	29.476
	CFRP	47.74	18.04	60.75
42 MPa	Unconfined	42.84	-	-
	GFRP	47.99	5.15	12.022
	CFRP	52.22	9.38	21.9
64 MPa	Unconfined	64.67	-	-
	GFRP	70.2	5.53	8.551
	CFRP	72.39	7.72	11.94

For 30 MPa concrete specimens, the increase in strength was 29.47 percent by GFRP confinement but for the same specimens CFRP confinement provided an increment of 60.74

percent which is almost double than the strength increment provided by GFRP. Similarly, for 42 MPa concrete specimens, GFRP provided 12.02 percent additional strength while CFRP provided 21.9 percent increase in strength. As we move towards high strength concrete, for 64 MPa specimens the increase in strength provided by GFRP and CFRP was 8.56 and 11.94 percent which shows that the gap between GFRP and CFRP induced additional strength converges as the strength of unconfined concrete is increased. Figure 4-5 shows the comparison of compressive strength among unconfined, GFRP confined and CFRP confined specimens.

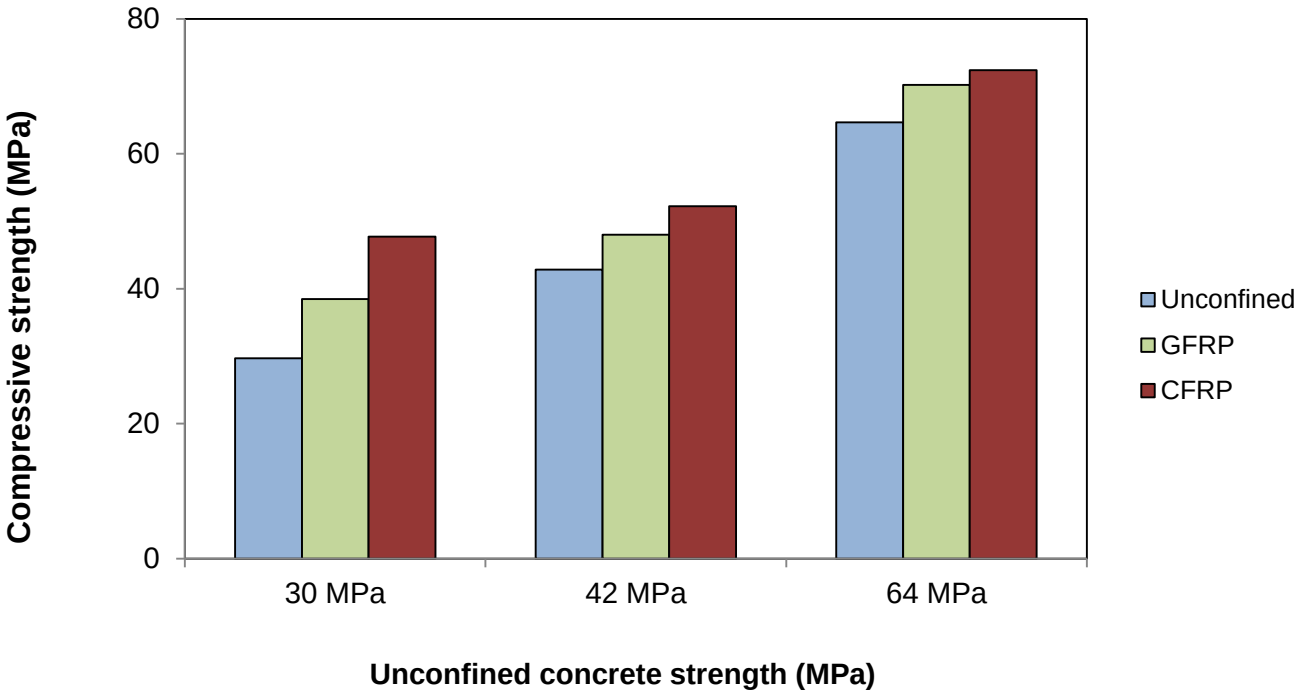

Figure 4-5 Comparison of the compressive strengths of unconfined and FRP confined concrete specimens.

Here it is found that the overall strength of the confined concrete depends on the type of confinement as well as on the original strength of the concrete to which the confinement is applied as confirmed by (Pessiki et al. 2001). In that study CFRP and GFRP were wrapped on concrete cylinders having 150 mm diameter and 610 mm height. The testing of these

cylinders indicated the confined compressive strength depends on the properties of confinement provided as well as on the original unconfined strength of concrete.

4.2.2 Stress-strain Response

The specimens were subjected to axial compressive test during which the applied stresses were recorded along with the corresponding strains in order to plot their stress-strain response.

4.2.2.1 Control Specimens

Strain gauges and rosettes were used to measure the strains induced in specimens and with the help of the strains recorded following stress-strain response have been developed. Figure 4-6, 4-7 and 4-8 show the measured stress-strain response of 30 MPa, 42 MPa and 64 MPa concrete respectively.

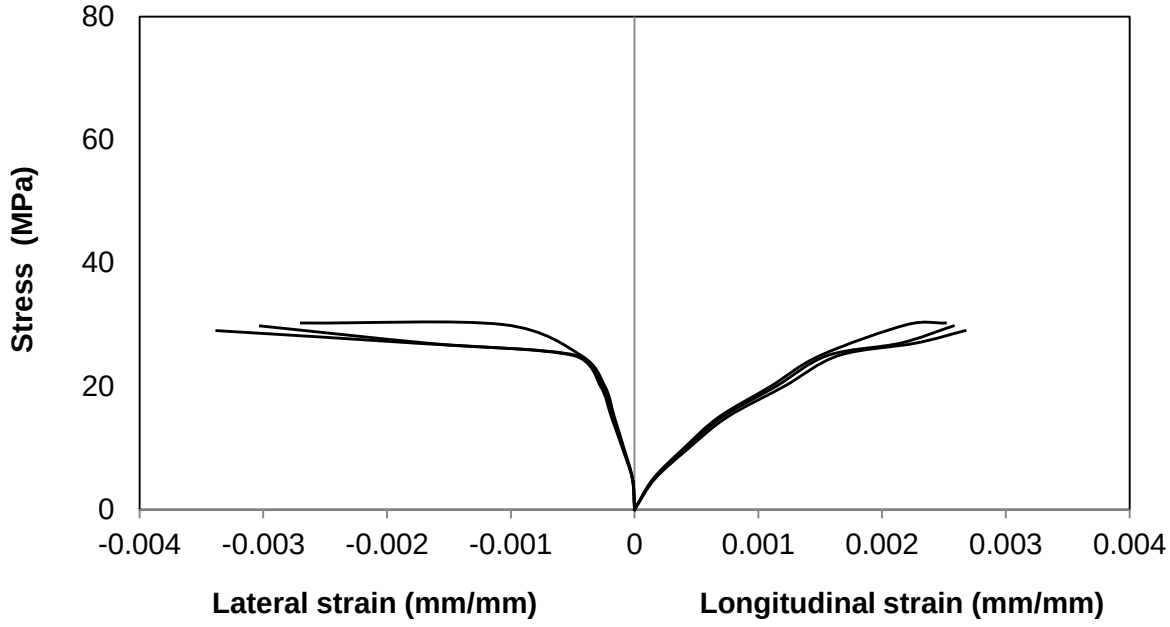

Figure 4-6 Stress-strain response of 30 MPa unconfined concrete

In figure 4-6, it can be observed that stress-strain curves are comparatively flatter with high strain values showing ductile stress-strain response.

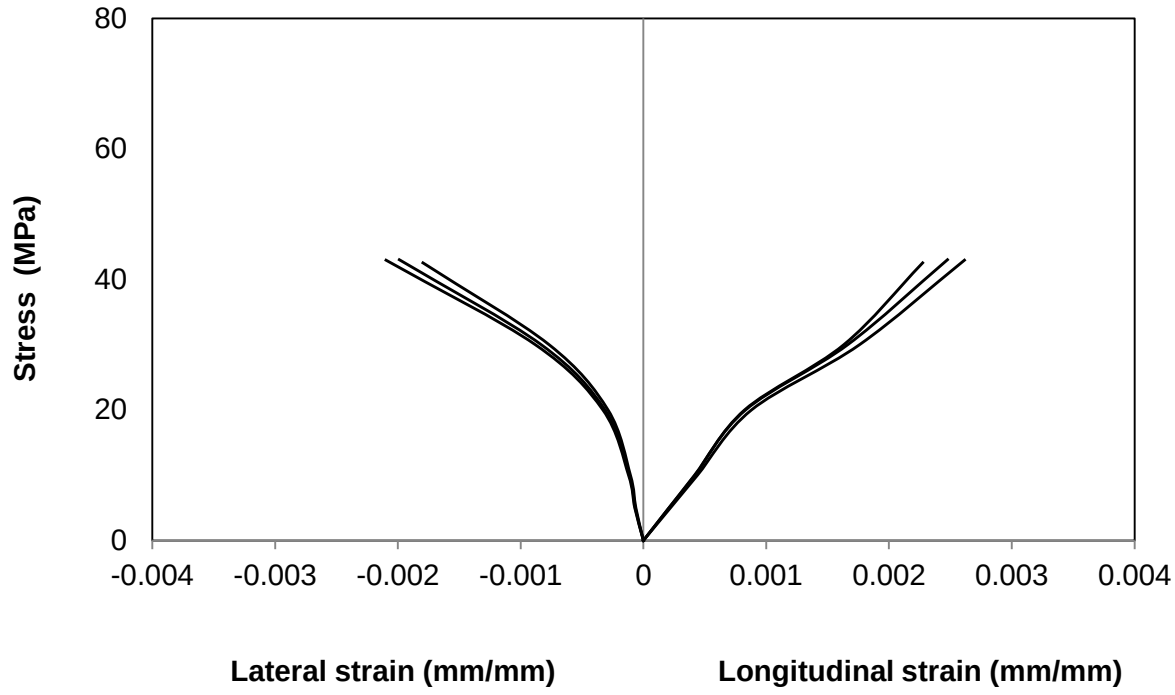

Figure 4-7 Stress-strain response of 42 MPa unconfined concrete

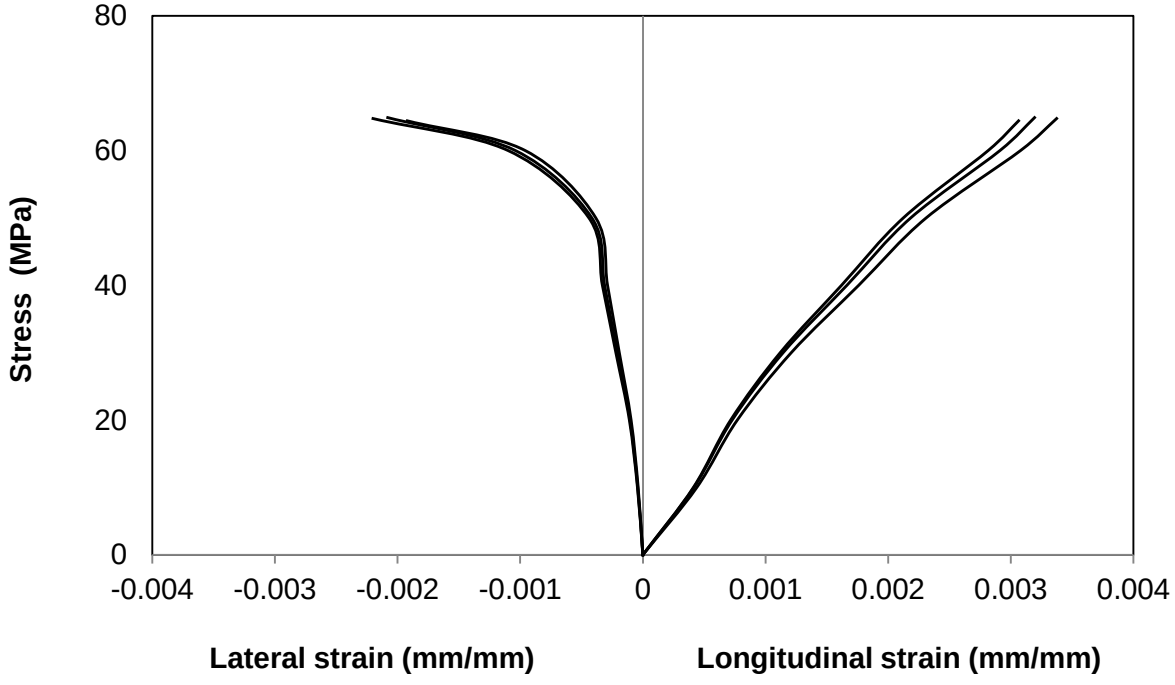

Figure 4-8 Stress-strain response of 64 MPa unconfined concrete

In figure 4-8, it can be observed that stress-strain curves are comparatively steeper with higher stress values and lesser strain values showing stiffer stress-strain response.

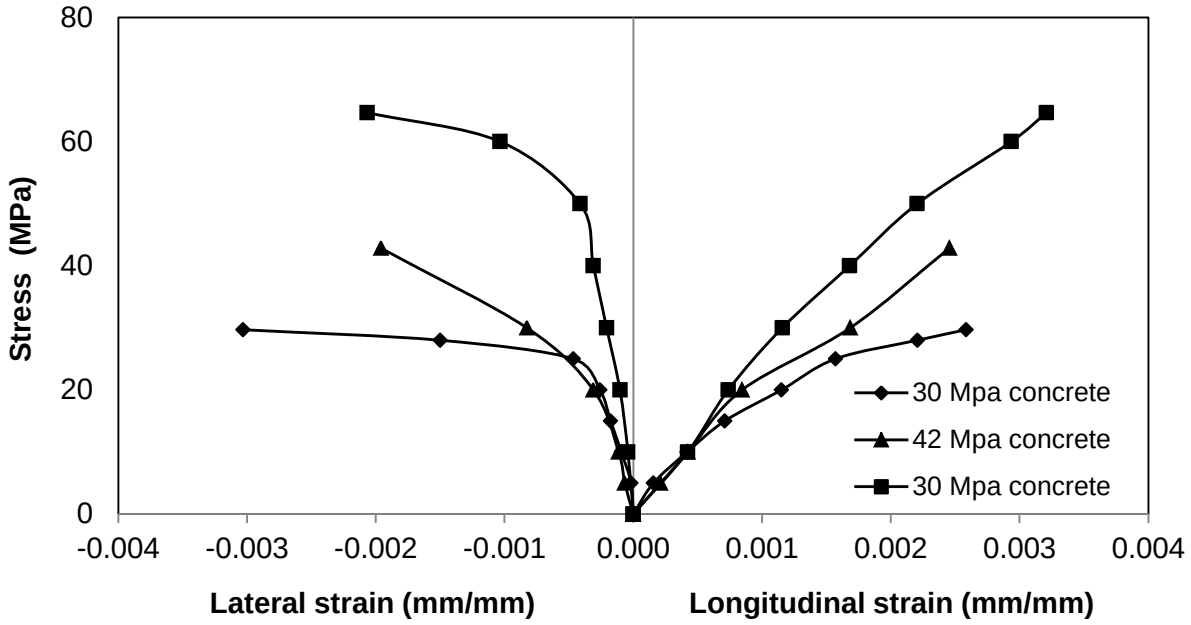

Figure 4-9 Stress-strain response of unconfined concrete specimens.

In figure 4-9, the comparative performance of the three batches used in this research is displayed. It can be seen that 30 MPa concrete shows a ductile behavior as compared to other concrete batches with lower stress values and higher strain values in stress-strain response while 64 MPa concrete shows a stiffer behavior with higher stress values and lower corresponding strains.

Figure 4-10 shows the volumetric strain response of the control specimens. The volumetric strain (ε_v) can be measured by adding the longitudinal strain (ε_l) and twice of hoop strain (ε_h). The longitudinal strain in axial compression test is a measure of contraction in a specimen while the lateral strain indicates expansion in the specimen in an axis perpendicular to the direction of loading. While calculating volumetric strain, if longitudinal strain is taken as positive then lateral strain is taken as negative. The volumetric strain is given by

$$\varepsilon_v = \varepsilon_l + 2\varepsilon_h$$

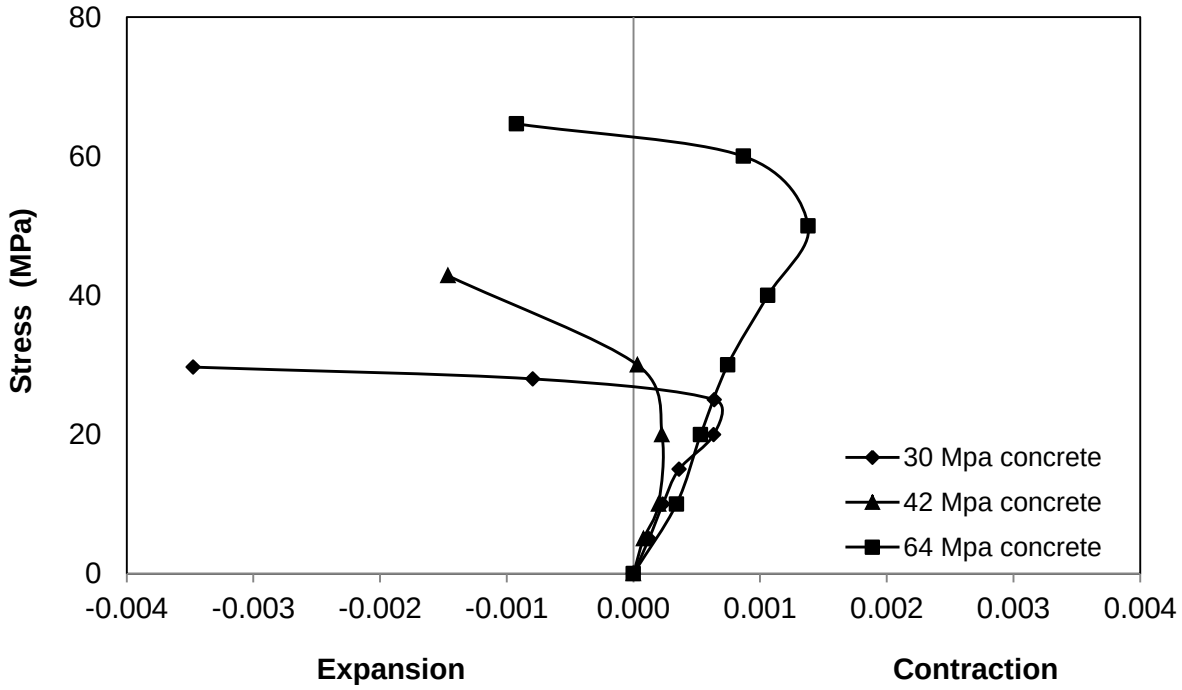

Figure 4-10 Volumetric strain response for unconfined concrete

The volumetric stress-strain response indicates that the specimens undergo contraction in longitudinal direction under axial compressive loading and then just before failure the specimens start expanding laterally indicating higher strains in lateral direction.

4.2.2.2 GFRP Wrapped Specimens

The stress strain response of 30 MPa, 42 MPa and 64 MPa GFRP confined specimens is shown in figures 4-11, 4-12 and 4-13 respectively. It can be observed that the GFRP confinement has enhanced the strength and ductility of the specimens. In figure 4-11, it can be observed that stress-strain curves are comparatively flatter with high strain values showing ductile stress-strain response while in figure 4-13, it can be observed that stress-strain curves are comparatively steeper with higher stress values and lesser strain values showing stiffer stress-strain response.

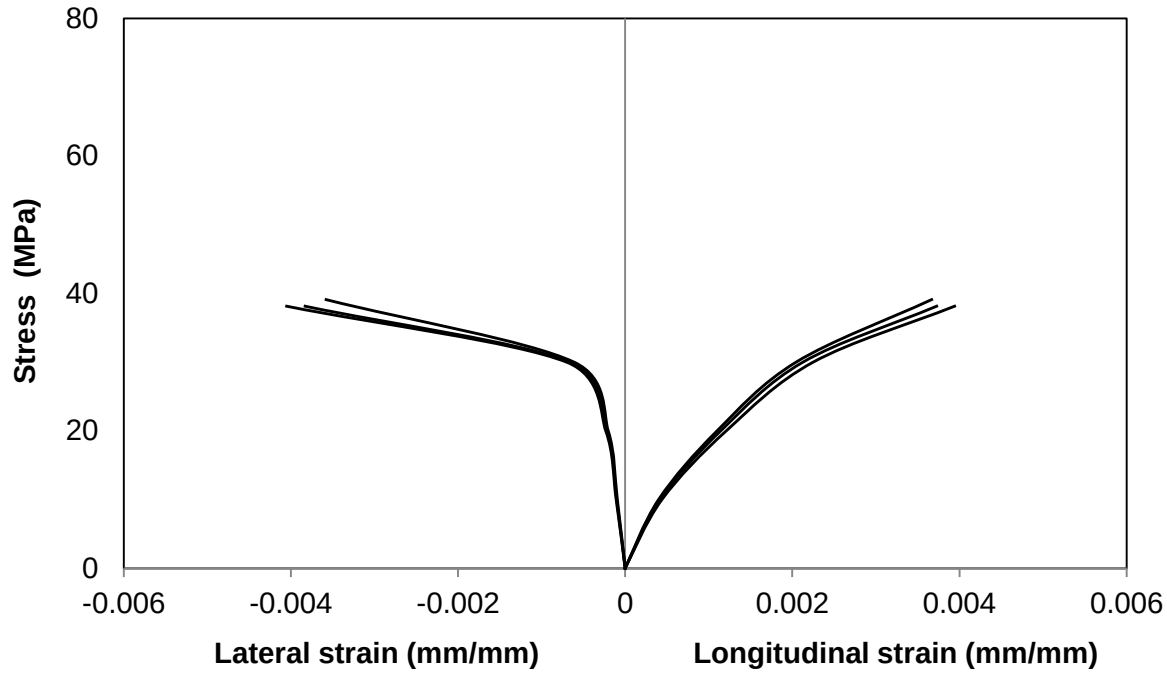

Figure 4-11 Stress-strain response of 30 MPa GFRP confined concrete

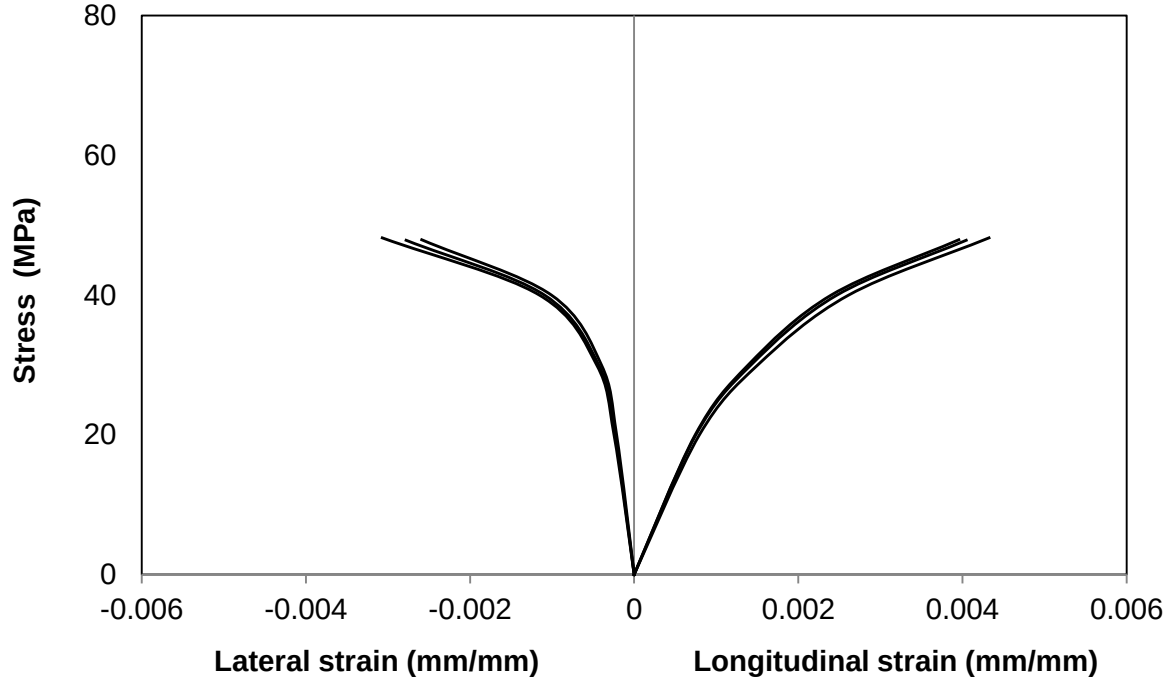

Figure 4-12 Stress-strain response of 42 MPa GFRP confined concrete

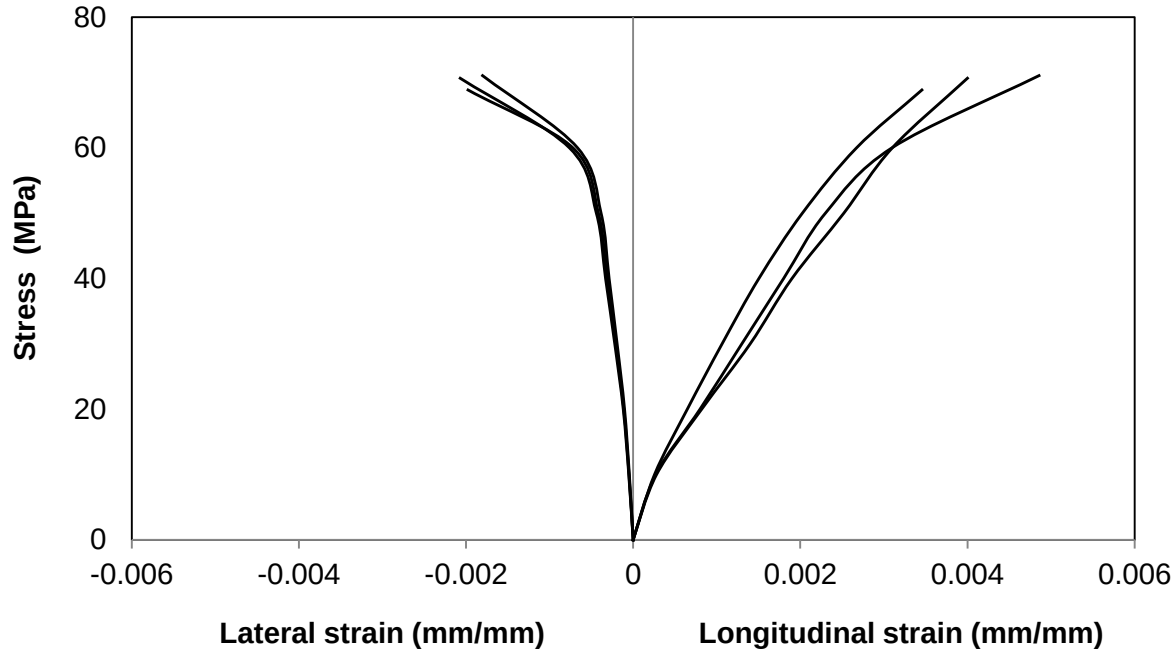

Figure 4-13 Stress-strain response of 64 MPa GFRP confined concrete

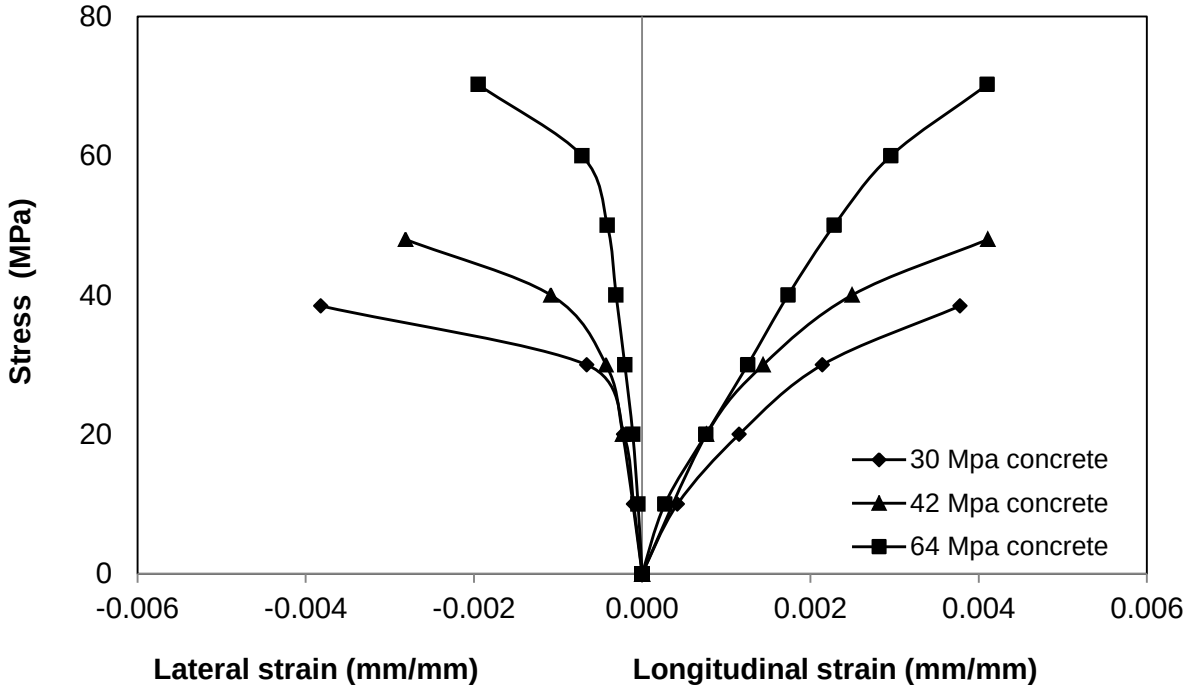

Figure 4-14 Stress-strain response of GFRP confined concrete specimens

In figure 4-14, 30 MPa concrete shows a ductile behavior as compared to other concrete batches with lower stress values and higher strain values in stress-strain response while 64

MPa concrete shows a stiffer behavior with higher stress values and lower corresponding strains.

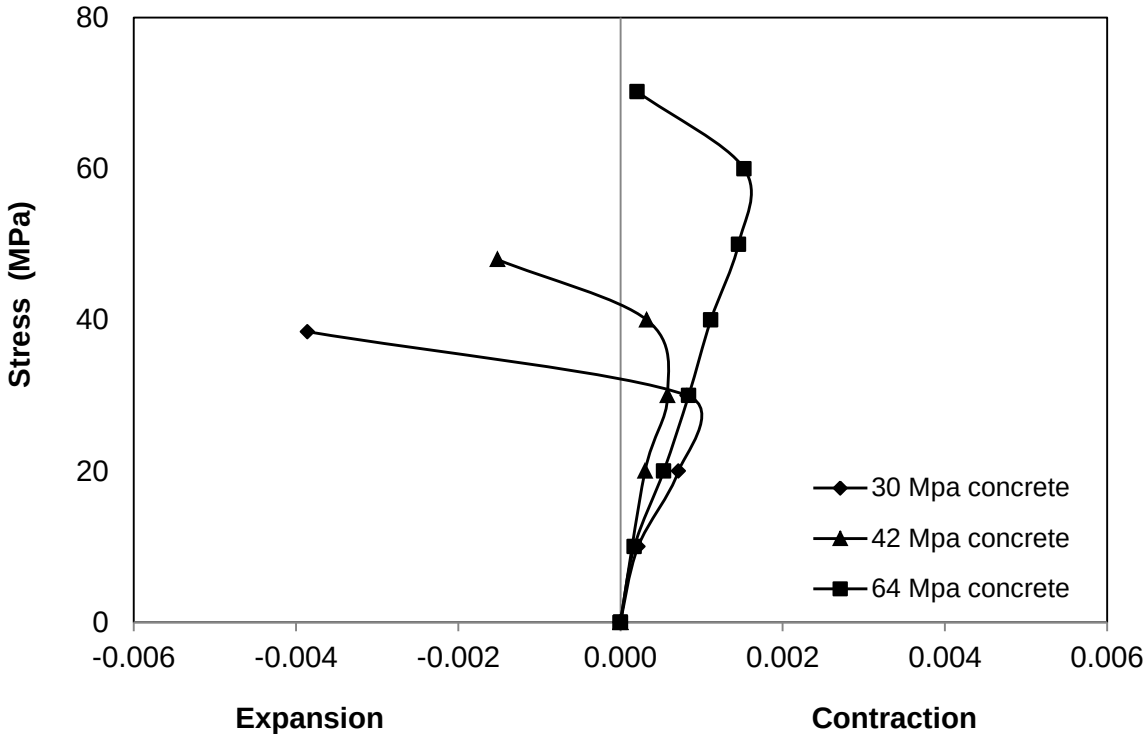

Figure 4-15 Volumetric strain response for GFRP confined concrete specimens

The volumetric stress-strain response of GFRP confined specimens follows the similar pattern like unconfined specimens in which the specimens undergo contraction when subjected to axial compressive loading as shown in figure 4-15. They absorb energy upto their capacity and then start expanding in lateral direction but due to confinement the specimens absorb more energy than the unconfined specimens. This can be justified by the fact that the confinement resists the lateral expansion which enables the confined specimens to withstand more loads before expanding.

During expansion, the confining FRP wrap participates in absorbing energy which enhances ductility of the GFRP confined specimens. As a result, the GFRP confined specimens undergo more expansion before failure as compared to the unconfined specimens.

4.2.2.3 CFRP Wrapped Specimens

The stress strain response of 30 MPa, 42 MPa and 64 MPa GFRP confined specimens is shown in figures 4-16, 4-17 and 4-18 respectively. It can be observed that the CFRP confinement has enhanced the strength and ductility of the specimens. In figure 4-16, it can be observed that stress-strain curves are comparatively flatter with high strain values showing ductile stress-strain response while in figure 4-18, it can be observed that stress-strain curves are comparatively steeper with higher stress values and lesser strain values showing stiffer stress-strain response.

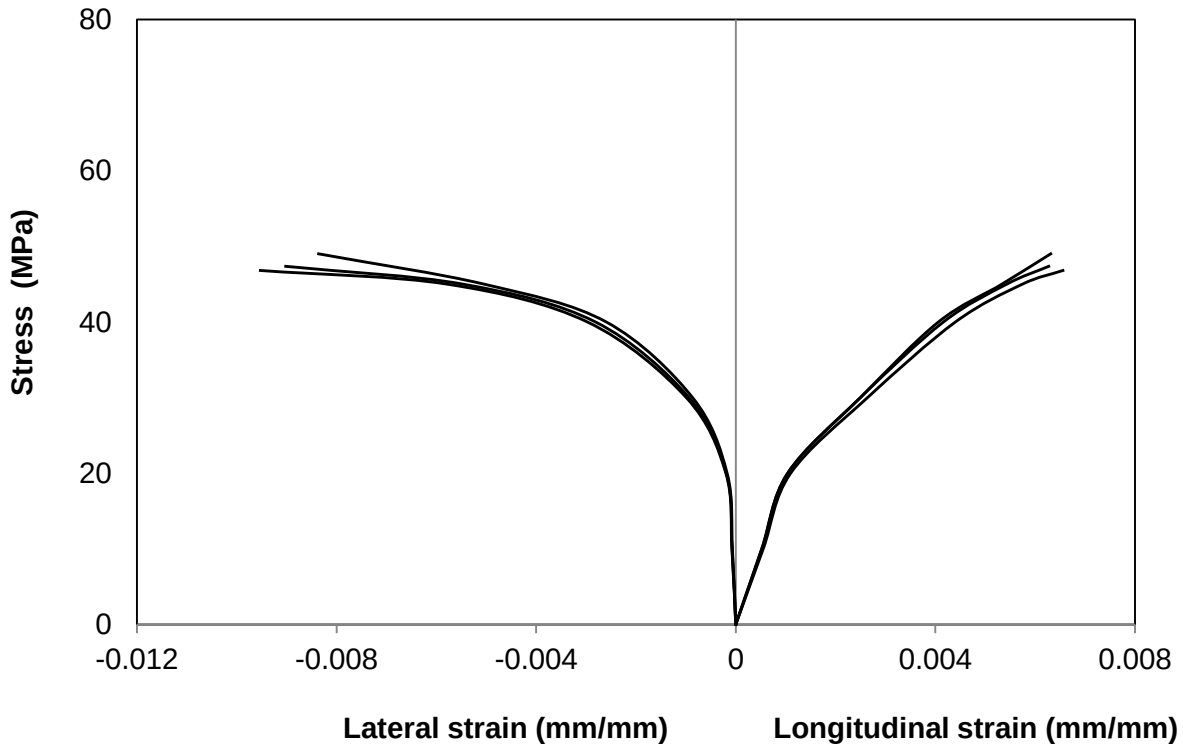

Figure 4-16 Stress-strain response of 30 MPa CFRP confined concrete

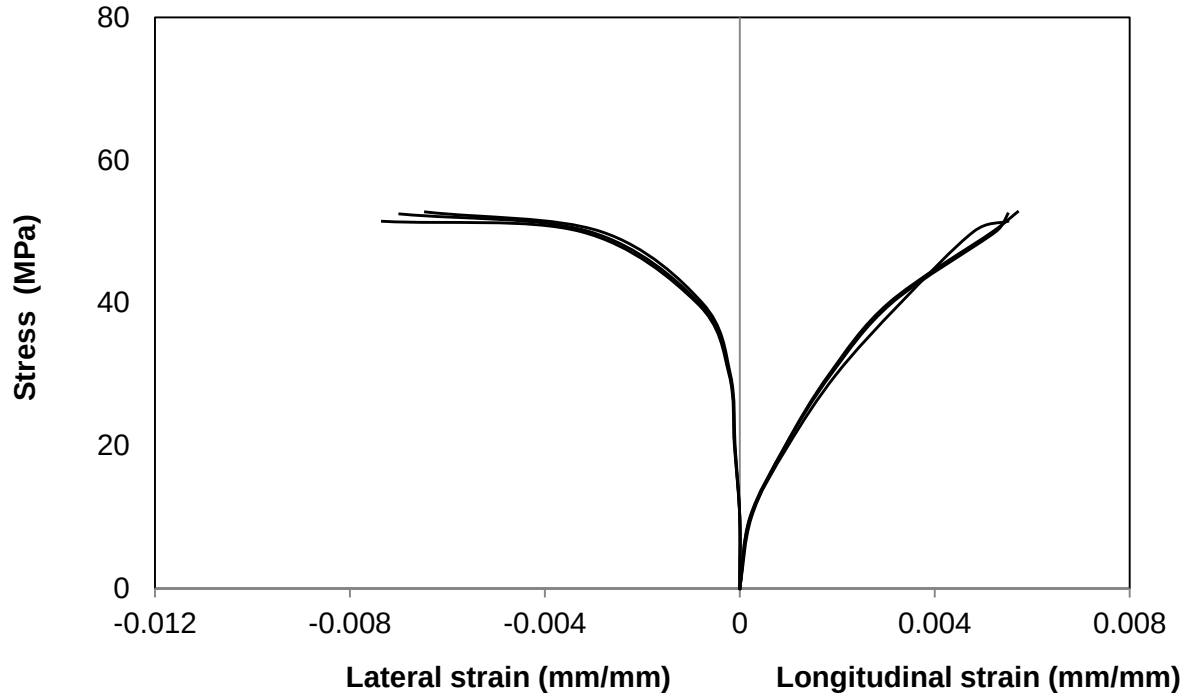

Figure 4-17 Stress-strain response of 42 MPa CFRP confined concrete

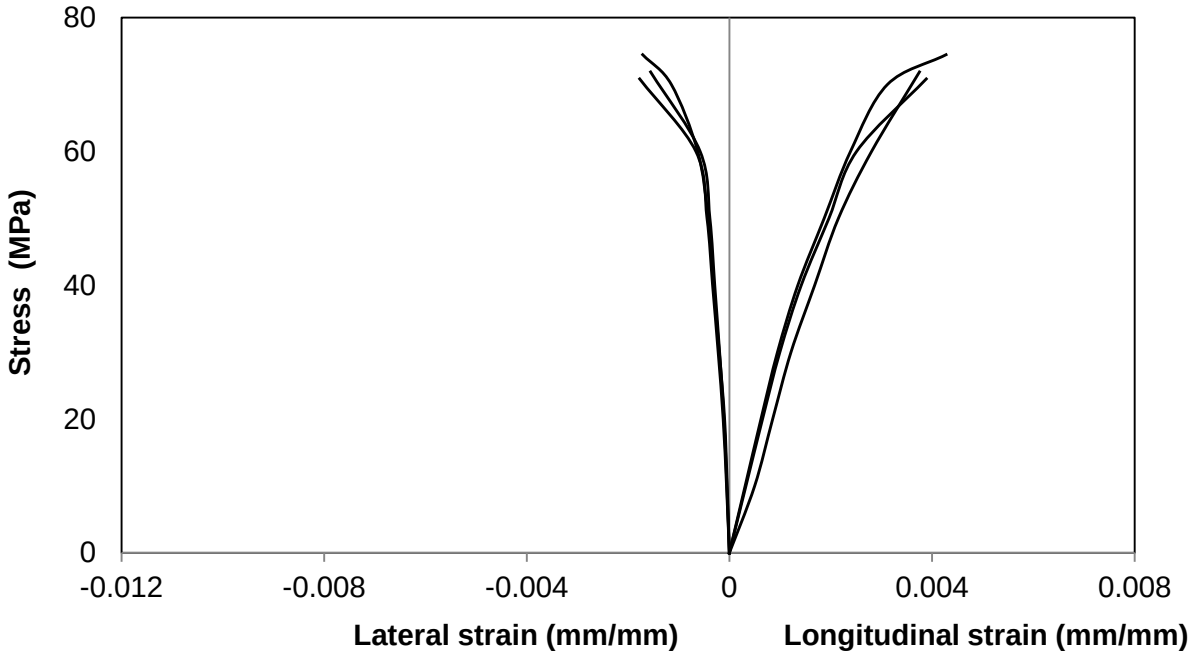

Figure 4-18 Stress-strain response of 64 MPa CFRP confined concrete

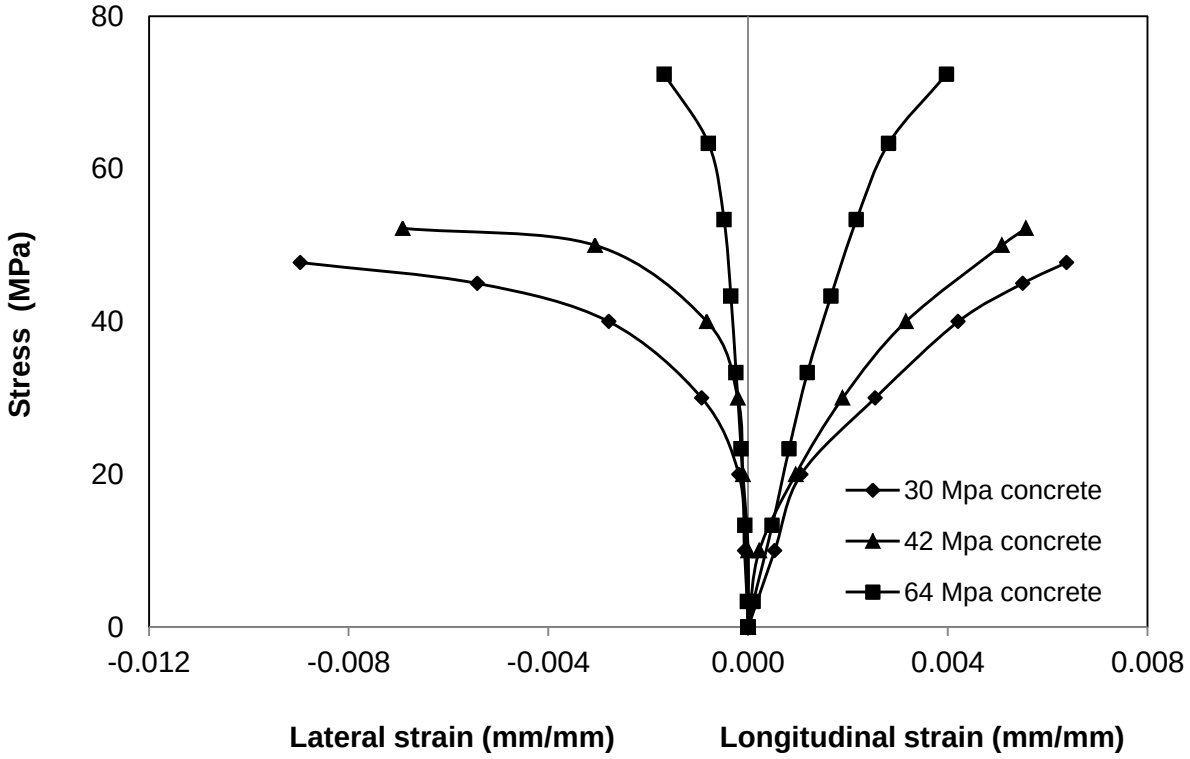

Figure 4-19 Stress-strain response of CFRP confined concrete specimens

In figure 4-19, the comparison of stress-strain response of CFRP confined specimens is shown. Here it can be observed that 30 MPa concrete shows a ductile behavior as compared to other concrete batches with lower stress values and higher strain values in stress-strain response while 64 MPa concrete shows a stiffer behavior with higher stress values and lower corresponding strains both in longitudinal and hoop direction.

The CFRP confined specimens show higher enhancement as compared to GFRP confined specimens. The CFRP confined specimens absorb more energy and show contraction under higher loading. In figure 4-20, it is clear that CFRP confinement is enabling specimens to take more loads without changing volume. The specimens resist both contraction as well as expansion as compared to GFRP confinement.

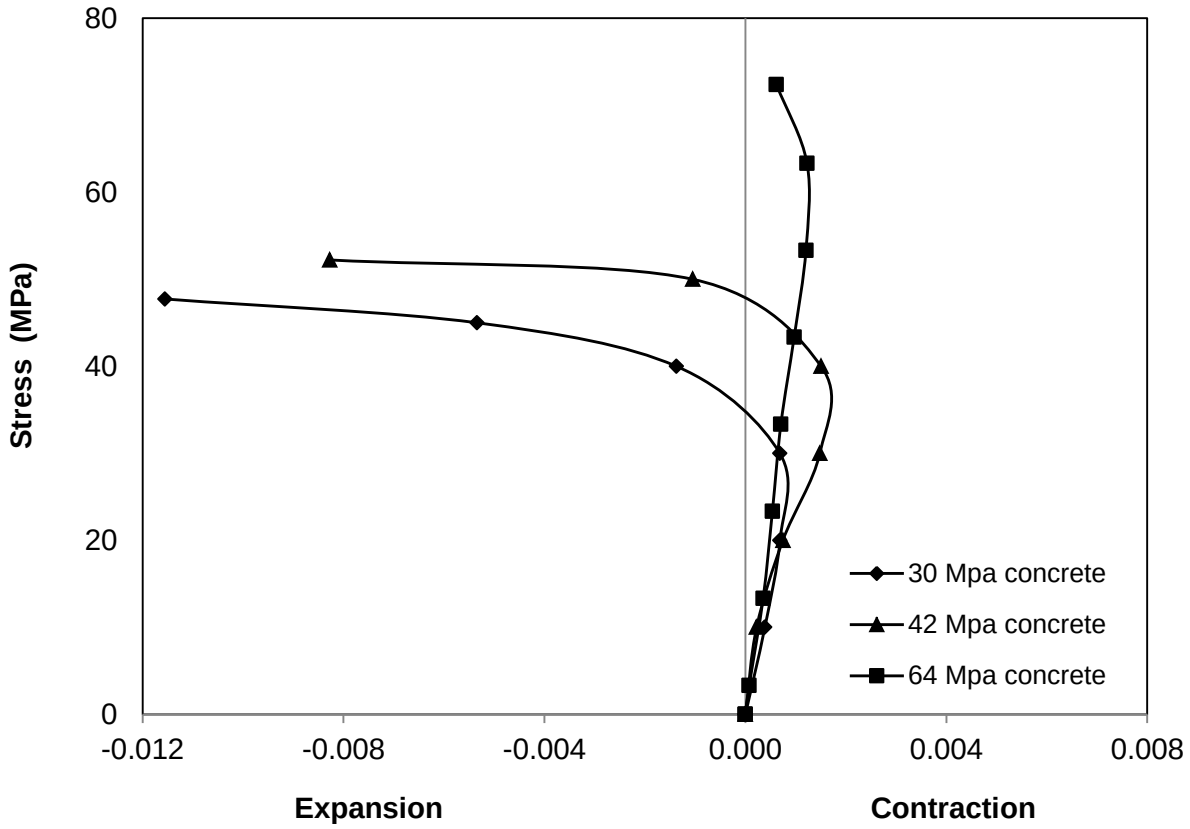

Figure 4-20 Volumetric strain response for CFRP confined concrete

During expansion, CFRP wrap takes part in absorbing energy along with concrete resulting in more ductile behavior as seen in 30 and 42 MPa concrete specimens where the specimens fail at higher lateral strains. The difference in behavior of 64 MPa concrete is due to the admixture which make it brittle.

The stress strain response other than 64 MPa concrete has been confirmed by previous studies on the behavior of CFRP wrapped concrete (Bisby et al. 2007; Rahai et al. 2008).

4.2.2.4 Stress-strain Plots of GFRP and CFRP Wrapped Specimens with Unconfined Specimens.

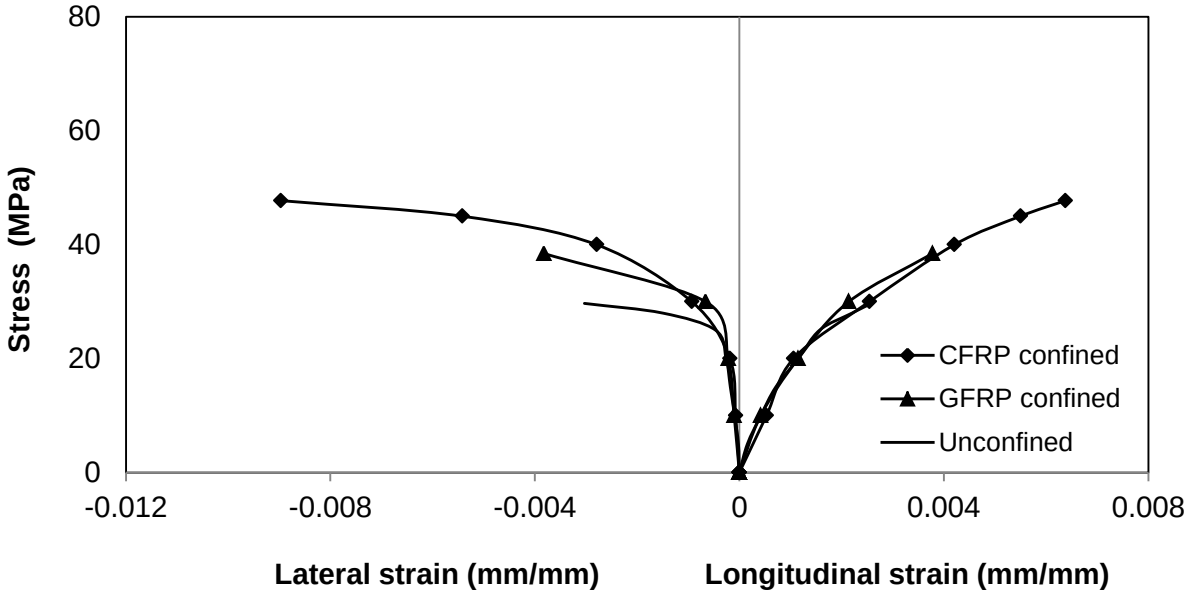

Figure 4-21 Stress-strain response of 30 MPa confined & unconfined concrete

In figure 4-21, it can be seen that the enhancement in strength as well as ductility is more pronounced in CFRP specimens as compared to GFRP confined specimens. Both FRPs enable concrete to undergo more strains in longitudinal as well as hoop direction.

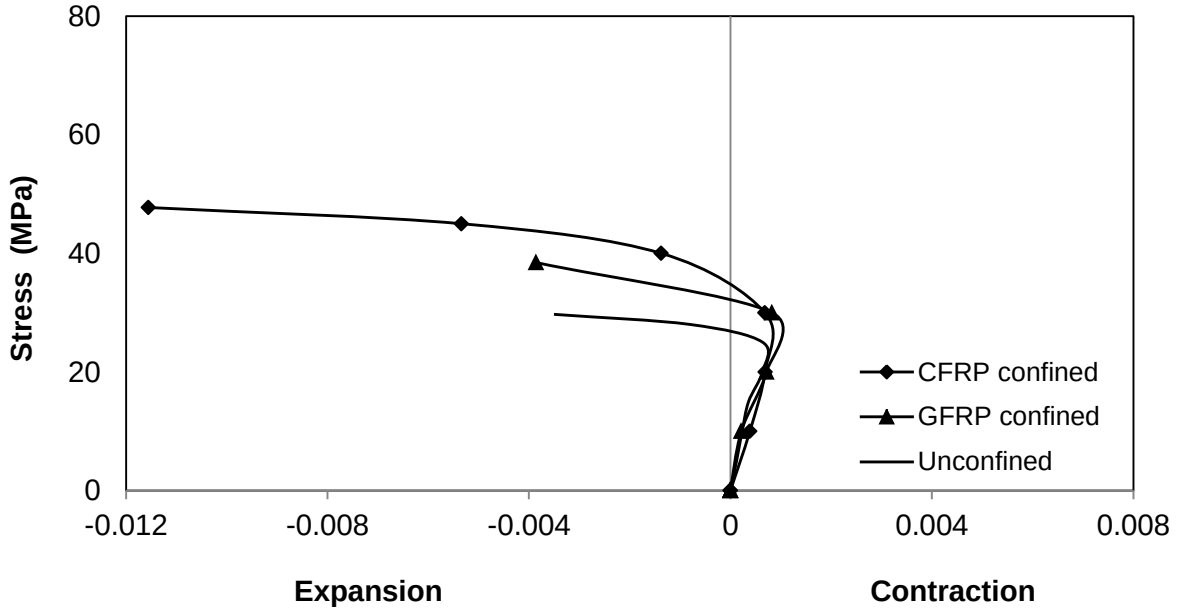

Figure 4-22 Volumetric strain response for 30 MPa Confined & unconfined concrete

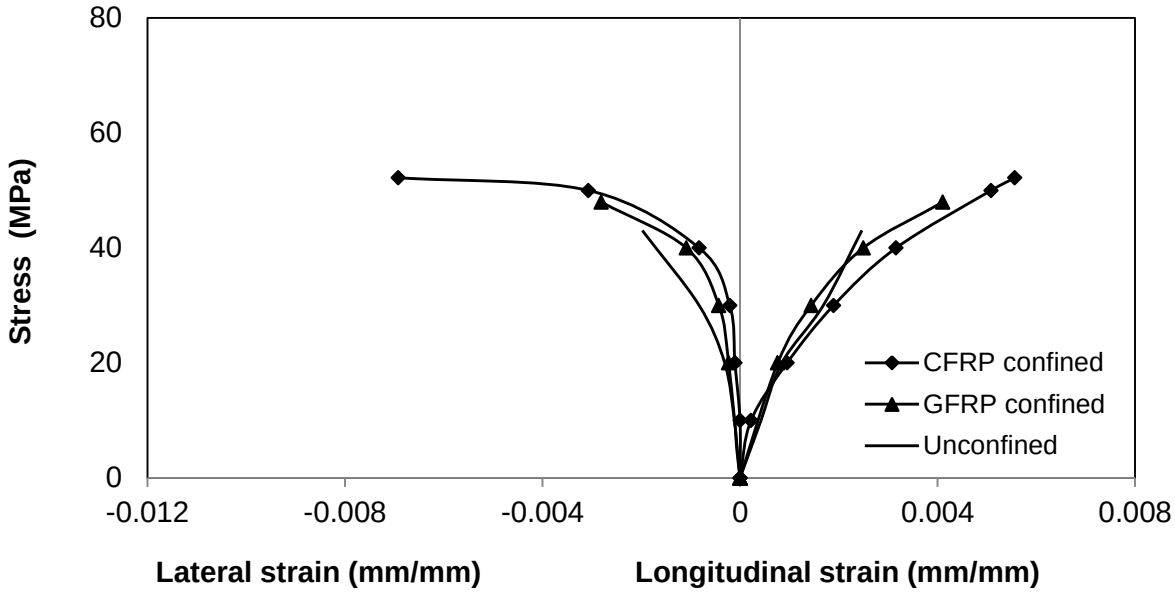

Figure 4-23 Stress-strain response of 42 MPa confined & unconfined concrete

For 42 MPa concrete specimens, CFRP confined specimens show more enhancements in strength as well as ductility as compared to GFRP confined specimens as shown in figure 4-23. Similarly, the volumetric stress-strain response also shows that GFRP and CFRP enhance the ductile behavior of concrete as indicated by higher strains undergone by concrete before failure.

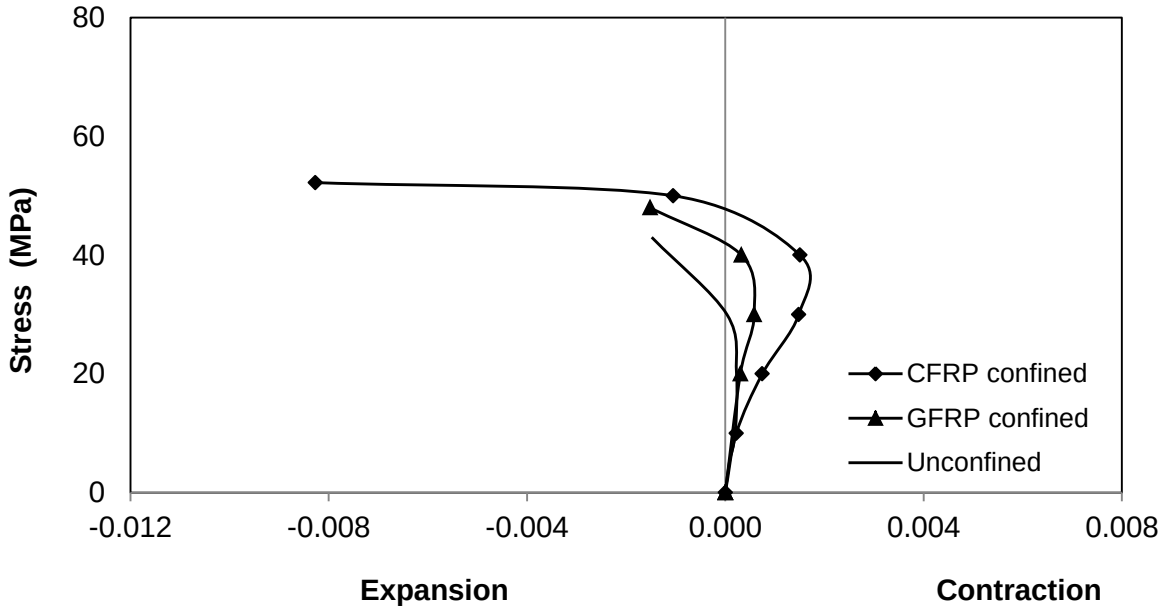

Figure 4-24 Volumetric strain response for 42 MPa confined & unconfined concrete

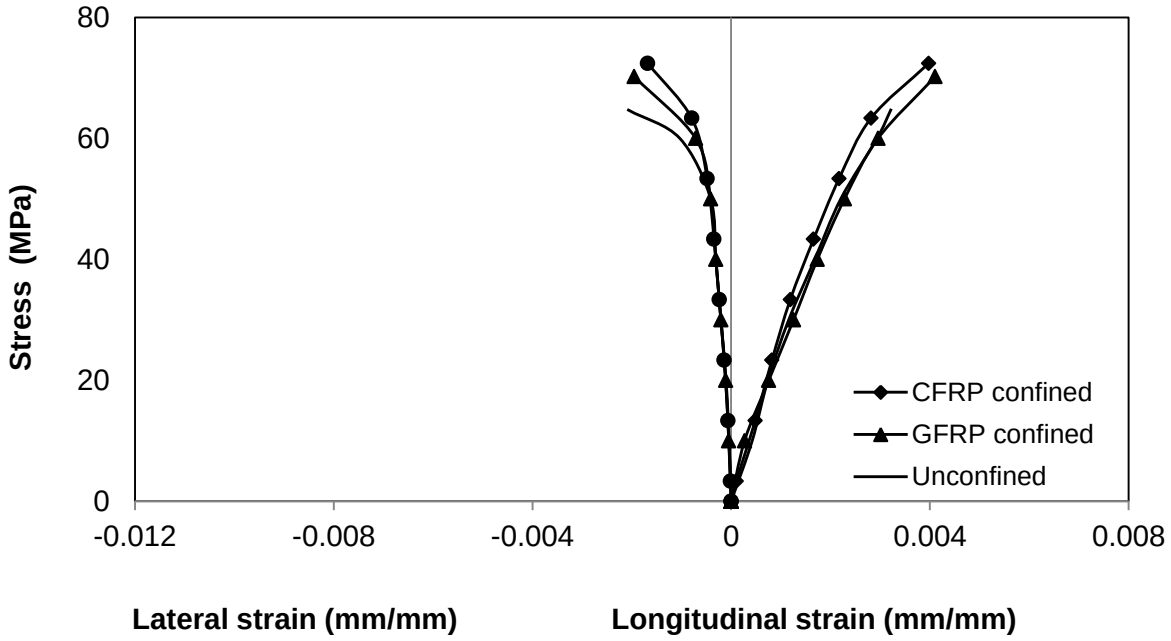

Figure 4-25 Stress-strain response of 64 MPa confined & unconfined concrete

The behavior of 64 MPa concrete is more brittle due to the admixtures used to get high strength and the use of FRP makes it even stiffer therefore, the only enhancement the FRPs have imparted is the increase in strength alone as shown in figure 4-25.

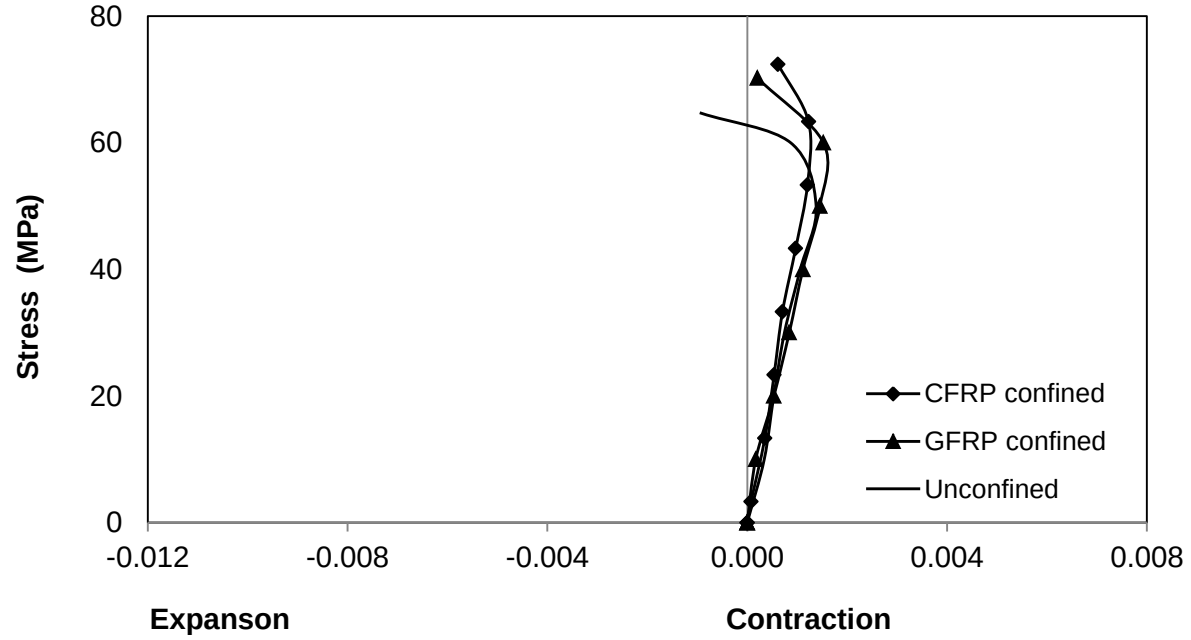

Figure 4-26 Volumetric strain response for 64 MPa Confined & unconfined concrete

4.2.3 Stress and Stiffness Response of FRP Confined Concrete

Stiffness was evaluated using the stress-strain response by calculating the slopes m_1, and m_2 at the bifurcation points as proposed by (Samaan et al. 1998). The initial slope of the curve is m_1 and the slope after the bifurcation point is m_2 as shown in figure 4-27.

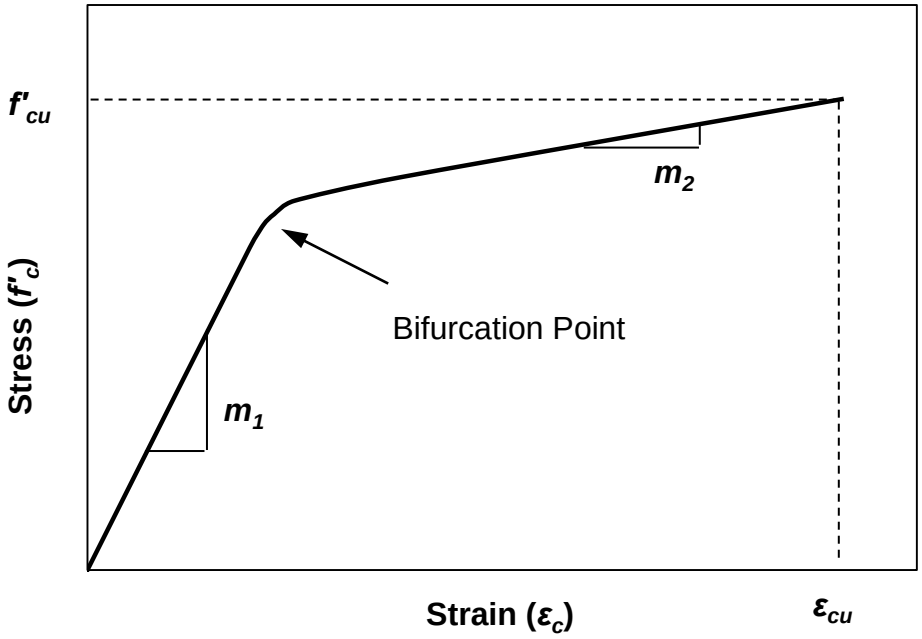

Figure 4-27 Evaluation of stiffness from stress-strain response

4.2.3.1 Maximum Stress and Average Stress.

The strengths of the confined specimens depend on the type of confinement provided to them but the effectiveness of the confining material also depends on the original unconfined strength of the concrete. As an average, the strength of normal strength concrete has been enhanced from 29.7 MPa to 38.45 MPa by confining it with GFRP and it can be enhanced up to 47.74 MPa by CFRP confinement. But the confinement does not follow the same pattern as the unconfined strength of concrete increases as shown in table 4-7 for higher concrete strengths.

Table 4-7 Maximum stress and average stress of specimens.

No.	Confinement provided	Max Axial Stress	Average Axial Stress
		Mpa	Mpa
1	30 MPa Unconfined	29.79	29.70
2		30.27	
3		29.03	
4	30 MPa GFRP	38.13	38.45
5		39.09	
6		38.13	
7	30 MPa CFRP	47.37	47.74
8		49.02	
9		46.82	
10	42 MPa Unconfined	43.02	42.84
11		42.54	
12		42.95	
13	42 MPa GFRP	47.85	47.99
14		47.92	
15		48.19	
16	42 MPa CFRP	52.47	52.22
17		52.75	
18		51.44	
19	64 MPa Unconfined	64.88	64.67
20		64.40	
21		64.74	
22	64 MPa GFRP	68.87	70.20
23		71.07	
24		70.67	
25	64 MPa CFRP	74.46	72.39
26		71.88	

4.2.3.2 Stiffness

The stiffness in longitudinal direction increases from 1.00 to 1.11 times in case of GFRP and it increases from 1.03 to 1.16 times in case of CFRP as the unconfined strength of concrete increases as tabulated in table 4-8 and shown in figure 4-28. This is due to the fact that the stiffness in longitudinal direction mainly depends on the mechanical properties of concrete and the role of FRP is not much significant. The stiffness of CFRP was confirmed by a previous study (Rahai et al. 2008). If we compare the stiffness of specimens confined with GFRP with those confined with CFRP, there is very little difference. The stiffness in longitudinal direction is increasing because the admixtures used to get higher strengths in

concrete make the concrete more stiff as compared to the concrete that has been prepared without using admixtures.

Table 4-8 Stiffness of unconfined and confined concrete specimens

Unconfined Specimens Strength	Confinement provided	m_1		m_2		Comparison of m_1 to Non wrapped m_1		Comparison of m_2 to m_1 (wrapped)	
		Axial	Hoop	Axial	Hoop	Axial	Hoop	Axial	Hoop
30 MPa	Unconfined	23.89	97.53	12.69	18.66	1.00	1.00	-	-
	GFRP	23.89	100.07	10.18	99.06	1.00	1.03	0.43	0.43
	CFRP	24.67	108.25	8.18	108.30	1.03	1.11	0.33	0.33
42 MPa	Unconfined	23.58	75.60	17.80	36.29	1.00	1.00	-	-
	GFRP	24.11	77.06	11.68	86.76	1.02	1.02	0.48	0.48
	CFRP	25.36	80.55	9.84	16.31	1.08	1.07	0.39	0.39
64 MPa	Unconfined	23.66	141.94	20.44	58.06	1.00	1.00	-	-
	GFRP	26.33	143.02	17.11	202.91	1.11	1.01	0.65	0.65
	CFRP	27.56	149.46	22.51	79.83	1.16	1.05	0.82	0.82

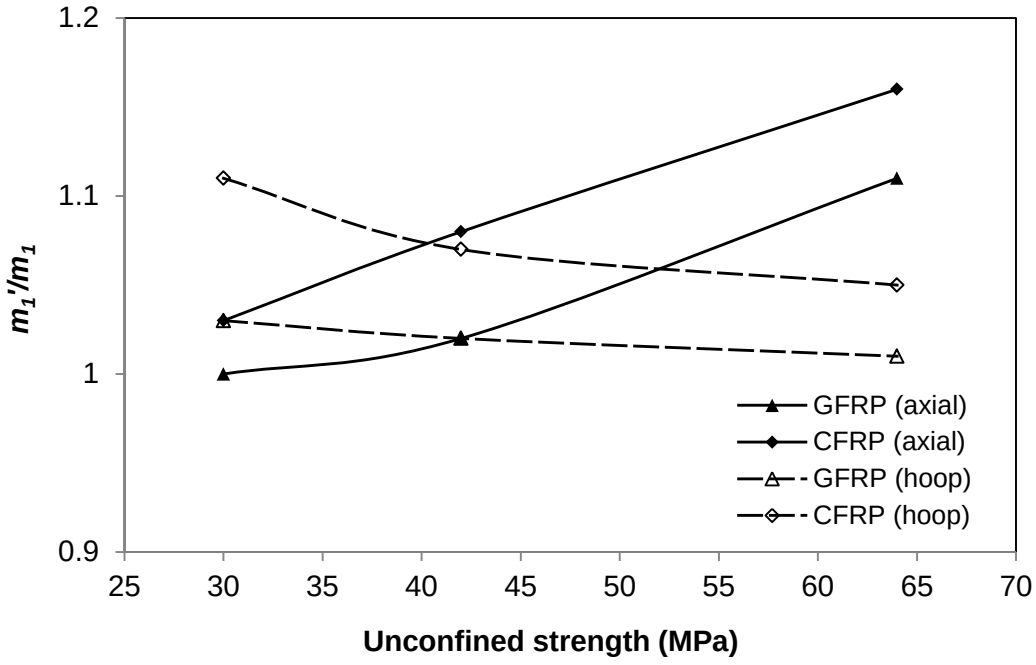

Figure 4-28 Comparison of stiffness of confined specimens

In hoop direction the stiffness increases but the increment in stiffness reduces as the unconfined strength of concrete increases. This is due to the reduction of effectiveness of FRP confinement at higher strengths of concrete.

The stiffness decreases from *m1* to *m2* in all the cases. This is due to the fact that before bifurcation point the load is carried by concrete alone which is much stiffer as compared to

the combination of concrete and FRP confinement where the load is partly carried by concrete and partly by the FRP confinement.

4.2.3.3 Axial Stress

Table 4-9 Axial stress values at 0.0008, 0.002 and 0.003 for unconfined and confined concrete specimens.

Unconfined Specimens Strength	Confinement provided	Strength at 0.0008 strain	Strength at 0.002 strain	Strength at 0.003 strain
		Mpa	Mpa	Mpa
30 MPa	Unconfined	15.68	28.14	-
		15.47	28.22	-
		15.59	27.96	-
	GFRP	15.81	29.82	32.97
		15.72	29.71	32.88
		15.56	30.14	33.14
	CFRP	15.88	30.08	34.14
		15.79	30.19	33.73
		15.71	29.93	33.86
42 MPa	Unconfined	19.57	30.12	-
		19.72	29.94	-
		19.69	30.27	-
	GFRP	19.72	31.91	37.62
		19.89	31.79	37.48
		19.93	32.13	37.23
	CFRP	19.91	32.11	39.82
		20.08	32.27	39.69
		20.12	31.96	40.17
64 MPa	Unconfined	20.42	45.12	63.34
		20.33	45.34	-
		20.09	44.97	64.15
	GFRP	20.59	45.98	60.91
		20.38	46.12	61.27
		20.63	46.37	61.07
	CFRP	20.71	48.05	63.33
		20.66	47.82	62.96
		20.55	47.99	63.27

Values of stress corresponding to axial strain limits of 0.0008, 0.002 and 0.003 are tabulated below in Table 4-9. The stress of the wrapped and non-wrapped specimens in Table 4-9 shows values of stress which are similar at an axial strain of 0.0008. Initially the slope is linear up to 0.008 value of strain. At strains of 0.002 and 0.003 the wrapped specimens show an increased value of stress when compared to the non-wrapped specimens. Thus the 0.0008 strain limit was chosen as the limiting curvature to calculate the deformability factor.

Wrapped concrete specimens show a bilinear load strain curve. The slope of the stress-strain curve is linear to a strain value of about 0.002. After the bifurcation point the concrete and the wrap start acting together and the specimens take up a different slope, which is lower than the initial slope.

4.2.4 Strain

The strain to failure of the specimens was recorded using the strain gauge. Gauges were attached both in the vertical and horizontal direction and hence both the values of axial and hoop strain were recorded. The maximum value of strain is recorded and the values are tabulated in the Table 4-10.

Table 4-10 Axial and hoop strain values unconfined and confined concrete specimens

Unconfined strength	Type of Confinement	Average Longitudinal Strain at Failure	Average Lateral Strain at Failure	% Increase in Longitudinal Strain	% Increase in Hoop Strain
30 MPa	Unconfined	0.0026	0.0014	0.00	0.00
	GFRP Wrapped	0.0045	0.0051	73.08	264.29
	CFRP Wrapped	0.0064	0.0090	145.37	540.55
42 MPa	Unconfined	0.0029	0.0019	0.00	0.00
	GFRP Wrapped	0.0041	0.0045	41.67	136.84
	CFRP Wrapped	0.0056	0.0069	91.95	264.15
64 MPa	Unconfined	0.0032	0.0022	0.00	0.00
	GFRP Wrapped	0.0041	0.0047	27.84	113.64
	CFRP Wrapped	0.0052	0.0049	61.99	122.73

In non-wrapped plain concrete specimens the hoop strain value was lower than the axial strain values. The ratio between the lateral and longitudinal strains varied from 0.15 to 0.20. The increase in hoop strains of the wrapped specimens was noted to be much higher than the axial strain increase as shown in Table 4-10. The CFRP confined specimens showed an increase of 5 times the strain of the non-wrapped specimens while GFRP wrapped specimens showed increase of up to 2 times the strain of unconfined specimens. The increase in strain is due to the enhancement provided by the FRP confinement to concrete.

4.2.5 Ductility

Ductility of a material is its capacity to absorb energy. Ductile materials allow better stress distribution and warning to impending failure. In the case of concrete wrapped specimens, ductility of the specimens is given in terms of deformability which is defined as the ratio of energy absorption (or area under load-deflection curve) at ultimate to energy absorption at limiting curvature (Vijay and Ganga Rao 1995). In these tests deformability was calculated by finding the total energy under the curve up to failure and calculating the ratio between total energy and energy at a limiting strain of 0.0008, 0.002, and 0.003. In this section, energy absorption of unconfined and confined concrete specimens is discussed.

4.2.5.1 Energy Absorption

The Stress-strain response curves were used to calculate the area under the curve that represents the energy absorbed by the wrapped concrete cylinders compared to the non-wrapped concrete cylinders. The area under the curve at a limiting strain of 0.0008, 0.002 and 0.003 is used to calculate the deformability factor. The ratios of energy absorption within limiting strains in longitudinal and hoop direction are given in Table 4-11 and Table 4-12.

Table 4-11 Comparison of energy absorption of unconfined and confined concrete specimens in longitudinal direction.

Confinement provided	Total Area	Area under 0.0008 strain	Area under 0.002 strain	Area under 0.003 strain	Ratio of Areas		
	Kpa	Kpa	Kpa	Kpa	0.0008 Strain	0.002 strain	0.003 strain
Unconfined	130.10	6.27	32.56	52.91	20.74	4.00	2.46
	129.29	6.19	32.40	52.70	20.89	3.99	2.45
	129.93	6.24	32.37	52.58	20.84	4.01	2.47
GFRP	243.94	6.32	33.70	71.42	38.57	7.24	3.42
	242.92	6.29	33.55	71.13	38.63	7.24	3.42
	251.85	6.22	33.64	71.51	40.46	7.49	3.52
CFRP	368.26	6.35	33.93	72.39	57.98	10.85	5.09
	373.53	6.32	33.90	72.18	59.14	11.02	5.17
	376.27	6.28	33.67	71.85	59.88	11.18	5.24
Unconfined	159.27	7.83	37.64	60.53	20.35	4.23	2.63
	154.49	7.89	37.68	60.54	19.59	4.10	2.55
	162.74	7.88	37.85	60.86	20.66	4.30	2.67
GFRP	301.18	7.89	38.87	81.52	38.18	7.75	3.69
	297.38	7.96	38.96	81.56	37.38	7.63	3.65
	313.70	7.97	39.21	81.86	39.35	8.00	3.83
CFRP	384.05	7.96	39.18	83.11	48.22	9.80	4.62
	394.38	8.03	39.44	83.45	49.10	10.00	4.73
	382.68	8.05	39.30	83.41	47.55	9.74	4.59
Unconfined	370.29	8.17	47.49	109.89	45.33	7.80	3.37
	232.64	8.13	47.53	78.34	28.61	4.89	2.97
	382.18	8.04	47.07	109.67	47.56	8.12	3.48
GFRP	390.46	8.24	48.18	109.86	47.41	8.10	3.55
	487.45	8.15	48.05	109.90	59.79	10.14	4.44
	430.61	8.25	48.45	110.42	52.18	8.89	3.90
CFRP	466.08	8.28	49.54	113.51	56.26	9.41	4.11
	423.63	8.26	49.35	113.01	51.26	8.58	3.75
	431.46	8.22	49.34	113.19	52.49	8.74	3.81

Table 4-12 Comparison of energy absorption of unconfined and confined concrete specimens in hoop direction.

Confinement provided	Total Area	Area under 0.0008 strain	Area under 0.002 strain	Area under 0.003 strain	Ratio of Areas		
	Kpa	Kpa	Kpa	Kpa	0.0008 Strain	0.002 strain	0.003 strain
Unconfined	226.37	10.50	43.25	82.75	21.56	5.23	2.74
	216.47	10.47	43.07	82.40	20.68	5.03	2.63
	234.83	10.49	43.13	82.46	22.39	5.44	2.85
GFRP	293.39	11.25	47.70	93.10	26.07	6.15	3.15
	286.15	11.29	47.74	93.19	25.35	5.99	3.07
	301.23	11.20	47.67	93.06	26.89	6.32	3.24
CFRP	561.98	11.94	50.98	100.98	47.05	11.02	5.57
	540.41	11.91	50.88	100.93	45.37	10.62	5.35
	583.50	11.87	50.92	101.14	49.17	11.46	5.77
Unconfined	198.56	12.02	55.34	88.44	16.52	3.59	2.25
	193.89	11.96	55.30	88.43	16.21	3.51	2.19
	199.68	11.91	54.94	87.82	16.76	3.63	2.27
GFRP	339.07	15.25	64.70	126.06	22.23	5.24	2.69
	329.66	15.16	64.39	125.73	21.75	5.12	2.62
	352.13	14.94	63.95	125.20	23.58	5.51	2.81
CFRP	571.44	16.04	67.19	130.80	35.62	8.51	4.37
	543.10	15.94	66.87	130.14	34.06	8.12	4.17
	585.01	16.09	67.10	130.51	36.35	8.72	4.48
Unconfined	337.35	23.01	95.93	150.94	14.66	3.52	2.23
	330.28	22.91	95.42	150.12	14.42	3.46	2.20
	339.10	22.81	95.22	149.86	14.87	3.56	2.26
GFRP	352.34	23.56	101.04	159.71	14.95	3.49	2.21
	346.97	23.45	100.55	158.94	14.80	3.45	2.18
	357.37	23.53	101.02	159.71	15.19	3.54	2.24
CFRP	360.41	25.33	105.47	165.93	14.23	3.42	2.17
	352.92	25.55	105.60	165.92	13.81	3.34	2.13
	361.06	25.64	106.07	166.68	14.08	3.40	2.17

Table 4-11 and table 4-12 show the ratio of area under curve at 0.0008, 0.002 and 0.003 strains for the three batches of concrete used in this research work. The average of all three batches will be the deformability factors of unconfined and confined concrete at specified limiting strains and are given in the table 4-13 and 4-14.

Table 4-13 Deformability factors for unconfined, GFRP confined and CFRP confined concrete specimens in longitudinal direction.

Type of Confinement	Deformability Factor		
	Limiting Strain=0.0008	Limiting Strain=0.002	Limiting Strain=0.003
Unconfined	27.1742	5.0489	2.78
GFRP Wrapped	43.5517	8.0537	3.71
CFRP Wrapped	53.5423	9.9248	4.57

Table 4-14 Deformability factors for unconfined, GFRP confined and CFRP confined concrete specimens in hoop direction.

Type of Confinement	Deformability Factor		
	Limiting Strain=0.0008	Limiting Strain=0.002	Limiting Strain=0.003
Unconfined	17.5627	4.1080	2.40
GFRP Wrapped	21.2005	4.9784	2.69
CFRP Wrapped	32.1929	7.6234	4.02

The deformability factors are a measure of finding deformations induced in a specimen under unit load. In longitudinal direction, the deformability factors of the concrete have been enhanced by the confining pressure provided by GFRP and CFRP which means that the confined concrete is able to absorb more energy as compared to unconfined concrete by taking more loads.

In hoop direction, the deformability factors of the unconfined concrete have been enhanced by using GFRP and CFRP which enable the confined concrete to absorb more energy as compared to unconfined concrete by being more ductile in lateral or hoop direction.

Energy absorbed by GFRP confined specimens is 1.33 to 1.99 times the energy absorbed by control specimens in longitudinal direction whereas energy absorbed in hoop direction is 1.05 to 1.3 times the energy absorbed by unconfined concrete specimens. CFRP confined specimens show 1.34 to 2.87 times the energy absorbed by unconfined concrete specimens while in hoop direction this increment in energy absorption is 1.07 to 2.4 times.

Table 4-15 Comparison of energy absorption by unconfined and confined concrete specimens in longitudinal direction.

Unconfined Specimens Strength	Confinement provided	Total Area Kpa	Average Total Area	Total Area ratio of confined to unconfined
30 MPa	Unconfined	130.10	129.78	1.00
		129.29		
		129.93		
	GFRP	243.94	246.24	1.90
		242.92		
		251.85		
	CFRP	368.26	372.69	2.87
		373.53		
		376.27		
42 MPa	Unconfined	159.27	158.83	1.00
		154.49		
		162.74		
	GFRP	301.18	304.08	1.91
		297.38		
		313.70		
	CFRP	384.05	387.04	2.44
		394.38		
		382.68		
64 MPa	Unconfined	370.29	328.37	1.00
		232.64		
		382.18		
	GFRP	390.46	436.17	1.33
		487.45		
		430.61		
	CFRP	466.08	440.39	1.34
		423.63		
		431.46		

In longitudinal direction, the energy absorption increases because the FRP confinement enables concrete to take more loads as compared to unconfined concrete as shown in table 4-15. Whereas, in hoop direction, the energy absorption increases because FRP confinement enables concrete to undergo more hoop strains as compared to that undergone by unconfined concrete as tabulated in table 4-16.

Table 4-16 Comparison of energy absorption by unconfined and confined concrete specimens in hoop direction.

Unconfined Specimens Strength	Confinement provided	Total Area kPa	Average Total Area	Total Area ratio
30 MPa	Unconfined	226.37	225.89	1.00
		216.47		
		234.83		
	GFRP	293.39	293.59	1.30
		286.15		
		301.23		
	CFRP	561.98	561.96	2.49
		540.41		
		583.50		
42 MPa	Unconfined	198.56	197.37	1.00
		193.89		
		199.68		
	GFRP	339.07	340.29	1.72
		329.66		
		352.13		
	CFRP	571.44	566.51	2.87
		543.10		
		585.01		
64 MPa	Unconfined	337.35	335.58	1.00
		330.28		
		339.10		
	GFRP	352.34	352.23	1.05
		346.97		
		357.37		
	CFRP	360.41	358.13	1.07
		352.92		
		361.06		

Moreover the increment in the energy absorption reduces as the unconfined strength of specimens increases in longitudinal as well as hoop direction for both types of FRP confinements provided because of the reduction of effectiveness of FRP confinement at higher strengths of concrete. The behaviour of CFRP regarding amount of energy absorption was confirmed by a previous study (Rahai et al. 2008).

4.3 Visual Observations

In addition to mechanical strength tests, visual observations were also made to observe the failure modes and patterns. It was observed that the majority of the high strength concrete cylinders failed with an abrupt failure. Figure 4-29 demonstrates the failure modes of specimens wrapped with GFRP and CFRP. All the confined specimens failed in an explosive manner by the sudden rupture of the FRP wrap due to hoop tension. Localized failure was avoided by providing 100 mm of overlap. For all confined specimens, delamination was not observed at the overlap location of the wrap.

(a) Unconfined

(b) GFRP Confined

(c) CFRP confined

Figure 4-29 Failure modes of unconfined and CFRP confined specimens.

4.4 Summary

The results from tests were conducted to analyze the effects of confinement of concrete cylinders using two different types of wraps i.e GFRP and CFRP. Variation in strength, and ductility due to variation in unconfined concrete strength and use of different types of FRP confinements have been provided. The results obtained to determine each parameter of stiffness confinement have been analyzed and discussed. Mechanical properties of unconfined and confined concrete have been discussed by plotting stress-strain response in longitudinal, hoop and volumetric aspects.

It was observed that CFRP provide better confinement as compared to GFRP wraps. The strength of unconfined concrete also affects the degree of confinement action. Normal strength concrete attains higher strain tolerance as compared to high strength concrete as steeper and longer stress-strain curves are obtained in stress-strain response. The volumetric strain response of the specimens showed that high strength concrete undergoes lesser expansion as compared to normal strength concrete. CFRP enables the specimens to take more loads and undergo lesser expansion as compared to GFRP. Both FRPs enhanced the stiffness of concrete but this enhancement reduced with an increase in the unconfined concrete strength. CFRP confined specimens showed stiffer stress-strain response as compared to GFRP specimens.

CHAPTER 5

5 ANALYTICAL EVALUATION

5.1 Introduction

The values of strength due to confinement determined through experimental testing are correlated to different mathematical models given by different FRC design guidelines. The values are compared with experimental results for each batch concrete cylinders. Calculations are provided for each guideline using all the strengths in Appendix A.

5.2 Design Guidelines and Models:

Different models and design guidelines have been developed for prediction of confinement pressure, confined axial compressive strength, axial load carrying capacity and other parameters for FRP confined concrete. The most prominent well known design guidelines are American Concrete Institute (ACI 440.2R-2008), Canadian Standard Association (CSA-S806-02), Intelligent Sensing for Innovative Structures (ISIS M04-2001) and European CEB/FIP Model Code 2010 (*fib bulletin 14*).

5.2.1 American Concrete Institute (ACI Committee-440-2R-2008)

This code helps us predict the strength and design of FRP wrap systems for increasing the strength and ductility of the members, and also discusses how to control the quality of the system. ACI suggests following formula for calculation of axial load carrying capacity and confined axial compressive strength of the member

$$P_u = 0.85 f'_{cc}(A_g - A_{st}) + f_y A_{st} \quad (1)$$

$$f'_{cc} = f'_c + 3.3 k_a \Psi_f f_l \quad (2)$$

$$f_l = \frac{2 \in_{fe} E_f n t_f}{D} \quad (3)$$

Where

P_u = Axial load carrying capacity
f'_{cc} = Compressive strength of confined concrete
A_g = Cross sectional area of the confined concrete
A_{st} = Longitudinal reinforcing steel area
f_y = Yield strength of longitudinal bars
Formula for confined strength is as follows
f'_c = Unconfined concrete compressive strength
f_l = Lateral confinement pressure

n = number of FRP layers
t_f = Thickness of FRP layer
E_f = Modulus of Elasticity of FRP
ε_{fe} = FRP effective strain
ε_{fe} = FRP effective strain = $k_e \varepsilon_{fu}$
$k_e = 0.55$
Ψ_f = FRP strength reduction factor = 0.95

5.2.2 CSA-S806-02

The confined strength of concrete that is wrapped with FRP is given by the following equation

$$f'_{cc} = 0.85 f'_c + k_l k_s f_l \quad (4)$$

The factor k_l is also used by past researchers in their studies that can be solved by the following empirical relation

$$k_l = 6.7(f_l)^{-0.17} \quad (5)$$

Where k_s is the shape factor which is equal to 1 in circular cross sectional shapes.

f_l can be calculated as:

$$f_l = \frac{2nt_f f_{frp}}{D} \quad (6)$$

f_{frp} will be least of the following values i.e., 0.004 E_f and 0.75* ultimate FRP strain.

5.2.3 Intelligent Sensing for Innovative Structures Canada (ISIS M04 2001)

The confined strength of concrete can be obtained by the expression given below:

$$f'_{cc} = f'_c(1+\alpha_{pr}\omega_w) \quad (7)$$

where

f'_{cc} = Compressive strength of concfined specimen

α_{pr} = Performance coefficient = 1 for circular columns

ω_w = Volumetric strength ratio

ω_w can be found out by equation (8)

$$\omega_w = \frac{f_l}{f'_c} \quad (8)$$

where

f_l = Lateral confinement pressure

f_l can be found out by the following equation (9)

$$f_l = \frac{2N_b f_{frpu} t_{frp}}{D_g} \quad (9)$$

N_b = Number of layers of FRP

f_{frpu} = Ultimate strength of FRP

t_{frp} = Thickness per layer of FRP

D_g = Diameter of the member

ISIS imposes a limitation of minimum confining pressure for design purposes to be taken equal to 4 MPa.

5.2.4 European CEB/FIP Model Code 2010

The European CEB/FIP Model Code 2010 uses the guidelines provided in *Technical Report by the Fédération Internationale du Béton, fib Bulletin 14, 2001* based on the model

presented by two researchers named Spoelstra and Monti (fib 2001; Spoelstra and Monti 1999). There are two methods for prediction of finding the FRP-confined compressive strength and corresponding ultimate strains as follows:

5.2.4.1 *fib* Approximate Method

As the name implies approximate predictions are obtained by this procedure and the confined strengths are calculated directly by empirical relations that consist of few parameter and neglect the secant modulus of elasticity at ultimate stress ($E_{sec,u}$).

The formula for confined strength is as:

$$f'_{cc} = f'_c\left(0.2 + 3\sqrt{\frac{f_l}{f'_c}}\right) \qquad (10)$$

$$f_l = \frac{1}{2} k_e \rho_f E_f \varepsilon_{fu} \qquad (11)$$

$k_e = 1$ for full wrap in circular sections
ε_{fu} = Ultimate tensile strain of FRP
E_f = Tensile modulus of Elasticity of FRP

b_f = width of FRP strip in partial wrapping
s = Pitch in partial wrapping
t_f = Thickness of FRP wrap
n = Number of wraps of FRP

k_e = Confinement effectiveness coefficient
ρ_f = volumetric ratio of FRP reinforcement

$$\rho_f = \frac{4nt_f}{10}\left(\frac{b_f}{s}\right) \quad \text{for circular sections} \qquad (12)$$

The ultimate load carrying capacity is given by

$$P_u = \lambda n f'_{cc} A_c + f_y A_{st} \qquad (13)$$

$\lambda = \text{Strength reduction factor}$

$\lambda = 0.8$

5.2.4.2 *fib* Exact Method

This method incorporates secant modulus of elasticity at ultimate stress ($E_{sec,u}$) along with intermediate moduli of elasticity and the corresponding stresses and strains. f_l can be found by equation (11). The parameters of the confinement model of fib exact method i.e confined stress (f_{cc}) and the corresponding strain (ε_{cc}) can be related to confining pressure (f_l) by the following relations

$$f_{cc} = f_c'\left[2.254\sqrt{1+7.94\frac{f_l}{f_c'}} - 2\frac{f_l}{f_c'} - 1.254\right] \qquad (14)$$

$$\varepsilon_{cc} = \varepsilon_c\left[1+5\left(\frac{f_{cc}}{f_c'}-1\right)\right] \qquad (15)$$

Where

$f_c' = \text{characteristic concrete compressive strength}$

The secant modulus of elasticity at ultimate stress ($E_{sec,u}$) is calculated from the following relation

$$E_{sec,u} = \frac{E_c}{1+2\beta\varepsilon_{fu}} \qquad (16)$$

Where

$$E_c = 4730\sqrt{f_c'} \qquad (17)$$

$$\beta = \frac{5700}{\sqrt{f_c'}} - 500 \qquad (18)$$

The strain at ultimate strength (ε_{cu}) is given by the following empirical relation

$$\varepsilon_{cu} = \varepsilon_{cc}\left[\frac{E_{cc}(E_c - E_{sec,u})}{E_{sec,u}(E_c - E_{cc})}\right]^{1-\frac{E_{cc}}{E_c}} \qquad (19)$$

Here

$$E_{cc} = \frac{f_{cc}}{\varepsilon_{cc}} \qquad (20)$$

The ultimate confined strength (f_{cu}) is calculated by the following relation

$$f_{cu} = \varepsilon_{cu} E_{sec,u} \qquad (21)$$

The calculations carried out by using these design guidelines are given in Appendix A.

5.3 Comparison of Analytical Models with Experimental Specimens

The Analytical models are compared with the experimental specimens in order to observe the predicted results with the actual results obtained during experimental work.

5.3.1 Theoretical Stress-strain response

The Stress-strain response of each of the specimens was drawn using the ACI Model from the following Equations

$$f_c = E_c \varepsilon_c - \frac{(E_c - E_2)^2}{4 f'_c} \varepsilon_c^{\,2}$$

for $0 \le \varepsilon_c \le \varepsilon'_t$

$$f_c = f'_c + E_2 \varepsilon_c$$

for $\varepsilon'_t \le \varepsilon_c \le \varepsilon'_{ccu}$

$$where E_2 = \frac{f'_{cc} - f'_c}{\varepsilon'_{ccu}}$$

$$\varepsilon'_t = \frac{2 f'_c}{E_c - E_2}$$

$$here \varepsilon'_{ccu} = \varepsilon'_c \left[1.5 + 12 K_b \frac{f_l}{f'_c} \left(\frac{\varepsilon_{fe}}{\varepsilon'_c} \right)^{0.45} \right]$$

From this model we come up with stress-strain response as shown in figure 5-1 and 5-2.

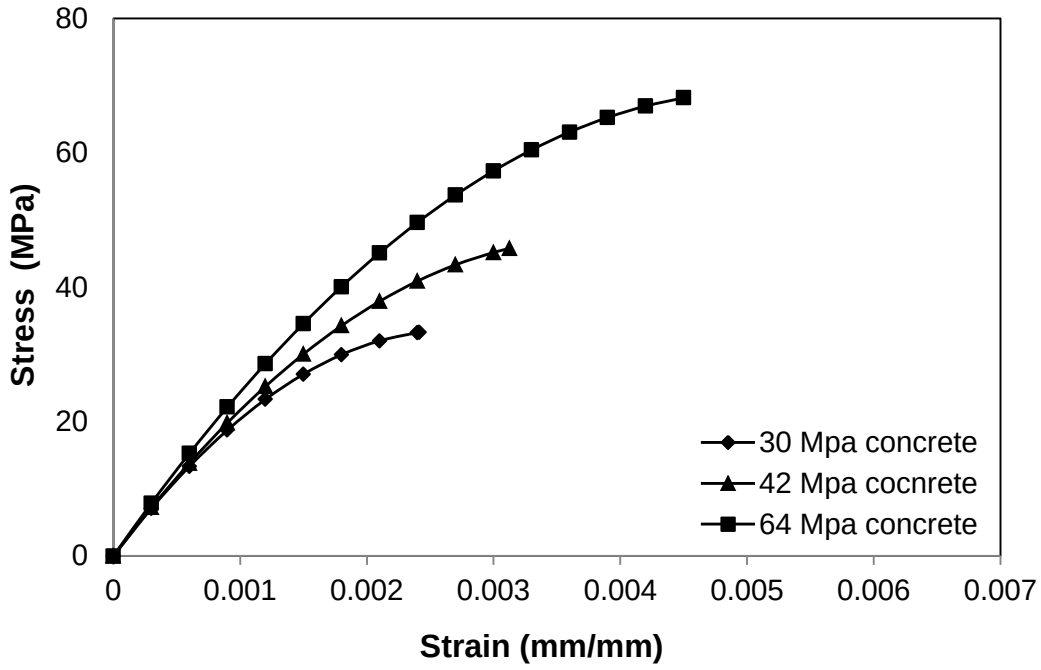

Figure 5-1 Theoretical Stress-strain response of GFRP confined concrete cylinders.

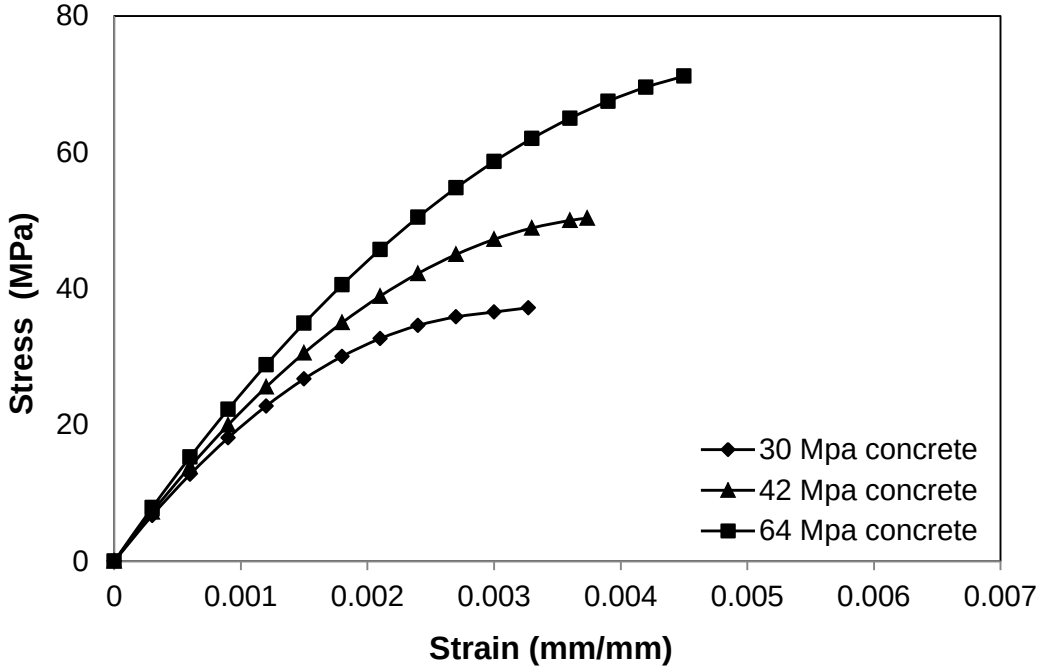

Figure 5-2 Theoretical Stress-strain response of CFRP confined concrete cylinders.

5.3.1.1 Comparison of Experimental and Theoretical Stress-strain response.

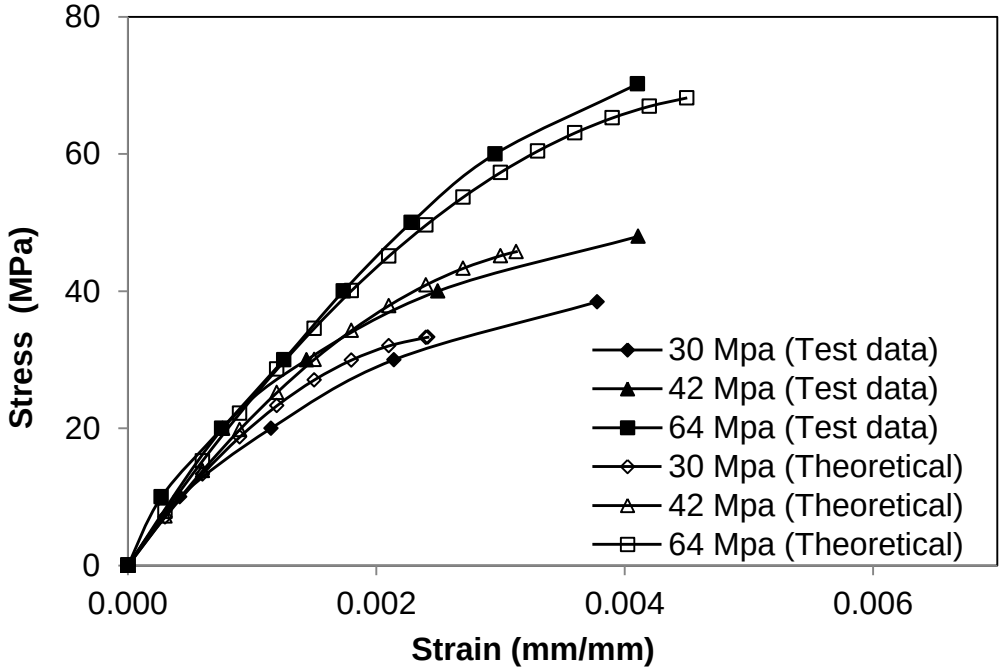

Figure 5-3 Comparison of experimental and theoretical Stress-strain response of GFRP confined concrete specimens.

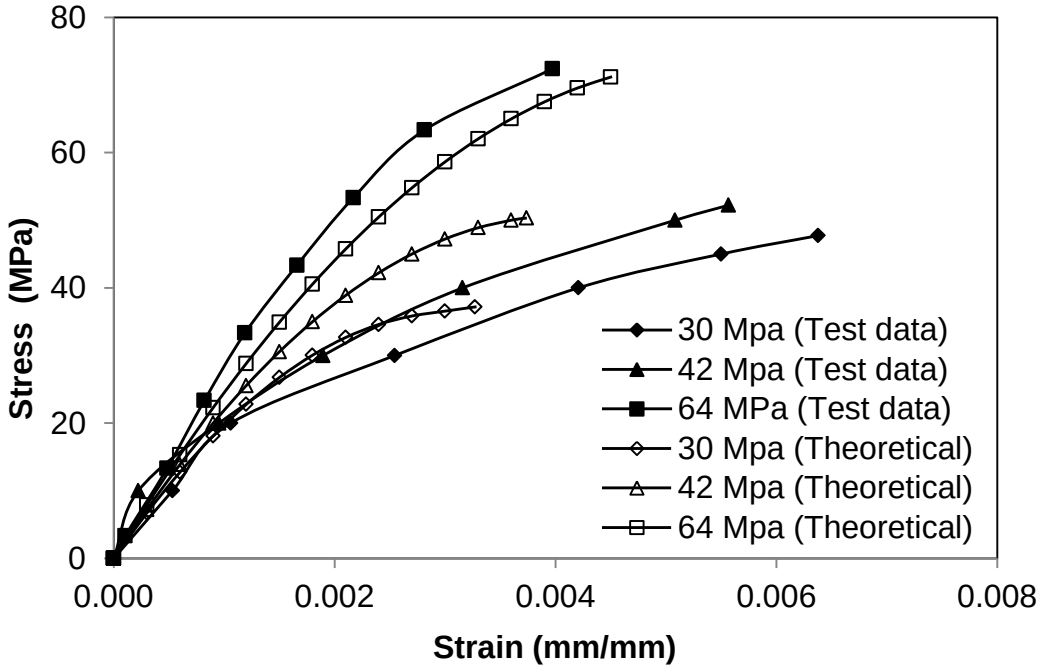

Figure 5-4 Comparison of experimental and theoretical stress-strain response of CFRP confined specimens.

The theoretical model underestimates the effectiveness of both GFRP and CFRP with respect to axial stress taken by the specimens as well as the strain induced in these confined specimens. The stress-strain response predicted by ACI model show stiffer behavior of confined concrete. However, the strain induced in specimens in case of high strength concrete is lesser than that predicted by ACI model for both GFRP and CFRP confinement as shown in figure 5-3 and 5-4. This is due to the chemical admixtures used to get high strength concrete that increase the elastic modulus of concrete and hence make it stiffer as compared to the concrete prepared without using such admixtures.

5.3.2 Compressive Strength

5.3.2.1 American Concrete Institute (ACI Committee-440-2R-2008)

The values of axial compressive strengths according to this analytical model are tabulated in the table 5-1 and shown in figure 5-5.

Table 5-1 Compressive strength of specimens confined with GFRP and CFRP.

Confinement	**Unconfined strengths**	**Theoretical Confined Strength**
	f'_c	f'_{cc}
	(Mpa)	**(Mpa)**
GFRP	29.7	33.34
	42.84	46.48
	64.67	68.32
CFRP	29.7	37.19
	42.84	50.33
	64.67	72.16

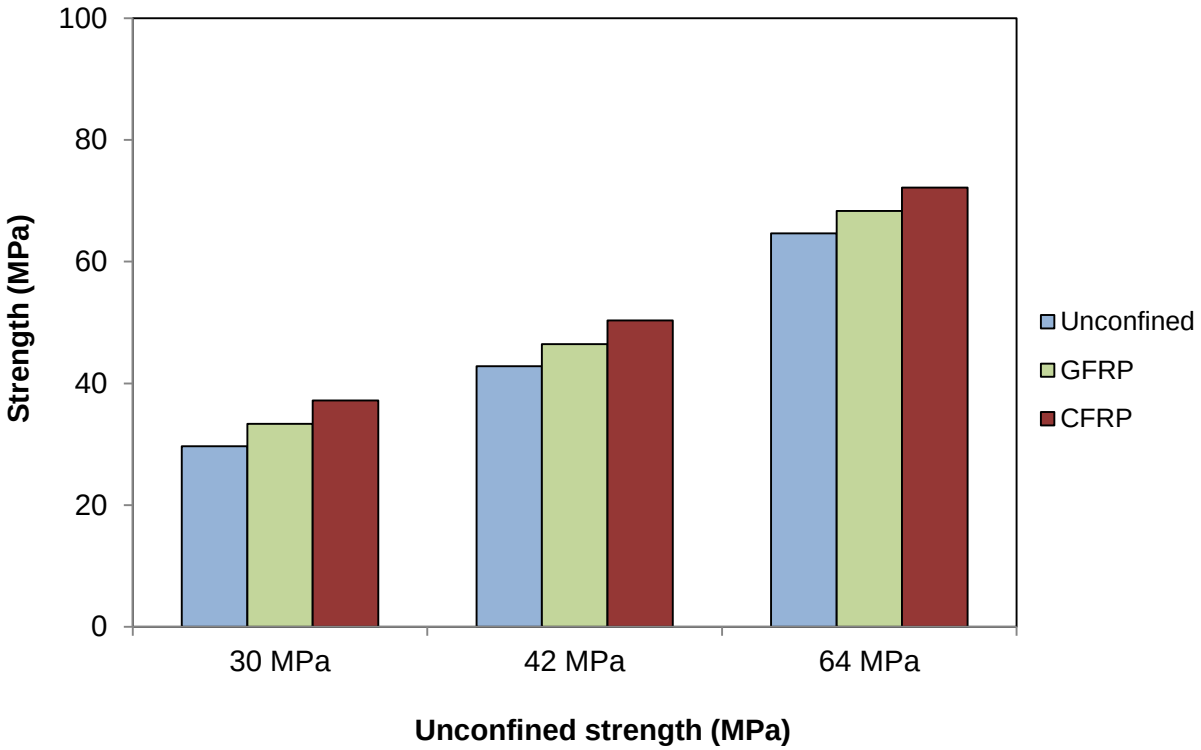

Figure 5-5 Theoretical compressive strengths according to ACI model.

5.3.2.2 CSA-S806-02

The values of axial compressive strengths according to this analytical model are less than the unconfined strengths of the specimens because of safety factors therefore the analytical strengths according to this model are taken equal to the unconfined specimens strengths and are tabulated in the table 5-2 and shown in figure 5-6.

Table 5-2 Compressive strength of specimens confined with GFRP and CFRP.

Confinement	Unconfined strength (MPa)	Confined Strength MPa (Theoretical)
GFRP	29.7	29.7
	42.84	42.84
	64.67	64.67
CFRP	29.7	33.61
	42.84	44.78
	64.67	64.67

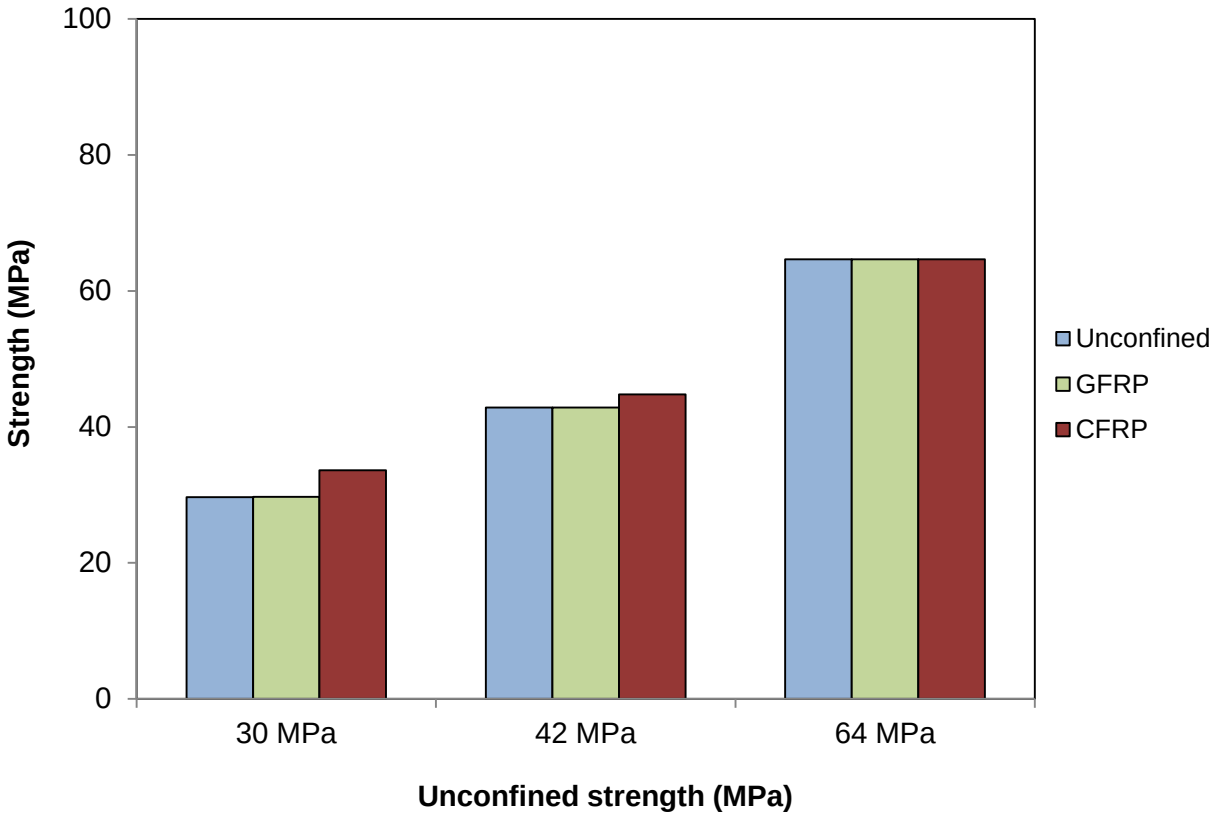

Figure 5-6 Theoretical compressive strengths according to CSA model.

5.3.2.3 Intelligent Sensing for Innovative Structures Canada (ISIS M04 2001)

The values of axial compressive strengths according to this analytical model are tabulated in the Table 5-3 and shown in figure 5-7.

Table 5-3 Compressive strength of specimens confined with GFRP and CFRP.

Confinement	Unconfined strength	Confined Strength (Theoretical)
GFRP	29.7	31.38
	42.84	44.95
	64.67	66.78
CFRP	29.7	34.16
	42.84	47.3
	64.67	69.13

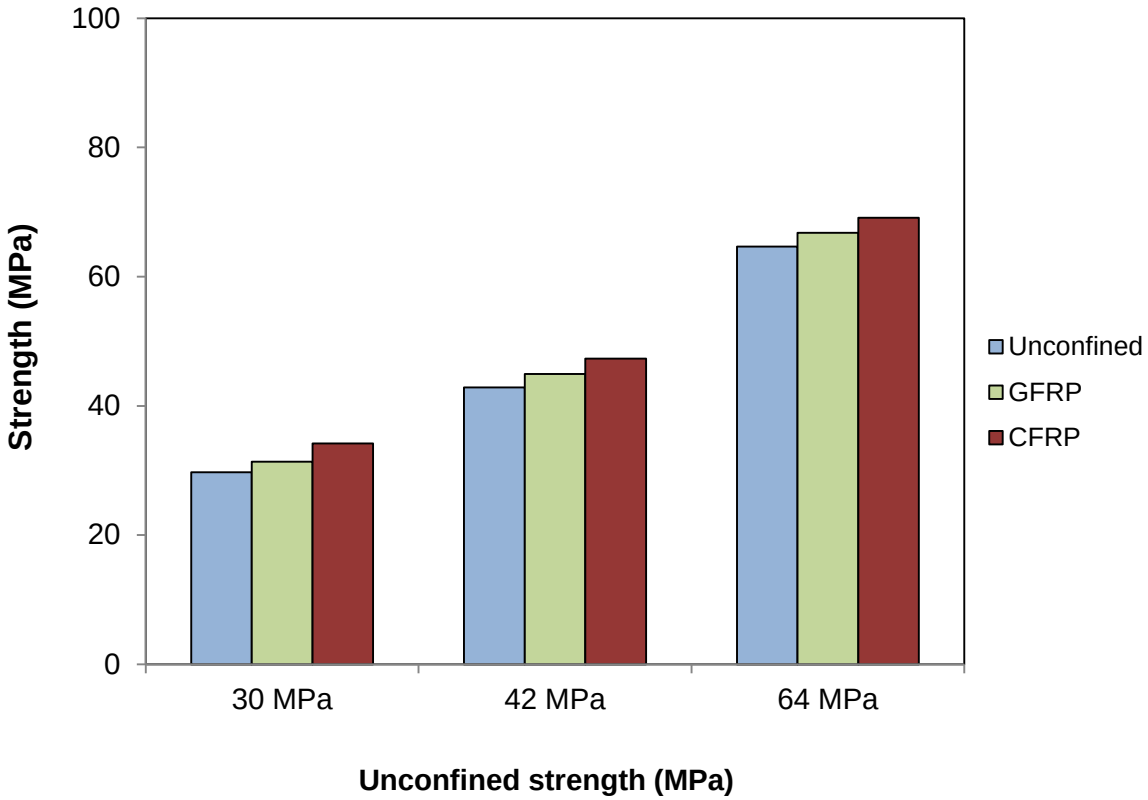

Figure 5-7 Theoretical compressive strengths according to ISIS model.

5.3.2.4 European CEB/FIP Model Code 2010

The values of axial compressive strengths according to this analytical model are tabulated in the table 5-4 and shown in figure 5-8 and 5-9 for both *fib* approximate method and *fib* exact method.

Table 5-4 Compressive strength of specimens confined with GFRP and CFRP.

Confinement	**Unconfined strengths**	***fib* approximate**	***fib* exact**
	f'_c	f'_{cc}	f'_{cc}
	(Mpa)	**(Mpa)**	**(Mpa)**
GFRP	29.7	28.89	36.82
	42.84	36.13	48.37
	64.67	46.79	69.84
CFRP	29.7	40.03	48.99
	42.84	49.51	64.11
	64.67	63.24	87.98

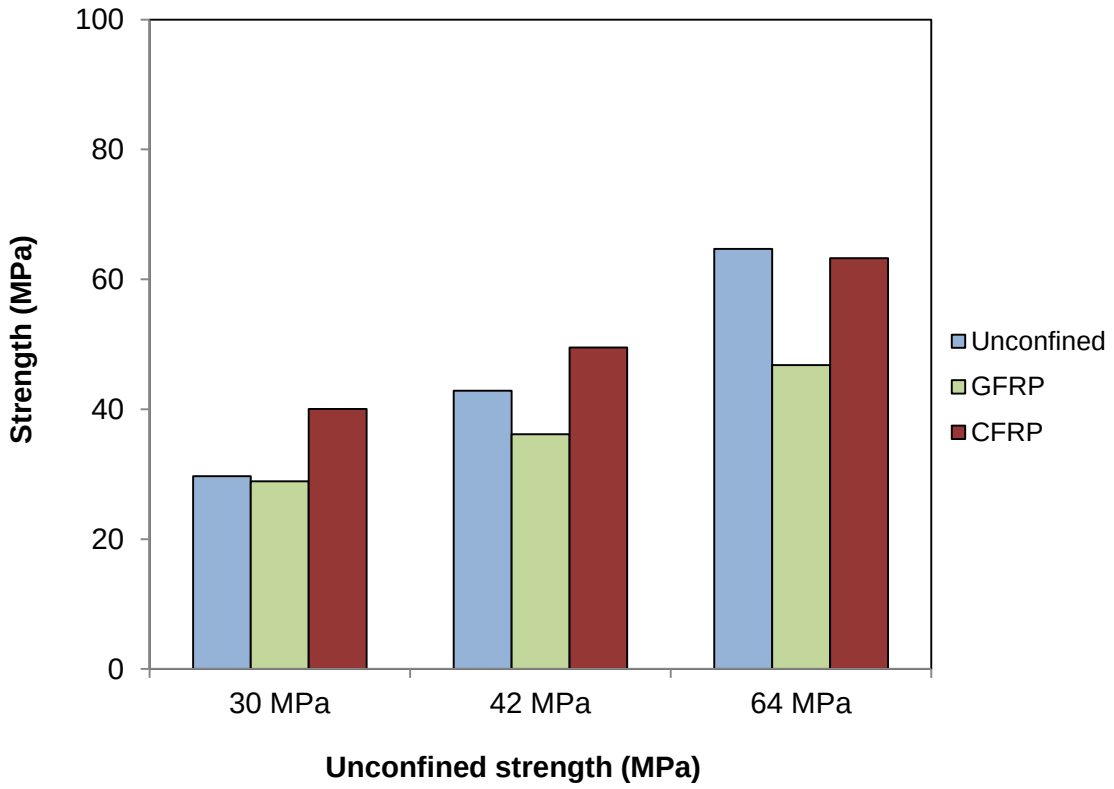

Figure 5-8 Theoretical compressive strengths according to *fib* approximate method.

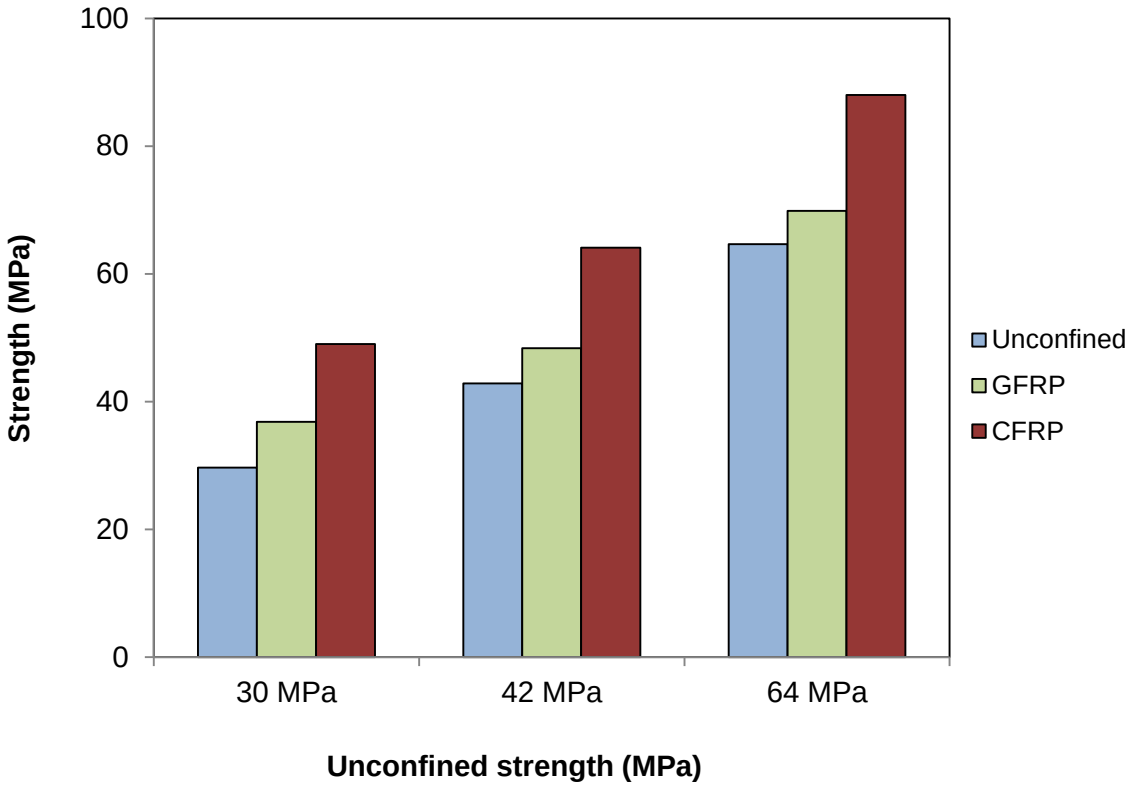

Figure 5-9 Theoretical compressive strengths according to fib exact method.

5.3.2.4 Comparison of Theoretical Compressive Strengths with Experimental Results

Table 5-5 Comparison of experimental and theoretical compressive strengths.

Confinement	Unconfined strengths	Experimental	ACI	CSA	ISIS	*fib* approximate	*Fib* exact
	f'_c (Mpa)	f'_{cc} (Mpa)	f'_{cc} (Mpa)	f'_{cc} (Mpa)	f'_{cc} (Mpa)	f'_{cc} (Mpa)	f'_{cc} (Mpa)
GFRP	29.7	38.45	33.34	29.7	31.38	28.89	36.82
	42.84	47.99	46.48	42.84	44.95	36.13	48.37
	64.67	70.20	68.32	64.67	66.78	46.79	69.84
CFRP	29.7	47.74	37.19	33.61	34.16	40.03	48.99
	42.84	52.22	50.33	44.78	47.3	49.51	64.11
	64.67	72.39	72.16	64.67	69.13	63.24	87.98

In table 5-5, it can be noted that at lower strengths of concrete all the guidelines predict conservative behavior for both GFRP and CFRP confined specimens but the predictions come closer as the unconfined strength of concrete increases. This is because of the safety factors applied while predicting the strengths of the confined specimens such as performance factor and unconfined strength reduction factor which impart greater variations in calculations at lower strengths of concrete and then these variations in calculations become smaller at higher strengths of concrete.

Among all the guidelines, *fib* exact guidelines give the closest predictions for both FRP but they overestimate the strength of CFRP confined specimens as the unconfined concrete strength increases from the domain of normal strength to high strength. ACI though more conservative than *fib* exact guidelines, gives good predictions at higher strengths of unconfined concrete as shown in figure 5-10 and 5-11. ISIS guidelines have a limitation of confining pressure provided by FRP which should be greater than 4 MPa. In this research, two layers of GFRP have been used in order to get a confining pressure of 4.46 MPa which means if single layer of GFRP had been used then ISIS could not predict the behavior of its confinement.

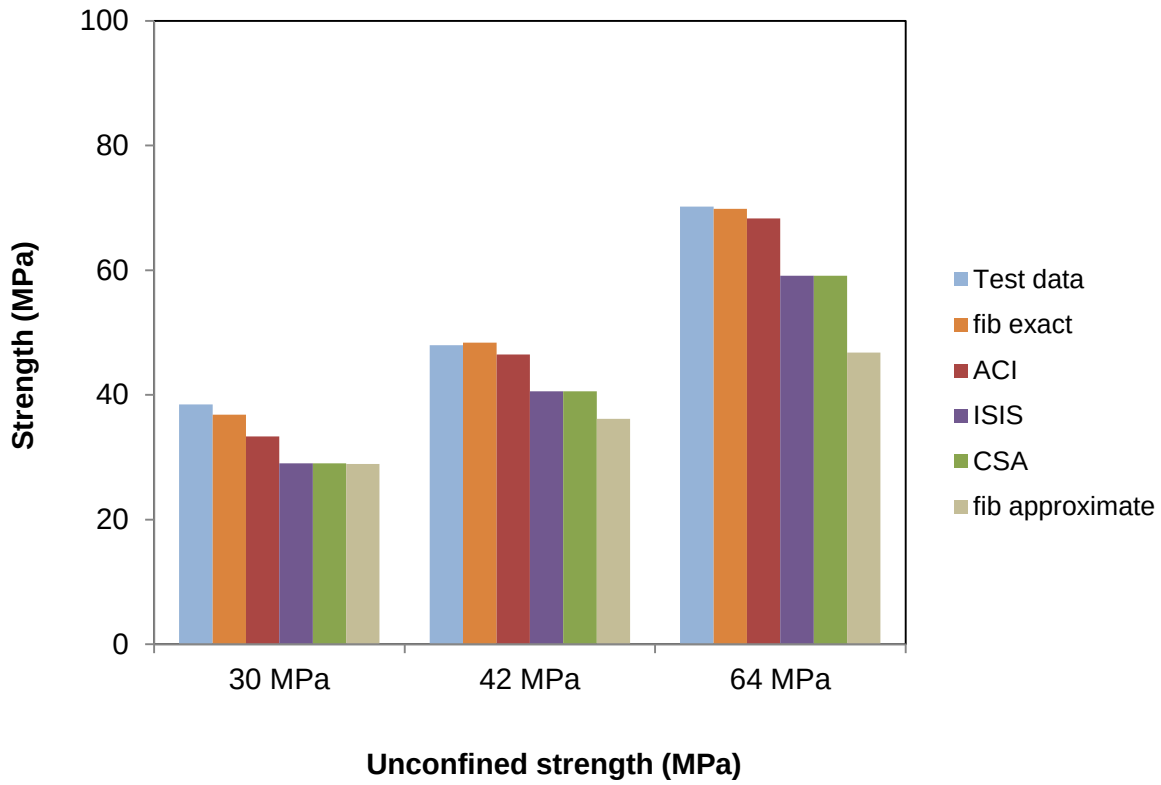

Figure 5-10 Comparison of experimental and theoretical compressive strength of specimens confined with GFRP.

fib approximate method and CSA guidelines give the most conservative predictions and are so high that GFRP confinement cannot be predicted by using these guidelines. This is because of the fact that *fib* approximate guidelines were developed for FRP that can provide high confining pressure and CSA uses a factor of 0.85 for reduction in unconfined concrete strength and GFRP provides lesser confining pressure than 15 percent of the unconfined strength even with 2 layers of GFRP wraps. As a result, the confined strength predicted by both these guidelines for GFRP wrapped specimens comes out to be lesser than the unconfined strength of the specimens. Therefore in this research, such lesser confined strengths are taken to be equal to unconfined strengths indicating no confining pressure provided by GFRP confinement as predicted by *fib* approximate and CSA guidelines.

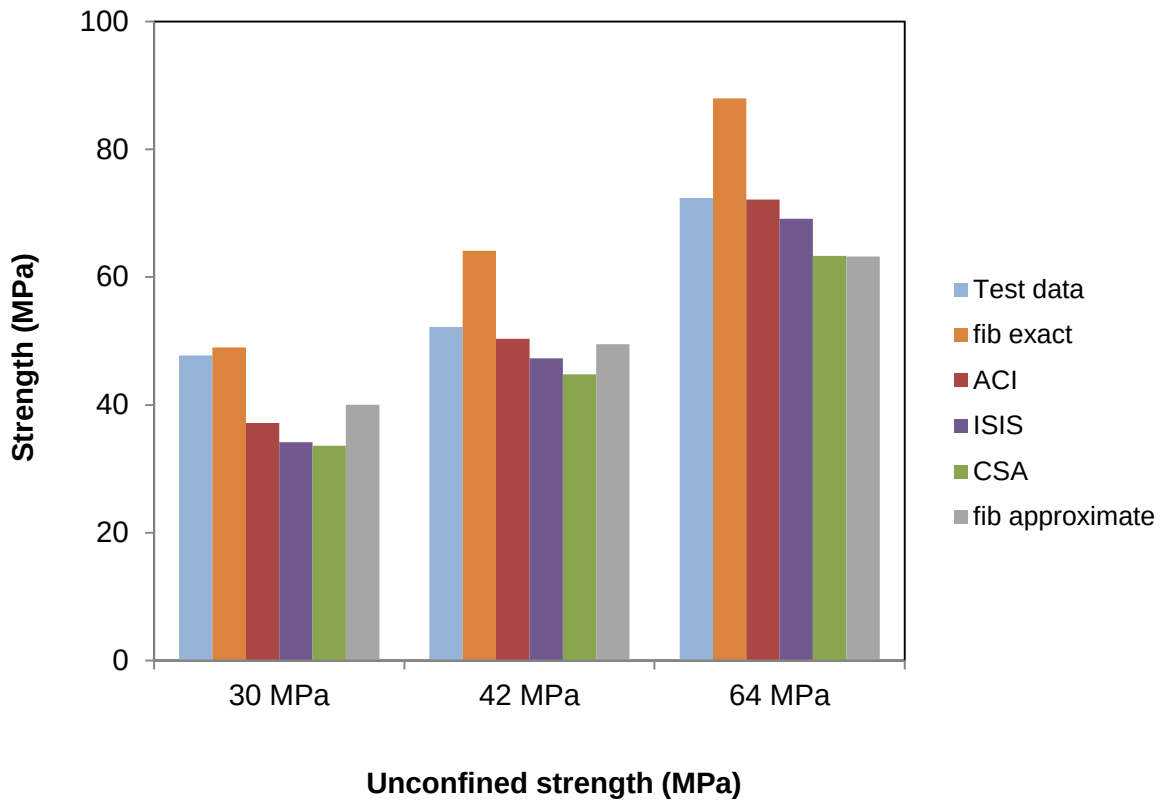

Figure 5-11 Comparison of experimental and theoretical compressive strength of specimens confined with CFRP.

fib exact guidelines give the closest predictions then comes ACI and ISIS guidelines and among all the guidelines CSA give the most conservative results as indicated in the figure 5-10 and figure 5-11.

The comparison of strength increments of confined specimens obtained from experimental results and predicted by theoretical guidelines is shown in figures 5-12, 5-13 and 5-14 for 30, 42 and 64 MPa respectively.

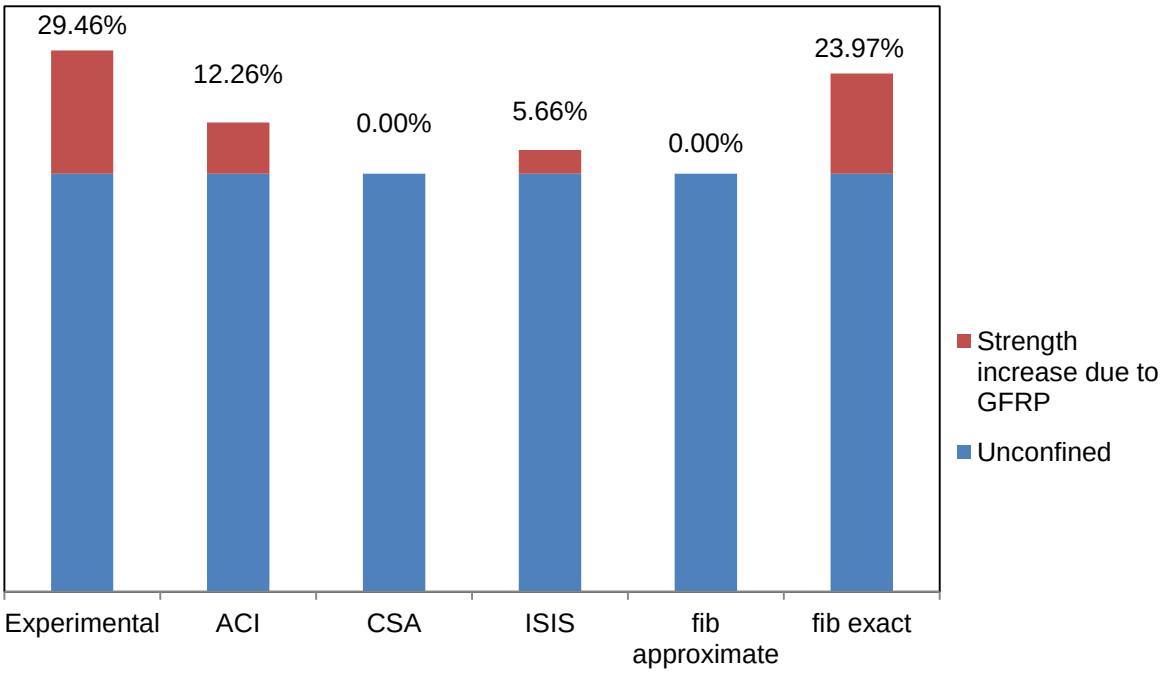

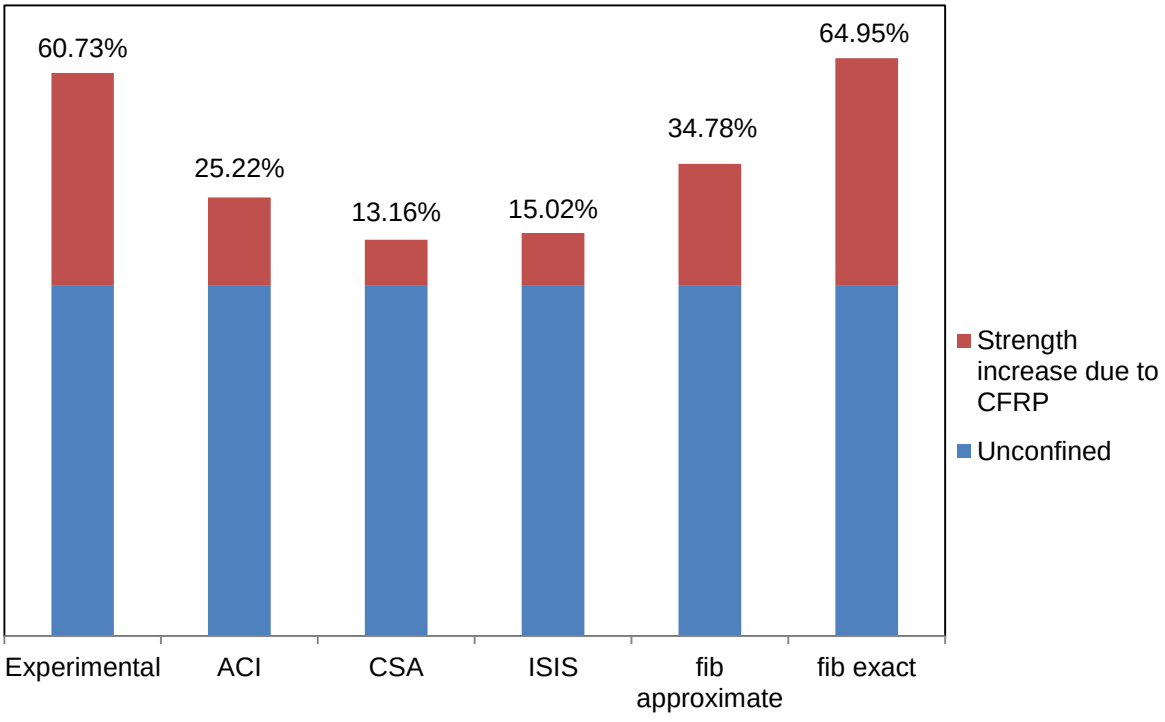

Figure 5-12 Comparison of theoretical and experimental results for 30 MPa concrete specimens.

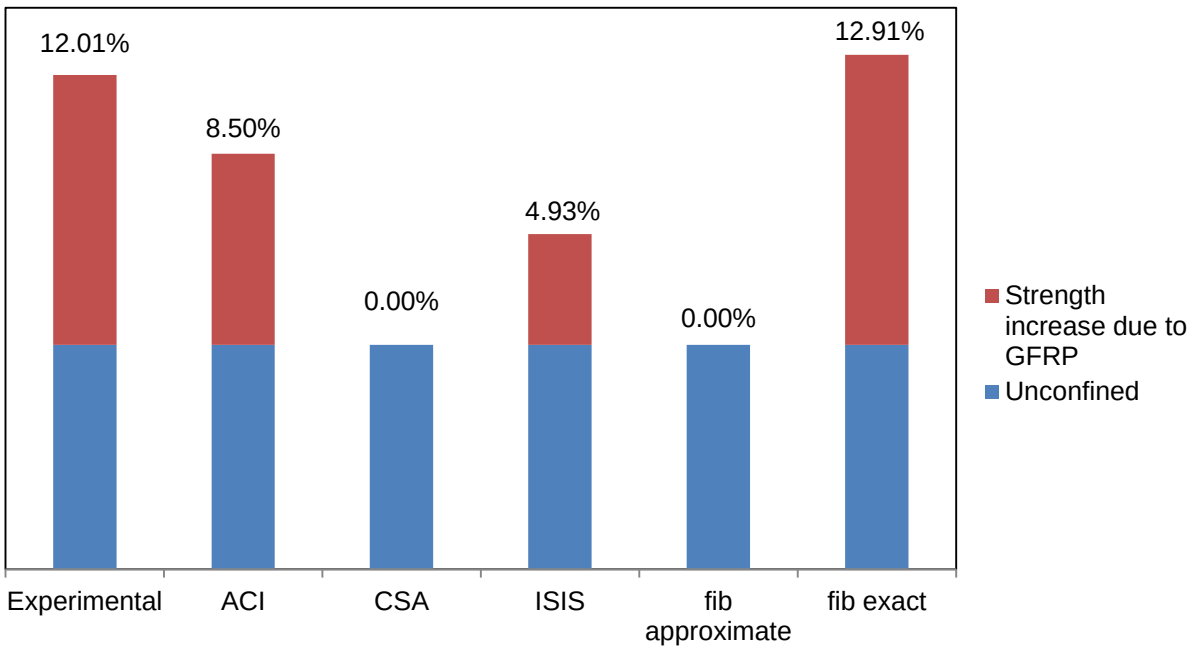

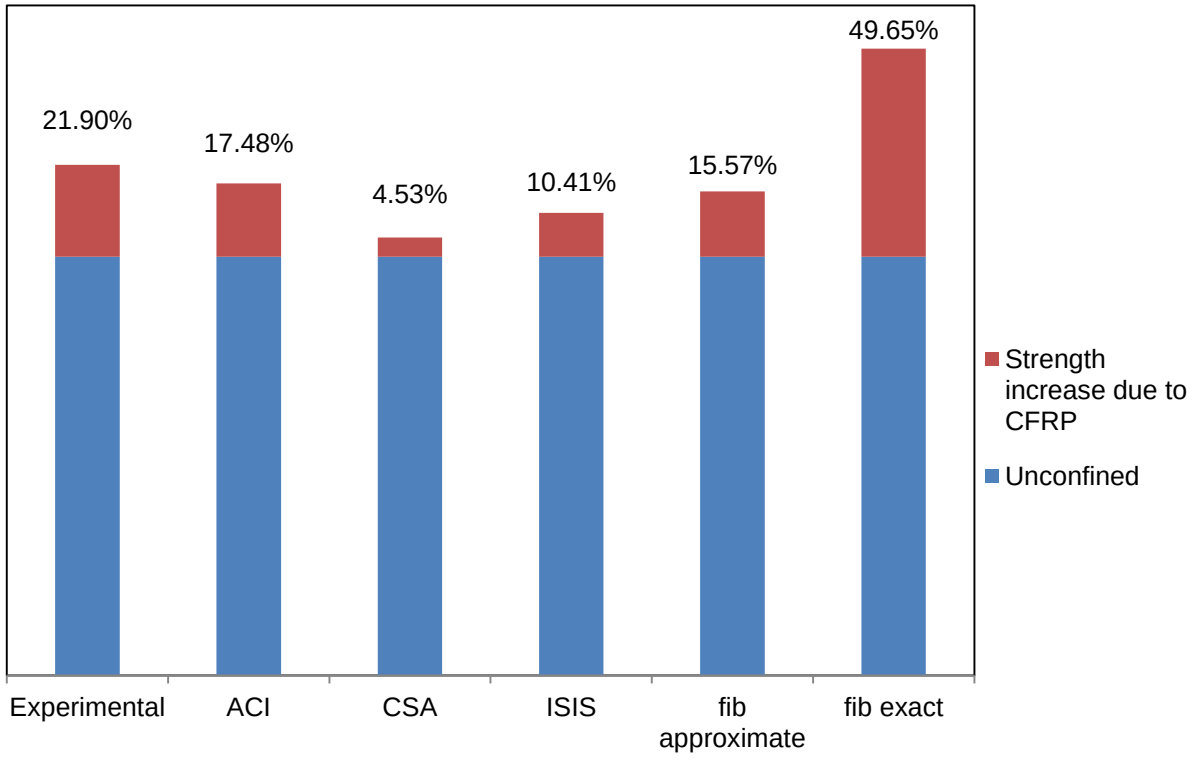

Figure 5-13 Comparison of theoretical and experimental results for 42 MPa concrete specimens.

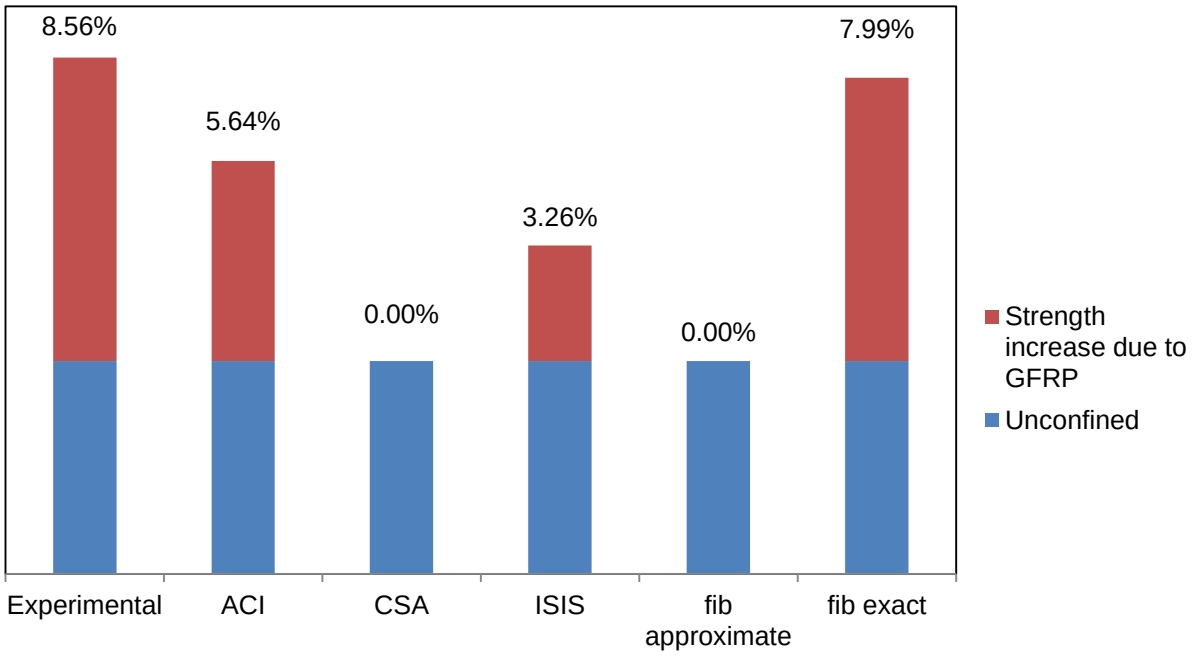

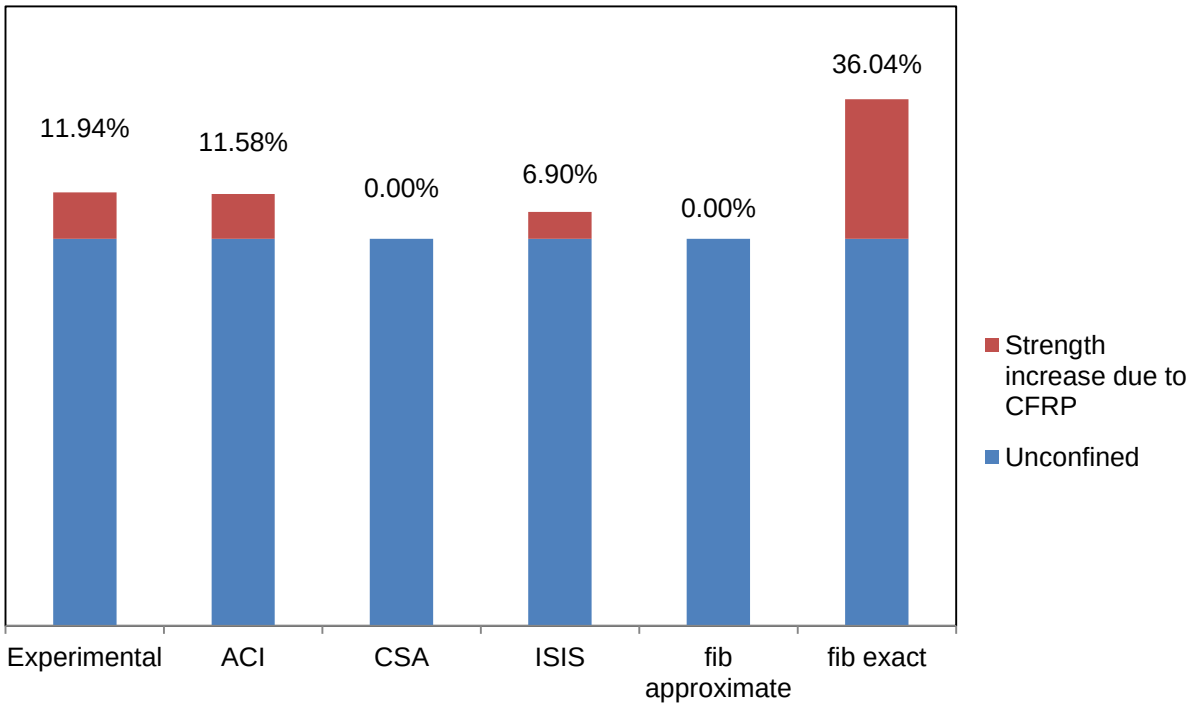

Figure 5-14 Comparison of theoretical and experimental results for 64 MPa concrete specimens.

5.3.3 Ultimate Load Carrying Capacity

5.3.3.1 American Concrete Institute (ACI Committee-440-2R-2008)

Table 5-6 Comparison of ACI model with experimental results for ultimate load carrying capacities of specimens.

Confinement	Unconfined strengths (MPa)	Experimental Load carrying capacity	ACI Load carrying capacity	
		Pu	***Pu***	Pu_{exp} **to** Pu_{ACI}
		kN	**kN**	
GFRP	29.7	699.79	517	1.35
	42.84	873.36	720.7	1.21
	64.67	1277.70	1059.2	1.21
CFRP	29.7	868.81	576.6	1.51
	42.84	950.40	780.38	1.22
	64.67	1317.56	1177	1.12

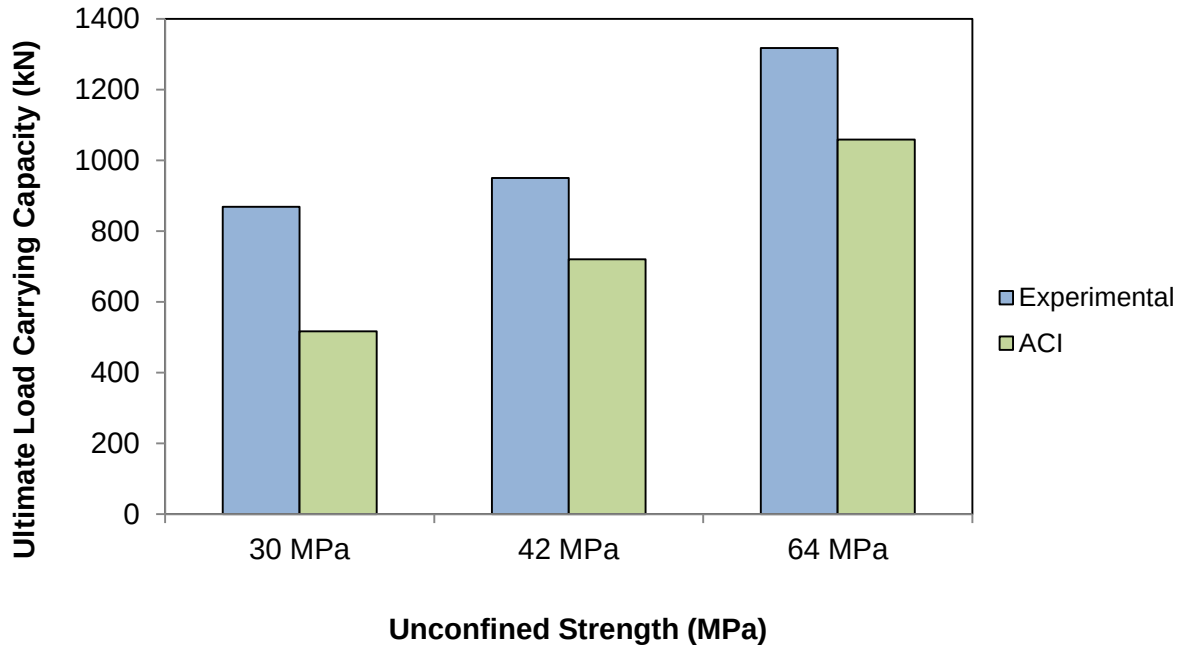

Figure 5-15 Theoretical ultimate load carrying capacity according to ACI model on GFRP confined specimens.

The experimental load carrying capacities are 1.21 to 1.35 times than that predicted by ACI for GFRP confined specimens and are 1.12 to 1.51 times for CFRP confined specimens as

shown in table 5-6. The predictions get closer to actual results at higher strengths of unconfined concrete as shown in figure 5-15 and 5-16.

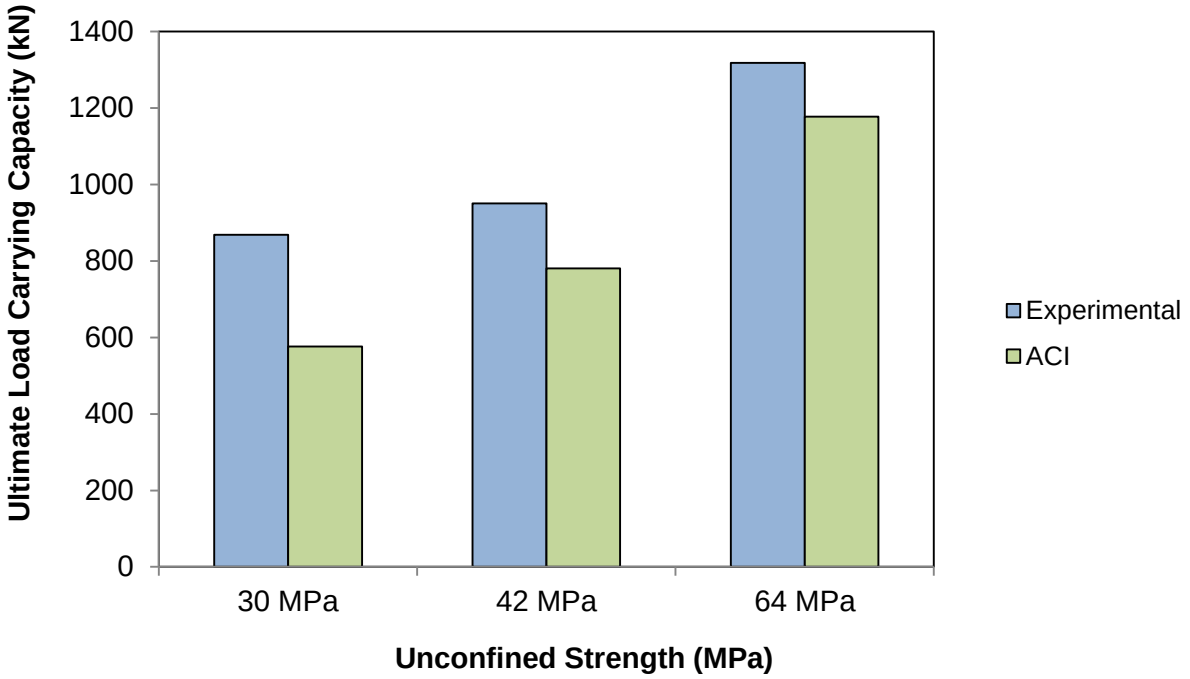

Figure 5-16 Theoretical ultimate load carrying capacity according to ACI model on CFRP confined specimens.

5.3.3.2 CSA-S806-02

Table 5-7 Comparison of CSA model with experimental results for ultimate load carrying capacities of specimens.

Confinement	Unconfined strengths MPa	Experimental Load carrying capacity	CSA Load carrying capacity	
		Pu	***Pu***	Pu_{exp} **to** Pu_{CSA}
		kN	**kN**	
GFRP	29.7	699.79	430.6	1.63
	42.84	873.36	605.87	1.44
	64.67	1277.70	876.53	1.46
CFRP	29.7	868.81	493	1.76
	42.84	950.40	641.83	1.48
	64.67	1317.56	876.53	1.50

The experimental load carrying capacities are 1.46 to 1.63 times than that predicted by CSA for GFRP confined specimens and are 1.50 to 1.76 times for CFRP confined specimens as

tabulated in table 5-7. The predictions get closer to actual results at higher strengths of unconfined concrete but they are still conservative as compared to the predictions given by ACI guidelines as shown in figure 5-17 and 5-18.

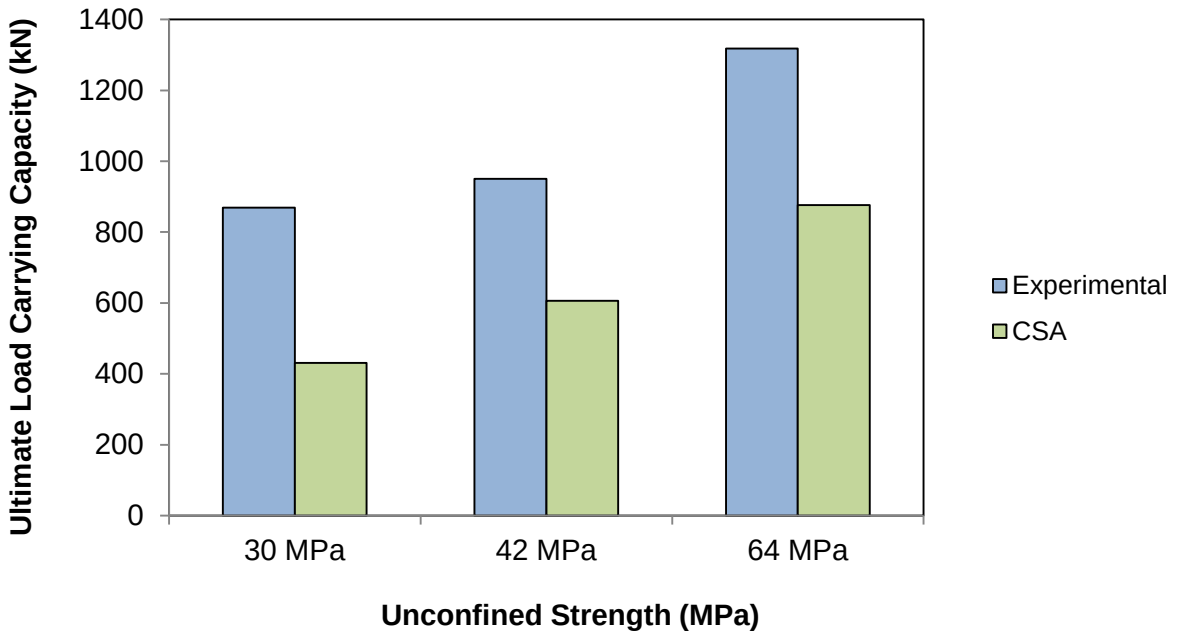

Figure 5-17 Theoretical ultimate load carrying capacity according to CSA model on GFRP confined specimens.

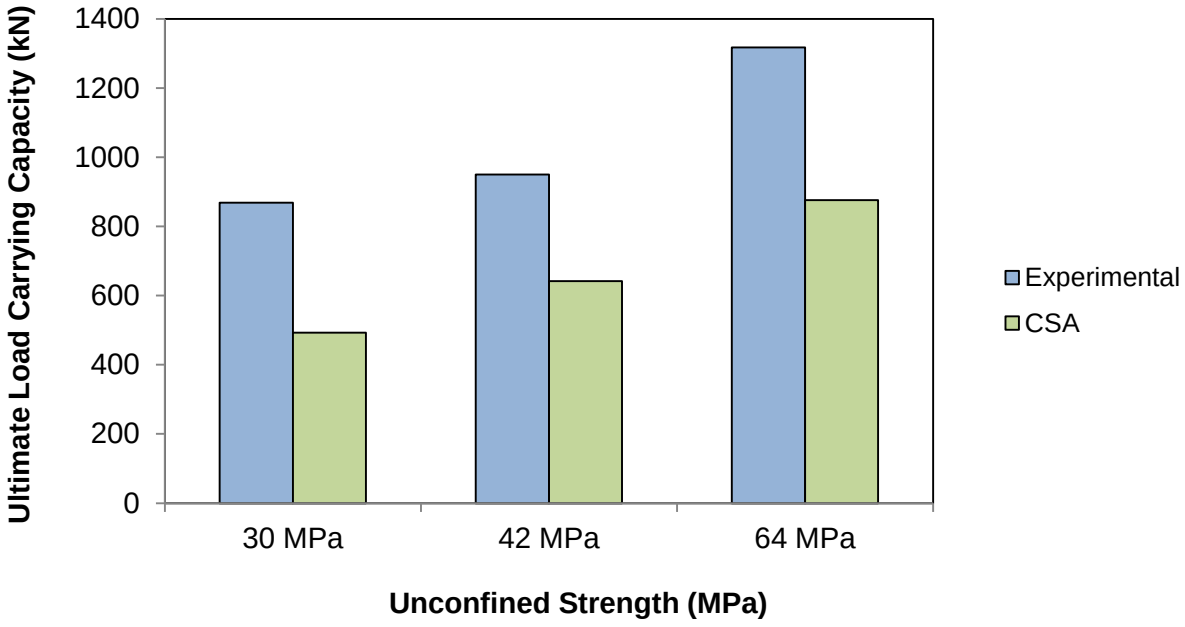

Figure 5-18 Theoretical ultimate load carrying capacity according to CSA model on CFRP confined specimens.

5.3.3.3 Intelligent Sensing for Innovative Structures (ISIS M04-2001)

Table 5-8 Comparison of ISIS model with experimental ultimate load carrying capacities of specimens.

Confinement	Unconfined strengths (MPa)	Experimental Load carrying capacity	ISIS Load carrying capacity	
		Pu	***Pu***	Pu_{exp} **to** Pu_{ISIS}
		kN	**kN**	
GFRP	29.7	699.79	456	1.53
	42.84	873.36	635.74	1.37
	64.67	1277.70	905.13	1.41
CFRP	29.7	868.81	495.25	1.75
	42.84	950.40	669	1.42
	64.67	1317.56	937	1.41

The experimental load carrying capacities are 1.41 to 1.53 times than that predicted by ISIS for GFRP confined specimens and are 1.41 to 1.75 times for CFRP confined specimens as tabulated in table 5-8. The predictions get closer to actual results at higher strengths of unconfined concrete but they are still conservative as compared to the predictions given by ACI guidelines more accurate than CSA guidelines as shown in figure 5-19 and 5-20.

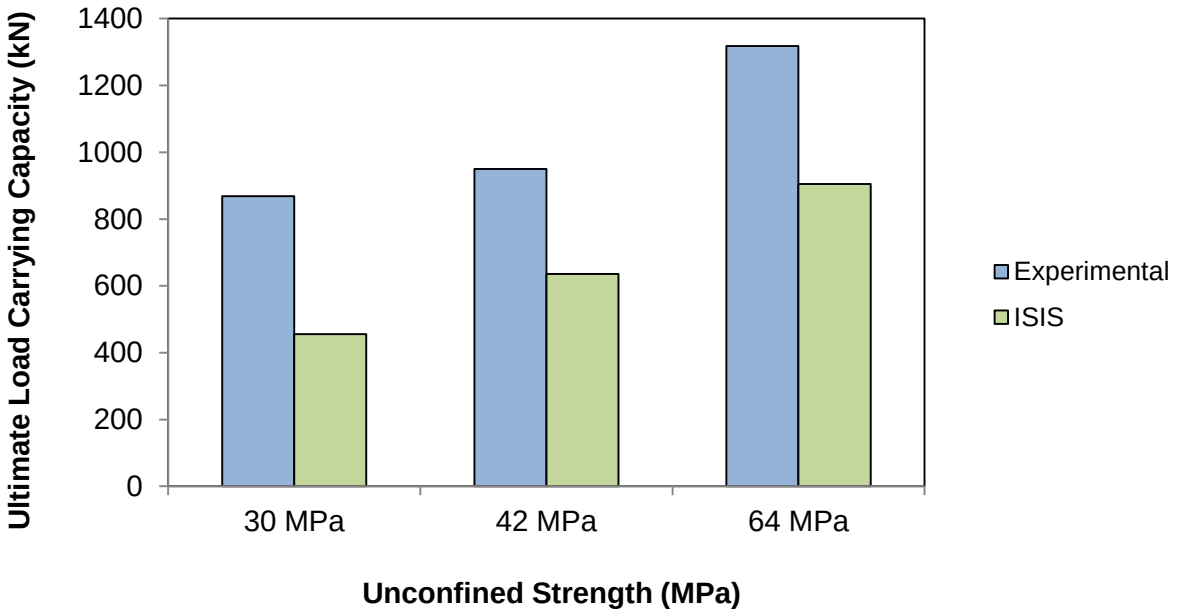

Figure 5-19 Theoretical ultimate load carrying capacity according to ISIS model on GFRP confined specimens.

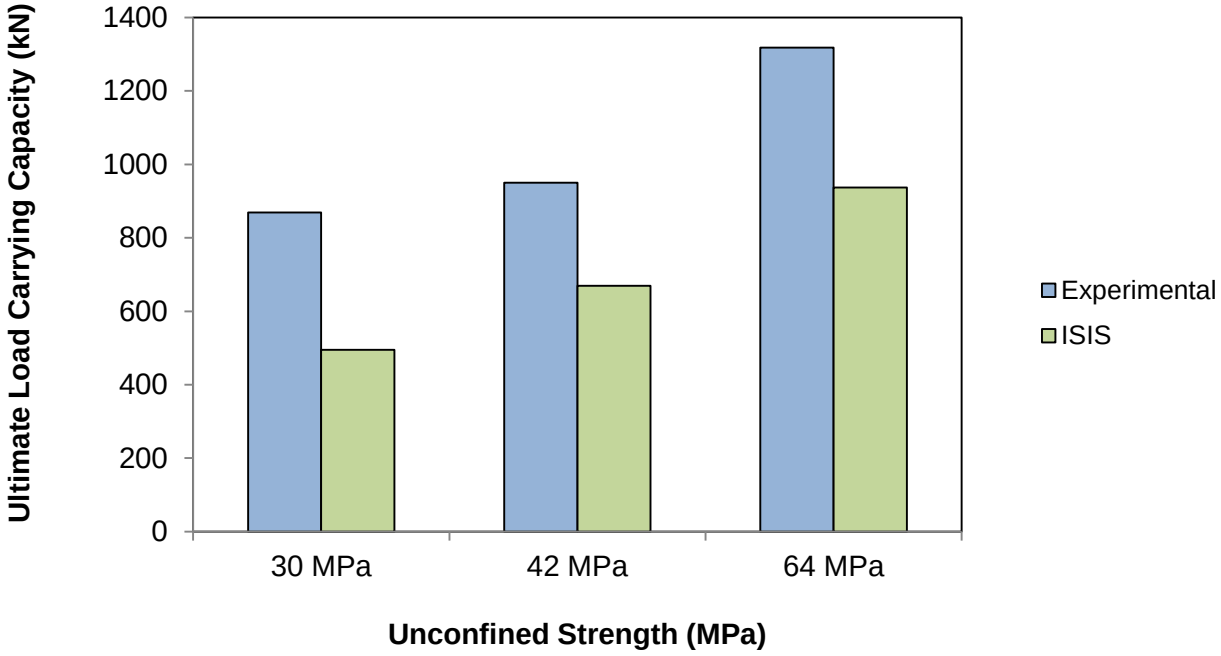

Figure 5-20 Theoretical ultimate load carrying capacity according to ISIS model on CFRP confined specimens.

5.3.3.4 CEB/FIP Model Code 2010 (*fib* bulletin 14)

Table 5-9 Comparison of CEB/FIP model code with experimental ultimate load carrying capacities of specimens.

Confinement	**Unconfined strengths (MPa)**	**Experimental**	***fib* approximate Load carrying capacity**		***fib* exact Load carrying capacity**	
		Pu	***Pu***	Pu_{exp} **to** $Pu_{fib\ a}$	***Pu***	Pu_{exp} **to** $Pu_{fib\ e}$
		kN	**kN**		**kN**	
GFRP	29.7	699.79	420.63	1.66	536.09	1.31
	42.84	873.36	526.02	1.66	704.26	1.24
	64.67	1277.70	681.34	1.88	1016.87	1.26
CFRP	29.7	868.81	584.16	1.49	713.3	1.22
	42.84	950.40	720.96	1.32	933.44	1.02
	64.67	1317.56	920.85	1.43	1280.93	1.03

The experimental load carrying capacities are 1.66 to 1.88 times than that predicted by *fib* approximate method for GFRP confined specimens and are 1.32 to 1.49 times for CFRP confined specimens as tabulated in table 5-9. Similarly, the experimental load carrying

capacities are 1.24 to 1.31 times than that predicted by *fib* exact method for GFRP confined specimens and are 1.02 to 1.22 times for CFRP confined specimens. The predictions get closer to actual results at higher strengths of unconfined concrete.

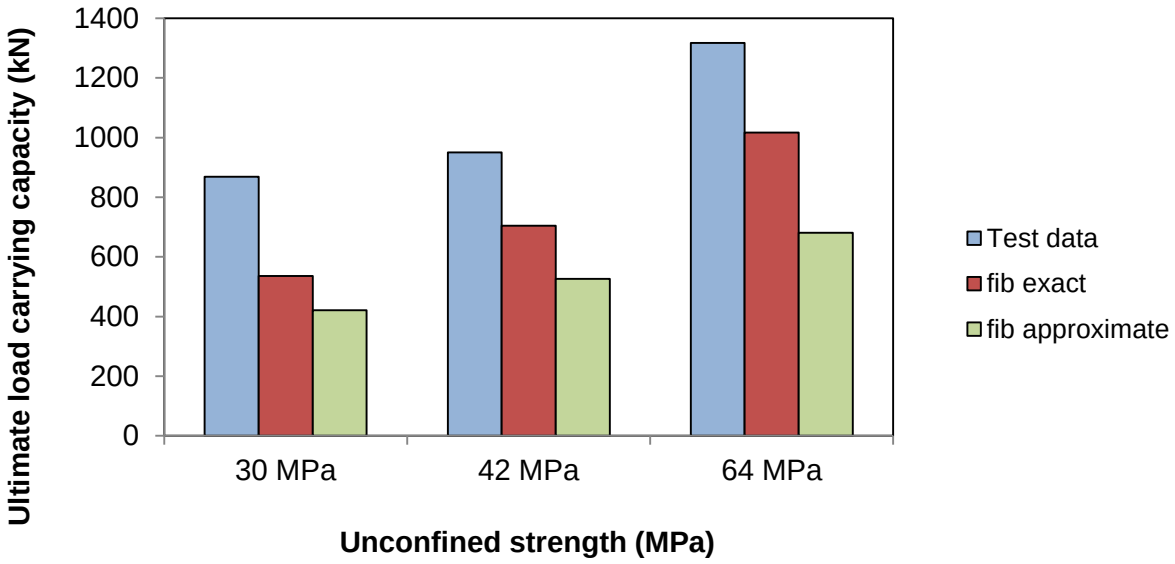

Figure 5-21 Theoretical ultimate load carrying capacity according to fib on GFRP confined specimens.

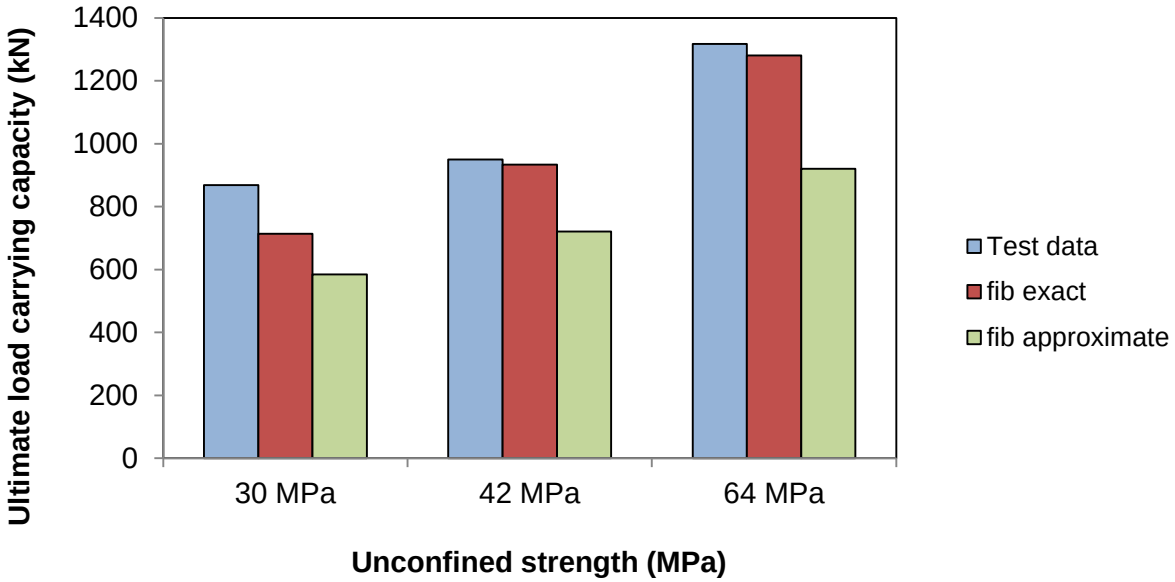

Figure 5-22 Theoretical ultimate load carrying capacity according to fib on CFRP confined specimens.

5.3.3.4 Comparison of all Theoretical Load Carrying Capacities with Actual Load Carrying Capacities.

Table 5-10 Comparison of all analytical models with experimental specimens for ultimate load carrying capacities.

Confinement	Unconfined strengths (MPa)	Experimental	ACI	CSA	ISIS	*fib approx*	*fib* exact
		Pu	***Pu***	***Pu***	***Pu***	***Pu***	***Pu***
		kN	**kN**	**kN**	**kN**	**kN**	**kN**
GFRP	29.7	699.79	517	430.6	456	420.63	536.09
	42.84	873.36	720.7	605.87	635.74	526.02	704.26
	64.67	1277.70	1059.2	876.53	905.13	681.34	1016.87
CFRP	29.7	868.81	576.6	493	495.25	584.16	713.3
	42.84	950.40	780.38	641.83	669	720.96	933.44
	64.67	1317.56	1177	876.53	937	920.85	1280.93

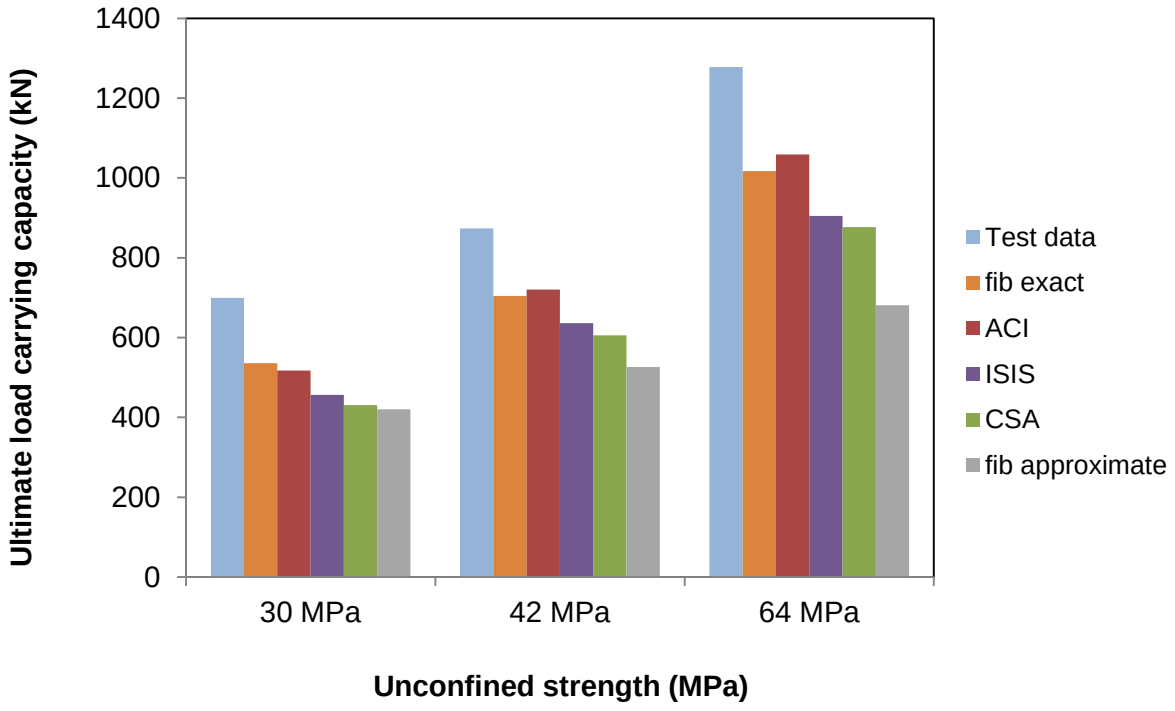

Figure 5-23 Comparison of analytical and experimental load carrying capacities of specimens wrapped with GFRP

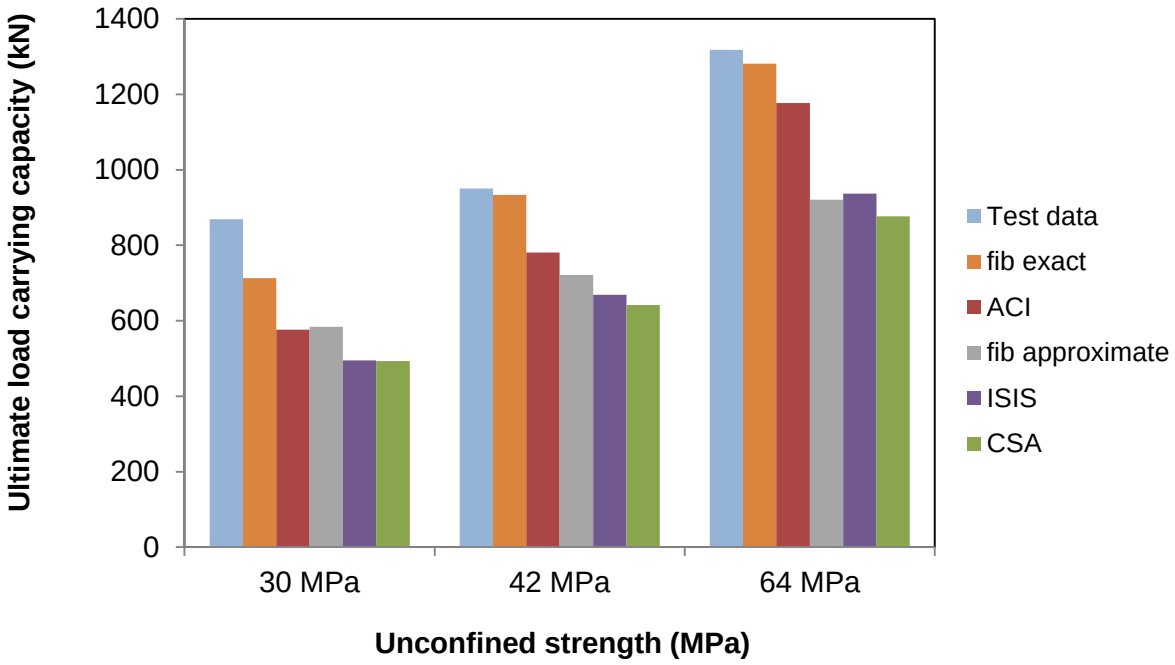

Figure 5-24 Comparison of analytical and experimental load carrying capacities of specimens wrapped with CFRP.

Table 5-10 shows that all the guidelines give conservative predictions but the predictions get closer to actual results at higher strengths of unconfined concrete. *fib* exact method gives the closest predictions CFRP as compared to other FRP confined concrete design guidelines. ACI gives the better predictions as compared to *fib* exact method in case of GFRP confinement. Among all the guidelines, *fib* approximate method gives the most conservative results in case of GFRP confinement while CSA gives the most conservative results in case of CFRP confinement as confirmed in a comparative study of models (Chaallal et al. 2006).

5.4 Summary

The analytical models used to calculate the strengths show conservative results. Among the analytical models, *fib* exact method has shown closest results in normal strength domains for both GFRP and CFRP confinement but it overestimates the CFRP confinement for high strength concrete. ACI guidelines give good predictions but they are conservative as compared to *fib* exact method. After ACI, comes ISIS model and then CSA and *fib*

approximate method show the most conservative strength values both for Axial Compressive strength as well as Ultimate Load Carrying Capacity. Moreover it has been observed that *fib* approximate method and CSA guidelines are not valid for GFRP confinement as *fib* approximate method is developed for FRPs that provide high confining pressure whereas CSA uses a factor of safety of 0.85 which mean 15% strength is reduced from unconfined strength and then confining strength is added to calculate the theoretical confined strength which in case of GFRP comes less than 15% of the unconfined strength. It is not appropriate to say that the theoretical confined strength is less than the unconfined strength therefore confined strength obtained by using *fib* approximate method and CSA guidelines is taken equal to the unconfined strength of the concrete specimens.

CHAPTER 6

6 CONCLUSIONS AND RECOMMENDATIONS

6.1 General

The present study compares the effectiveness of GFRP and CFRP for normal and high strength concrete. The effects of confinement have been studied with respect to the type of FRP used and the cylinder strength (f'_c). While studying the behavior of concrete cylinders under compression, various aspects have been compared which include the axial compressive strength, the ultimate load carrying capacity, stiffness, the longitudinal and hoop strains and the ductility. While studying ductility the energy absorption and the deformability factors were calculated and compared. The results obtained from the experimental work are compared with four different analytical confinement models to evaluate the performance of actual work. This comparison also identifies the most and least conservative confinement models for the prediction of axial compressive strength and the ultimate load carrying capacity of circular cylinders.

6.2 Conclusions

The conclusions derived from this research are as follows.

- The axial compressive strength of the concrete specimens is increased by confining them with FRPs. The specimens wrapped with CFRP show higher improvement in confined compressive strength from 12 to 60.75% whereas GFRP confined specimens show 8.56 to 29.47% increase in compressive strength.
- Effectiveness of FRP confinement reduces with increase in unconfined strength of substrate concrete.

- The increase in longitudinal (axial) strain in CFRP confined concrete is 1.99 to 2.22 times higher than GFRP confined concrete, whereas hoop strain in CFRP confined concrete is 1.08 to 2.04 times higher than that of GFRP confined concrete in 30 to 64 MPa unconfined concrete strengths. Both FRP confinements enhance the hoop strain far more than longitudinal strain but this enhancement effect reduces with increase in unconfined strength of concrete.
- Stiffness of FRP confined concrete is also affected by unconfined strength of concrete as it reduces by increase in unconfined concrete strength and vice versa.
- The increase in total energy absorption is more pronounced in CFRP confined concrete as compared to GFRP confined concrete; however this increment in total energy absorption reduces with an increase in the unconfined strength of concrete.
- The American Concrete Institute ACI 440.2R 2008, the Canadian Standard Association (CSA- S806 02), Intelligent Sensing for Innovative Structures Canada (ISIS M04 2001) and *fib* approximate method guidelines show conservative predictions of confined compressive strength of the concrete, however the predictions from these guidelines give closer confined strength results with increase in the unconfined concrete strength.
- Among all FRP design codes and guidelines, *fib* exact guidelines give the closest predictions for both FRPs, however it overestimates the strength of CFRP confined concrete with increase in unconfined concrete strength.
- ACI 440.2R 2008 gives conservative results as compared to *fib* exact guidelines and is less affected by strength of unconfined concrete.
- CSA-S806-02 guidelines show the most conservative results. This is attributed to the safety factor of 0.85 used by CSA-S806-02 for reduction of unconfined concrete strength which leads to underestimation of effectiveness of CFRP.

- For GFRP confinement, CSA-S806-02 and *fib* approximate guidelines give lower strength of the confined specimens than the unconfined specimens.

6.3 Recommendations for Future Work

Following recommendations are proposed from this study:

- Complete stress-stain curves with post peak response should be experimentally investigated with strain controlled test equipment to understand the ultimate confinement behaviour of Carbon and Glass fiber reinforced polymers.
- The effect of FRP confinement on low strength concrete of 3000 psi and less should be investigated.
- FRP confined high performance concrete columns should be tested and validated with confinement models.
- Comparative parametric study for aramid fibre reinforced polymer should be carried out and correlated with carbon fiber reinforced polymer and glass fiber reinforced polymer confinement.
- Actual seismic and fire destroyed concrete specimens should be tested/investigated for strength/confinement enhancement with different aramid fibre reinforced polymers.

7 REFERENCES

1. ACI 440.2 (2002). "Guide for the design and construction of externally bonded FRP systems for strengthening concrete structures." *American Concrete Institute, Farmington Hills, USA*.
2. Benzaid, R., and Mesbah, H.-A. (2013). "Circular and Square Concrete Columns Externally Confined by CFRP Composite: Experimental Investigation and Effective Strength Models."
3. Bisby, L., Take, W. A., and Caspary, A. (2007). "Effects of Unconfined Concrete Strength on FRP Confinement of Concrete." *International Institute for FRP in Construction*.
4. Chaallal, O., Hassan, M., and LeBlanc, M. (2006). "Circular columns confined with FRP: Experimental versus predictions of models and guidelines." *Journal of composites for Construction*, 10(1), 4-12.
5. CSA S806-02 (2002). "Design and construction of building components with fibre-reinforced polymers." *Canadian Standards Association*.
6. fib (2001). "Fédération internationale du Béton :Externally bonded FRP reinforcement for RC structures." *Bulletin No. 14, Technical Report*, Lausanne, Switzerland.
7. ISIS M04-01 (2001). "Externally Bonded FRP for Strengthening Reinforced Concrete Structures." *The Canadian Network of Centres of Excellence on Intelligent Sensing for Innovative Structures, Winnipeg, MB, Canada*.
8. Karabinis, A., and Rousakis, T. (2002). "Concrete confined by FRP material: a plasticity approach." *Engineering structures*, 24(7), 923-932.
9. Khaliq, W. (2012). "Performance characterization of high performance concretes under fire conditions." *PhD Dissertation*, Michigan State University, East Lansing, MI, 345.
10. Khaliq, W., and Kodur, V. (2011). "Thermal and mechanical properties of fiber reinforced high performance self-consolidating concrete at elevated temperatures." *Cement and Concrete Research*, 41(11), 1112-1122.
11. Lam, L., and Teng, J. (2003). "Design-oriented stress–strain model for FRP-confined concrete." *Construction and Building Materials*, 17(6), 471-489.

12. Li, G., Maricherla, D., Singh, K., Pang, S.-S., and John, M. (2006). "Effect of fiber orientation on the structural behavior of FRP wrapped concrete cylinders." *Composite structures*, 74(4), 475-483.
13. Matthys, S., Taerwe, L., and Audenaert, K. (1999). "Tests on axially loaded concrete columns confined by fiber reinforced polymer sheet wrapping." *ACI Special Publication*, 188.
14. Mirmiran, A., and Shahawy, M. (1997). "Behavior of concrete columns confined by fiber composites." *Journal of Structural Engineering*, 123(5), 583-590.
15. Nanni, A., Di Ludovico, M., and Parretti, R. (2004). "Shear strengthening of a PC bridge girder with NSM CFRP rectangular bars." *Advances in Structural Engineering*, 7(4), 297-309.
16. Nanni, A., Norris, M., and Bradford, N. (1993). "Lateral confinement of concrete using FRP reinforcement." *ACI Special Publication*, 138.
17. Parretti, R., and Nanni, A. "Axial testing of concrete columns confined with carbon FRP: Effect of fiber orientation." *Proc., CD Proc. of the third international conference on composites in infrastructure*.
18. Parretti, R., and Nanni, A. (2004). "Strengthening of RC members using near-surface mounted FRP composites: design overview." *Advances in Structural Engineering*, 7(6), 469-483.
19. Parvin, A., and Jamwal, A. S. (2005). "Effects of wrap thickness and ply configuration on composite-confined concrete cylinders." *Composite structures*, 67(4), 437-442.
20. Parvin, A., and Jamwal, A. S. (2006). "Performance of externally FRP reinforced columns for changes in angle and thickness of the wrap and concrete strength." *Composite structures*, 73(4), 451-457.
21. Pessiki, S., Harries, K. A., Kestner, J. T., Sause, R., and Ricles, J. M. (2001). "Axial behavior of reinforced concrete columns confined with FRP jackets." *Journal of composites for Construction*, 5(4), 237-245.
22. Picher, F., Rochette, P., and Labossiere, P. "Confinement of concrete cylinders with CFRP." *Proc., Proceedings of the First International Conference Composites in Infrastructure, Tucson, AZ*, 903.
23. Rahai, A., Sadeghian, P., and Ehsani, M. "Experimental Behavior of Concrete Cylinders Confined with CFRP Composites." *Proc., The 14th World Conference on Earthquake Engineering*, 12-17.

24. Rochette, P., and Labossiere, P. (2000). "Axial testing of rectangular column models confined with composites." *Journal of composites for Construction*, 4(3), 129-136.
25. Samaan, M., Mirmiran, A., and Shahawy, M. (1998). "Model of concrete confined by fiber composites." *Journal of Structural Engineering*, 124(9), 1025-1031.
26. Seible, F., Priestley, M. N., Hegemier, G. A., and Innamorato, D. (1997). "Seismic retrofit of RC columns with continuous carbon fiber jackets." *Journal of composites for Construction*, 1(2), 52-62.
27. Spoelstra, M. R., and Monti, G. (1999). "FRP-confined concrete model." *Journal of composites for Construction*, 3(3), 143-150.
28. Teng, J., Huang, Y., Lam, L., and Ye, L. (2007). "Theoretical model for fiber-reinforced polymer-confined concrete." *Journal of composites for Construction*, 11(2), 201-210.
29. Teng, J., and Lam, L. (2004). "Behavior and modeling of fiber reinforced polymer-confined concrete." *Journal of Structural Engineering*, 130(11), 1713-1723.
30. Wu, G., Lü, Z., and Wu, Z. (2006). "Strength and ductility of concrete cylinders confined with FRP composites." *Construction and Building Materials*, 20(3), 134-148.

APPENDIX A

CALCULATIONS BASED ON ANALYTICAL MODELS

A-1 Confined Compressive Strength and Ultimate Axial Load Carrying Capacity Using ACI Code 440.2R-08

$$P_u = 0.85 f'_{cc}(A_g - A_{st}) + f_y A_{st}$$

$$f'_{cc} = f'_c + 3.3 k_a \Psi_f f_l$$

$$f_l = \frac{2 \in_{fe} E_f n t_f}{D}$$

Where

P_u = Axial load carrying capacity
f'_{cc} = Compressive strength of confined concrete
A_g = Cross sectional area of the confined concrete
A_{st} = Longitudinal reinforcing steel area
f_y = Yield strength of longitudinal bars
Formula for confined strength is as follows
f'_c = Unconfined concrete compressive strength
f_l = Lateral confinement pressure

n = number of FRP layers
t_f = Thickness of FRP layer
E_f = Modulus of Elasticity of FRP
ε_{fe} = FRP effective strain
ε_{fe} = FRP effective strain = $k_e \varepsilon_{fu}$
$k_e = 0.55$
Ψ_f = FRP strength reduction factor = 0.95

k_a=k_b=1 (for circular cylinders)
Tabulating values from the supplier

A-1.1 For CFRP Sika Wrap Hex 230

$\in_{fe}$ = 0.55(0.0133) = 0.00731
E_f = 65402 MPa
n = 1

$t_f = 0.381\text{mm}$

$D = 152.4\text{mm}$

$k_a = 1$

Tabulating confined concrete cylinder strengths wrapped with CFRP

Solving for 30 MPa strength

$f'_c = 29.7\,\text{MPa}$

$$f_l = \frac{2(65402)(1)(0.381)(0.00731)}{152.4}$$

$f_l = 2.39\,\text{MPa}$

$f'_{cc} = 29.7 + 3.3(1)(0.95)(2.39)$

$f'_{cc} = 37.19\,\text{MPa}$

$P_u = 0.85 f'_{cc} A_c + A_{st} f_y$

$= 0.85(37.19)(0.018)\text{x}10^3\ \text{kN}$

$= 576.6\,\text{kN}$

Solving for 42 MPa strength

$f'_c = 42.84\,\text{MPa}$

$$f_l = \frac{2(65402)(1)(0.381)(0.00731)}{152.4}$$

$f_l = 2.39\,\text{MPa}$

$f'_{cc} = 42.84 + 3.3(1)(0.95)(2.39)$

$f'_{cc} = 50.33\,\text{MPa}$

$P_u = 0.85 f'_{cc} A_c + A_{st} f_y$

$= 0.85(50.33)(0.018)\text{x}10^3\ \text{kN}$

$= 780.38\,\text{kN}$

Solving for 64 MPa strength

$f'_c = 64.67\,\text{MPa}$

$$f_l = \frac{2(65402)(1)(0.381)(0.00731)}{152.4}$$

$$f_l = 2.39\,\text{MPa}$$

$$f'_{cc} = 29.7 + 3.3(1)(0.95)(2.39)$$

$$f'_{cc} = 72.16\,\text{MPa}$$

$$P_u = 0.85 f'_{cc} A_c + A_{st} f_y$$
$$= 0.85(72.16)(0.018)\text{x}10^3 \text{ kN}$$
$$= 1118.86\,\text{kN}$$

A-1.2 For GFRP Sika Wrap Hex 106G

$\in_{fe} = 0.55(0.0143) = 0.007865$
$E_f = 16215\,\text{MPa}$
$n = 2$
$t_f = 0.33\,\text{mm}$
$D = 152.4\,\text{mm}$
$k_a = 1$
Tabulating confined concrete cylinder strengths wrapped with GFRP

Solving for 30 MPa strength

$$f'_c = 29.7\,\text{MPa}$$

$$f_l = \frac{2(16215)(2)(0.33)(0.007865)}{152.4}$$

$$f_l = 1.1046\,\text{MPa}$$

$$f'_{cc} = 29.7 + 3.3(1)(0.95)(1.1046)$$

$$f'_{cc} = 33.34\,\text{MPa}$$

$$P_u = 0.85 f'_{cc} A_c + A_{st} f_y$$
$$= 0.85(33.34)(0.018)\text{x}10^3 \text{ kN}$$
$$= 517\,\text{kN}$$

Solving for 42 MPa strength

$$f_c' = 42.84\,\text{MPa}$$

$$f_l = \frac{2(16215)(2)(0.33)(0.007865)}{152.4}$$

$$f_l = 1.1046\,\text{MPa}$$

$$f_{cc}' = 42.84 + 3.3(1)(0.95)(1.1046)$$

$$f_{cc}' = 46.48\,\text{MPa}$$

$$P_u = 0.85 f_{cc}' A_c + A_{st} f_y$$
$$= 0.85(46.48)(0.018)\text{x}10^3\ \text{kN}$$
$$= 720.7\,\text{kN}$$

Solving for 64 MPa strength

$$f_c' = 64.67\,\text{MPa}$$

$$f_l = \frac{2(16215)(2)(0.33)(0.007865)}{152.4}$$

$$f_l = 1.1046\,\text{MPa}$$

$$f_{cc}' = 64.67 + 3.3(1)(0.95)(1.1046)$$

$$f_{cc}' = 68.32\,\text{MPa}$$

$$P_u = 0.85 f_{cc}' A_c + A_{st} f_y$$
$$= 0.85(68.32)(0.018)\text{x}10^3\ \text{kN}$$
$$= 1059.2\,\text{kN}$$

A-2 Confined compressive strength and ultimate axial load carrying capacity Using CSA S806-02

$$f_{cc}' = 0.85 f_c' + k_l k_s f_l$$

The factor k_l is also used by past researchers in their studies that can be solved by the following empirical relation

$$k_l = 6.7(f_l)^{-0.17}$$

Where k_s is the shape factor which is equal to 1 in circular cross sectional shapes. f_l can be calculated as:

$$f_l = \frac{2nt_f f_{frp}}{D}$$

f_{frp} will be least of the following values i.e., 0.004 E_f and 0.75* ultimate FRP strain.

A-2.1 For CFRP Sika Wrap Hex 230

CSA design guideline limits FRP strain to 0.004

$E_f = 65402\,\text{MPa}$

$n = 1$

$t_f = 0.381\,\text{mm}$

$D = 152\,\text{mm}$

Ultimate strength of FRP = f_{frp} = lesser of $0.004(65402)$ or $0.75(894)$

$f_{frp} = 261.608$

$k_1 = 6.7(k_s f_l)^{-0.17}$

$k_s = 1 \quad (\text{for circular section})$

$$f_l = \frac{2nt_f f_{frp}}{D}$$

$$f_l = \frac{2(1)(0.381)(261.608)}{152.4}$$

$f_l = 1.308$

$k_1 = 6.7(1.308)^{-0.17}$

$k_1 = 6.40$

Solving for 30 MPa strength

$f'_c = 29.7\,\text{MPa}$

$f'_{cc} = 0.85(29.7) + (6.40)(1)(1.308)$

$f'_{cc} = 33.61\,\text{MPa}$

$P_u = \alpha f'_{cc} A_c + A_{st} f_y$

$\alpha = 0.85 - 0.0015 f'_c$

$= 0.85 - 0.0015(29.7)$

$= 0.80545$

$P_u = 0.80545(33361)(0.018)\text{x}10^3\ \text{kN}$

$= 493\,\text{kN}$

Solving for 42 MPa strength

$f_c' = 42.84\,\text{MPa}$

$f_{cc}' = 0.85(42.48) + (6.40)(1)(1.308)$

$f_{cc}' = 44.78\,\text{MPa}$

$P_u = \alpha f_{cc}' A_c + A_{st} f_y$

$\alpha = 0.85 - 0.0015 f_c'$

$= 0.85 - 0.0015(42.84)$

$= 0.78574$

$P_u = 0.78574(4478)(0.018)\text{x}10^3\ \text{kN}$

$= 641.83\,\text{kN}$

Solving for 64 MPa strength

$f_c' = 64.67\,\text{MPa}$

$f_{cc}' = 0.85(64.67) + (6.40)(1)(1.308)$

$f_{cc}' = 63.34\,\text{MPa}$

As $f'_{cc} < f'_c$ therefore it can be stated that there is no confining strength according to CSA code

Hence $f'_{cc} = f'_c$

$P_u = \alpha f_{cc}' A_c + A_{st} f_y$

$\alpha = 0.85 - 0.0015 f_c^{'}$

$= 0.85 - 0.0015(64.67)$

$= 0.752995$

$P_u = 0.752995(64.67)(0.018)\text{x}10^3\ \text{kN}$

$= 876.53\,\text{kN}$

A-2.2 For GFRP Sika Wrap Hex 106G

CSA design guideline limits FRP strain to 0.004

$E_f = 16215\,\text{MPa}$

$n = 2$

$t_f = 0.33\,\text{mm}$

$D = 152\,\text{mm}$

Ultimate strength of FRP = f_{frp} = lesser of $0.004(16215)$ or $0.75(244)$

$$f_{frp} = 64.86\,\text{MPa}$$
$$k_1 = 6.7(k_s f_l)^{-0.17}$$
$$k_s = 1 \quad (\text{for circular section})$$

$$f_l = \frac{2nt_f f_{frp}}{D}$$
$$f_l = \frac{2(2)(0.33)(64.86)}{152.4}$$
$$f_l = 0.5618$$
$$k_1 = 6.7(0.5618)^{-0.17}$$
$$k_1 = 7.39$$

Solving for 30 MPa strength

$$f_c' = 29.7\,\text{MPa}$$
$$f_{cc}' = 0.85(29.7) + (7.39)(1)(0.5618)$$
$$f_{cc}' = 29.03\,\text{MPa}$$

As $f'_{cc} < f'_c$ therefore it can be stated that there is no confining strength according to CSA code

Hence $f'_{cc} = f'_c$

$$P_u = \alpha f_{cc}' A_c + A_{st} f_y$$
$$\alpha = 0.85 - 0.0015 f_c'$$
$$= 0.85 - 0.0015(29.7)$$
$$= 0.80545$$
$$P_u = 0.80545(29.7)(0.018) \times 10^3 \text{ kN}$$
$$= 430.59\,\text{kN}$$

Solving for 42 MPa strength

$$f_c' = 42.84\,\text{MPa}$$
$$f_{cc}' = 0.85(42.84) + (7.39)(1)(0.5618)$$
$$f_{cc}' = 40.56\,\text{MPa}$$

As $f'_{cc} < f'_c$ therefore it can be stated that there is no confining strength according to CSA code

Hence $f'_{cc} = f'_c$

$$P_u = \alpha f'_{cc} A_c + A_{st} f_y$$
$$\alpha = 0.85 - 0.0015 f'_c$$
$$= 0.85 - 0.0015(42.84)$$
$$= 0.78574$$
$$P_u = 0.78574(4284)(0.018)\text{x}10^3 \text{ kN}$$
$$= 605.87 \text{kN}$$

Solving for 64 MPa strength

$$f'_c = 64.67 \text{MPa}$$
$$f'_{cc} = 0.85(64.67) + (7.39)(1)(0.5618)$$
$$f'_{cc} = 59.12 \text{MPa}$$

As $f'_{cc} < f'_c$ therefore it can be stated that there is no confining strength according to CSA code

Hence $f'_{cc} = f'_c$

$$P_u = \alpha f'_{cc} A_c + A_{st} f_y$$
$$\alpha = 0.85 - 0.0015 f'_c$$
$$= 0.85 - 0.0015(64.67)$$
$$= 0.752995$$
$$P_u = 0.752995(64.67)(0.018)\text{x}10^3 \text{ kN}$$
$$= 876.53 \text{kN}$$

A-3 Confined compressive strength and ultimate axial load carrying capacity Using ISIS M04 2001

A-3.1 For CFRP Sika Wrap Hex 230

$$n = 1$$
$$t_f = 0.381 \text{mm}$$
$$\in_{fe} = 0.0133$$
$$E_f = 65402 \text{psi}$$

$$f_l = \frac{2N_b f_{frpu} t_{frp}}{D_g}$$

N_b = Number of layers of FRP

f_{frpu} = Ultimate strength of FRP = 894

t_{frp} = Thickness per layeof FRP = 0.381mm

D_g = Diameter of the member = 152.4 mm

α_{pr} = Performance Coefficient = 1

ω_w = Volumetric Strength ratio

$$\omega_w = \frac{f_l}{f_c'}$$

$$f_l = \frac{2(1)(894)(0.381)}{152.4}$$

$f_l = 4.46$ MPa

$f_{cc}' = f_c'(1+\alpha_{pr}\omega_w)$

Solving for 30 MPa strength

f'_c=29.7 MPa

$$\omega_w = \frac{4.46}{29.7}$$

$= 0.15$

$f_{cc}' = f_{c'}(1+\alpha_{pr}\omega_w)$

$f_{cc}' = 29.7(1+1*0.15)$

$= 34.16$ MPa

$P_u = \alpha f_{cc}' A_c + A_{st} f_y$

$\alpha = 0.85 - 0.0015 f_c'$

$= 0.85 - 0.0015(29.7)$

$= 0.80545$

$P_u = 0.80545(3416)(0.018)\text{x}10^3$ kN

$= 495.25$ kN

Solving for 42 MPa strength

$$\omega_w = \frac{4.46}{42.48}$$

$= 0.105$

$f_{cc}' = f_c'(1+\alpha_{pr}\omega_w)$

$f_{cc}' = 42.84(1+1*0.105)$

$= 47.3$ MPa

$$P_u = \alpha f'_{cc} A_c + A_{st} f_y$$
$$\alpha = 0.85 - 0.0015 f'_c$$
$$= 0.85 - 0.0015(42.84)$$
$$= 0.78574$$
$$P_u = 0.78574(47.3)(0.018) \text{x} 10^3 \text{ kN}$$
$$= 668.98 \text{kN}$$

Solving for 64 MPa strength

$$\omega_w = \frac{4.46}{64.67}$$
$$= 0.0689$$
$$f'_{cc} = f'_c(1 + \alpha_{pr} \omega_w)$$
$$f'_{cc} = 64.67(1 + 1 * 0.0689)$$
$$= 69.13 \text{MPa}$$

$$P_u = \alpha f'_{cc} A_c + A_{st} f_y$$
$$\alpha = 0.85 - 0.0015 f'_c$$
$$= 0.85 - 0.0015(64.67)$$
$$= 0.752995$$
$$P_u = 0.752995(69.13)(0.018) \text{x} 10^3 \text{ kN}$$
$$= 936.98 \text{kN}$$

A-3.2 For GFRP Sika Wrap Hex 106G

$$N_b = 2$$
$$t_f = 0.33 \text{mm}$$
$$E_f = 16215 \text{MPa}$$

$$f_l = \frac{2 N_b f_{frpu} t_{frp}}{D_g}$$
$$N_b = \text{Number of layers of FRP}$$
$$f_{frpu} = \text{Ultimate strength of FRP} = 244$$
$$t_{frp} = \text{Thickness per layeof FRP} = 0.33 \text{mm}$$
$$D_g = \text{Diameter of the member} = 152.4 \text{mm}$$
$$\alpha_{pr} = \text{Performance Coefficient} = 1$$
$$\omega_w = \text{Volumetric Strength ratio}$$

$$\omega_w = \frac{f_l}{f_c'}$$

$$f_l = \frac{2(2)(244)(0.33)}{152.4}$$

$$f_l = 2.113\,\text{MPa}$$

$$f_{cc}' = f_c'(1+\alpha_{pc}\omega_w)$$

Solving for 30 MPa strength

f'_c=29.7 MPa

$$\omega_w = \frac{2.113}{29.7}$$

$$= 0.071$$

$$f_{cc}' = f_c'(1+\alpha_{pr}\omega_w)$$

$$f_{cc}' = 29.7(1+1*0.071)$$

$$= 31.38\,\text{MPa}$$

$$P_u = \alpha f_{cc}' A_c + A_{st} f_y$$

$$\alpha = 0.85 - 0.0015 f_c'$$

$$= 0.85 - 0.0015(29.7)$$

$$= 0.80545$$

$$P_u = 0.80545(3138)(0.018)\text{x}10^3\ \text{kN}$$

$$= 454.95\,\text{kN}$$

Solving for 42 MPa strength

$$\omega_w = \frac{2.113}{42.48}$$

$$= 0.0497$$

$$f_{cc}' = f_{c'}(1+\alpha_{pr}\omega_w)$$

$$f_{cc}' = 42.84(1+1*0.0497)$$

$$= 44.95\,\text{MPa}$$

$$P_u = \alpha f_{cc}' A_c + A_{st} f_y$$

$$\alpha = 0.85 - 0.0015 f_c'$$

$$= 0.85 - 0.0015(42.84)$$

$$= 0.78574$$

$$P_u = 0.78574(4495)(0.018)\text{x}10^3\ \text{kN}$$

$$= 635.74\,\text{kN}$$

Solving for 64 MPa strength

$$\omega_w = \frac{2.113}{64.67}$$
$$= 0.0327$$
$$f'_{cc} = f'_c(1+\alpha_{pr}\omega_w)$$
$$f'_{cc} = 64.67(1+1*0.0327)$$
$$= 66.78\,\text{MPa}$$

$$P_u = \alpha f'_{cc} A_c + A_{st} f_y$$
$$\alpha = 0.85 - 0.0015 f'_c$$
$$= 0.85 - 0.0015(64.67)$$
$$= 0.752995$$
$$P_u = 0.752995(66.78)(0.018)\text{x}10^3\ \text{kN}$$
$$= 905.13\,\text{kN}$$

A-4 Confined compressive strength and ultimate axial load carrying capacity Using CEB/FIP Model Code (*fib* Bulletin 14)

A-4.1 Approximate Method

A-4.1.1 For CFRP Sika Wrap Hex 230

$$f_l = \frac{1}{2} k_e \rho_f E_f \in_{fu}$$

$k_e =$ Confinement effectiveness coefficient (accounting for effect of partial wrapping in circular sections)

$k_e = 1$ (For full wrap in circular sections)

$E_f =$ Tensile modulus of Elasticity of FRP

$E_f = 65402\,\text{MPa}$

$\rho_f =$ Volumetric ratio of FRP reinforcement

$$\rho_f = \frac{4nt_f}{D}\left(\frac{b_f}{s}\right) \quad \text{(For circular sections)}$$

$b_f =$ Width of FRP strip in partial wrapping

$s =$ pitch in partial wrapping

$t_f =$ Thickness of FRP wrap

$n =$ Number of wraps of FRP

$t_f = 0.381\,\text{mm}$

$n = 1$

$$\rho_f = \frac{4nt_f}{D}\left(\frac{b_f}{s}\right)$$

$$\rho_f = \frac{4(1)(0.015)}{152.4}(1) \qquad \text{as } \frac{b_f}{s} = 1$$

$$\rho_f = 0.01$$

Putting in equation 1, we get

$$f_l = \frac{1}{2}(1)(0.01)(65402)(0.0133)$$

$$f_l = 4.349\,\text{MPa}$$

Solving for 30 MPa strength

$$f'_{cc} = f'_c\left(0.2 + 3\sqrt{\frac{f_l}{f'_c}}\right)$$

$$f'_{cc} = 29.7\left(0.2 + 3\sqrt{\frac{4.35}{29.7}}\right)$$

$$f'_{cc} = 40.03\,\text{MPa}$$

$$P_u = \lambda f'_{cc} A_c + f_y A_{st}$$

$$= (0.8)(40.03)(0.0018)\text{x}10^3\ \text{kN}$$

$$= 584.16\,\text{kN}$$

Solving for 42 MPa strength

$$f'_{cc} = f'_c\left(0.2 + 3\sqrt{\frac{f_l}{f'_c}}\right)$$

$$f'_{cc} = 42.84\left(0.2 + 3\sqrt{\frac{4.35}{42.84}}\right)$$

$$f'_{cc} = 49.51\,\text{MPa}$$

$$P_u = \lambda f'_{cc} A_c + f_y A_{st}$$

$$= (0.8)(49.51)(0.0018)\text{x}10^3\ \text{kN}$$

$$= 720.96\,\text{kN}$$

Solving for 64 MPa strength

$$f'_{cc} = f'_c\left(0.2 + 3\sqrt{\frac{f_l}{f'_c}}\right)$$

$$f'_{cc} = 64.67\left(0.2 + 3\sqrt{\frac{4.35}{64.67}}\right)$$

$$f'_{cc} = 63.24\,\text{MPa}$$

$$P_u = \lambda f'_{cc} A_c + f_y A_{st}$$

$$= (0.8)(63.24)(0.018)\text{x}10^3\ \text{kN}$$

$$= 920.85\,\text{kN}$$

A-4.1.2 For GFRP Sika Wrap Hex 106G

$$f_l = \frac{1}{2} k_e \rho_f E_f \in_{fu}$$

$k_e =$ Confinement effectiveness coefficient (accounting for effect of partial wrapping in circular sections)

$k_e = 1$ (For full wrap in circular sections)

$E_f =$ Tensile modulus of Elasticity of FRP

$E_f = 16215\,\text{MPa}$

$\rho_f =$ Volumetric ratio of FRP reinforcement

$$\rho_f = \frac{4nt_f}{D}\left(\frac{b_f}{s}\right) \quad \text{(For circular sections)}$$

$b_f =$ Width of FRP strip in partial wrapping

$s =$ pitch in partial wrapping

$t_f =$ Thickness of FRP wrap

$n =$ Number of wraps of FRP

$t_f = 0.33\,\text{mm}$

$n = 2$

$$\rho_f = \frac{4nt_f}{D}\left(\frac{b_f}{s}\right)$$

$$\rho_f = \frac{4(2)(0.33)}{152.4}(1) \qquad \text{as } \frac{b_f}{s} = 1$$

$$\rho_f = 0.017$$

Putting in equation 1, we get

$$f_l = \frac{1}{2}(1)(0.017)(16215)(0.0143)$$

$$f_l = 1.97\,\text{MPa}$$

Solving for 30 MPa strength

$$f'_{cc} = f'_c\left(0.2 + 3\sqrt{\frac{f_l}{f'_c}}\right)$$

$$f'_{cc} = 29.7\left(0.2 + 3\sqrt{\frac{1.97}{29.7}}\right)$$

$$f'_{cc} = 28.89\,\text{MPa}$$

$$P_u = \lambda f'_{cc} A_c + f_y A_{st}$$

$$= (0.8)(28.89)(0.0018)\text{x}10^3\ \text{kN}$$

$$= 420.63\,\text{kN}$$

Solving for 42 MPa strength

$$f'_{cc} = f'_c\left(0.2 + 3\sqrt{\frac{f_l}{f'_c}}\right)$$

$$f'_{cc} = 42.84\left(0.2 + 3\sqrt{\frac{1.97}{42.84}}\right)$$

$$f'_{cc} = 36.13\,\text{MPa}$$

$$P_u = \lambda f'_{cc} A_c + f_y A_{st}$$

$$= (0.8)(36.13)(0.0018)\text{x}10^3\ \text{kN}$$

$$= 526.02\,\text{kN}$$

Solving for 64 MPa strength

$$f'_{cc} = f_c\left(0.2 + 3\sqrt{\frac{f_l}{f'_c}}\right)$$

$$f'_{cc} = 64.67\left(0.2 + 3\sqrt{\frac{1.97}{64.67}}\right)$$

$$f'_{cc} = 46.79\,\text{MPa}$$

$$P_u = \lambda f'_{cc} A_c + f_y A_{st}$$

$$= (0.8)(46.79)(0.0018)\text{x}10^3\ \text{kN}$$

$$= 681.34\,\text{kN}$$

A-4.2 Exact Method

A-4.2.1 For CFRP Sika Wrap Hex 230

Solving for 30 MPa strength

$f_c' = 29.7\,\text{MPa}$

$D = 152.4\,\text{mm}$

$k_e = 1\,(\text{For full wrap in circular cylinders})$

$E_f = 65402\,\text{MPa}$

$n = 1$

$t_f = 0.381\text{mm}$

$\frac{b_f}{s} = 1$

$\varepsilon_{fu} = 0.0133$

$$\rho_f = \frac{4nt_f}{D}\left(\frac{b_f}{s}\right)$$

$$= \frac{4(1)(0.381)(1)}{152.4} = 0.01$$

$$f_l = \frac{1}{2}k_e\rho_f E_f \varepsilon_{fu}$$

$$= \frac{1}{2}(1)(0.01)(65402)(0.0133)$$

$$= 4.349\,\text{MPa}$$

$$f_{cc} = f_c'\left[2.254\sqrt{1+7.94\frac{f_l}{f_c'}} - 2\frac{f_l}{f_c'} - 1.254\right]$$

$$= 7.84\left[2.254\sqrt{1+7.84\left(\frac{4.35}{29.7}\right)} - 2\left(\frac{4.35}{29.7}\right) - 1.254\right]$$

$$= 52\,\text{MPa}$$

$$\varepsilon_{cc} = \varepsilon_c\left[1+5\left(\frac{f_{cc}}{f_c'} - 1\right)\right]$$

$$= 0.0026\left[1+5\left(\frac{52}{29.7} - 1\right)\right]$$

$$= 0.0124$$

$$E_c = 4730\sqrt{f_c'}$$
$$= 4730\sqrt{29.7}$$
$$= 25777.4$$
$$\beta = \frac{5700}{\sqrt{f_c'}} - 500$$
$$= \frac{5700}{\sqrt{29.7}} - 500$$
$$= 545.91$$
$$E_{cc} = \frac{f_{cc}}{\varepsilon_{cc}} = \frac{52}{0.0124}$$
$$= 4193.55\text{MPa}$$

$$E_{sec,u} = \frac{E_c}{1 + 2\beta\varepsilon_{fu}}$$
$$= \frac{25777.4}{1 + 2(545.91)(0.0133)}$$
$$= 1660.78\text{MPa}$$
$$\varepsilon_{cu} = \varepsilon_{cc}\left[\frac{E_{cc}(E_c - E_{sec,u})}{E_{sec,u}(E_c - E_{cc})}\right]^{1-\frac{E_{cc}}{E_c}}$$

$$\varepsilon_{cc} = 0.0124\left[\frac{4193(25777.4 - 1660.78)}{1660.78(25777.4 - 4193.55)}\right]^{1-\frac{4193.55}{25777.4}}$$
$$= 0.0295$$
$$f_{cu} = \varepsilon_{cu}E_{sec,u} = 1660.78\text{x}0.0295 = 48.99\,\text{MPa}$$

$$P_u = \lambda f_{cu}A_c + f_y A_{st}$$
$$= (0.8)(48.99)(0.018)\text{x}10^3\ \text{kN}$$
$$= 713.3\,\text{kN}$$

Solving for 42 MPa strength

$$f_c' = 42.84\,\text{MPa}$$
$$D = 152.4\,\text{mm}$$
$$k_e = 1\,(\text{For full wrap in circular cylinders})$$
$$E_f = 65402\,\text{MPa}$$
$$n = 1$$
$$t_f = 0.381\,\text{mm}$$
$$\frac{b_f}{s} = 1$$

$$\varepsilon_{fu} = 0.0133$$

$$\rho_f = \frac{4nt_f}{D}(\frac{b_f}{s})$$

$$= \frac{4(1)(0.381)(1)}{152.4} = 0.01$$

$$f_l = \frac{1}{2}k_e\rho_f E_f \varepsilon_{fu}$$

$$= \frac{1}{2}(1)(0.01)(65402)(0.0133)$$

$$= 4.349\,\text{MPa}$$

$$f_{cc} = f_c'\left[2.254\sqrt{1+7.94\frac{f_l}{f_c'}} - 2\frac{f_l}{f_c'} - 1.254\right]$$

$$= 67.35\,\text{MPa}$$

$$\varepsilon_{cc} = \varepsilon_c\left[1+5\left(\frac{f_{cc}}{f_c'}-1\right)\right]$$

$$= 0.0112$$

$$E_c = 4730\sqrt{f_c'}$$

$$= 30958.92\,\text{MPa}$$

$$\beta = \frac{5700}{\sqrt{f_c'}} - 500$$

$$= 370.86$$

$$E_{cc} = \frac{f_{cc}}{\varepsilon_{cc}}$$

$$= 6013.39\,\text{MPa}$$

$$E_{sec,u} = \frac{E_c}{1+2\beta\varepsilon_{fu}}$$

$$= 2849.45\,\text{MPa}$$

$$\varepsilon_{cu} = \varepsilon_{cc}\left[\frac{E_{cc}(E_c - E_{sec,u})}{E_{sec,u}(E_c - E_{cc})}\right]^{1-\frac{E_{cc}}{E_c}}$$

$$= 0.0225$$

$$f_{cu} = \varepsilon_{cu}E_{sec,u} = 64.11\,\text{MPa}$$

$$P_u = \lambda f_{cu} A_c + f_y A_{st}$$
$$= (0.8)(64.11)(0.0018)\text{x}10^3 \text{ kN}$$
$$= 933.44\text{kN}$$

Solving for 64 MPa strength

$$f_c' = 64.67\,\text{MPa}$$
$$D = 152.4\,\text{mm}$$
$$k_e = 1\,(\text{For full wrap in circular cylinders})$$
$$E_f = 65402\,\text{MPa}$$
$$n = 1$$
$$t_f = 0.381\text{mm}$$
$$\frac{b_f}{s} = 1$$

$$\varepsilon_{fu} = 0.0133$$
$$\rho_f = \frac{4nt_f}{D}(\frac{b_f}{s})$$
$$= \frac{4(1)(0.381)(1)}{152.4} = 0.01$$
$$f_l = \frac{1}{2} k_e \rho_f E_f \varepsilon_{fu}$$
$$= \frac{1}{2}(1)(0.01)(65402)(0.0133)$$
$$= 4.349\,\text{MPa}$$

$$f_{cc} = f_c' \left[2.254\sqrt{1+7.94\frac{f_l}{f_c'}} - 2\frac{f_l}{f_c'} - 1.254 \right]$$
$$= 90.74\,\text{MPa}$$

$$\varepsilon_{cc} = \varepsilon_c \left[1+5\left(\frac{f_{cc}}{f_c'} - 1 \right) \right]$$
$$= 0.0096$$

$$E_c = 4730\sqrt{f_c'}$$
$$= 38037.55\text{MPa}$$
$$\beta = \frac{5700}{\sqrt{f_c'}} - 500$$

$= 208.8$

$$E_{cc} = \frac{f_{cc}}{\varepsilon_{cc}}$$

$= 9452.08\text{MPa}$

$$E_{sec,u} = \frac{E_c}{1+2\beta\varepsilon_{fu}}$$

$= 5803.64\text{MPa}$

$$\varepsilon_{cu} = \varepsilon_{cc}\left[\frac{E_{cc}(E_c - E_{sec,u})}{E_{sec,u}(E_c - E_{cc})}\right]^{1-\frac{E_{cc}}{E_c}}$$

$= 0.01515$

$f_{cu} = \varepsilon_{cu} E_{sec,u} = 87.976\text{MPa}$

$$P_u = \lambda f_{cu} A_c + f_y A_{st}$$

$= (0.8)(87.976)(0.0018)\text{x}10^3\ \text{kN}$

$= 1280.93\text{kN}$

A-4.2.1 For GFRP Sika Wrap Hex 106G

Solving for 30 MPa strength

$f_c' = 29.7\ \text{MPa}$

$D = 152.4\,\text{mm}$

$k_e = 1\,(\text{For full wrap in circular cylinders})$

$E_f = 16215\text{MPa}$

$n = 2$

$t_f = 0.33\,\text{mm}$

$$\frac{b_f}{s} = 1$$

$\varepsilon_{fu} = 0.0143$

$$\rho_f = \frac{4nt_f}{D}\left(\frac{b_f}{s}\right)$$

$= 0.017$

$$f_l = \frac{1}{2} k_e \rho_f E_f \varepsilon_{fu}$$

$$= \frac{1}{2}(1)(0.017)(16215)(0.0143)$$

$= 1.97\,\text{MPa}$

$$f_{cc} = f_c'\left[2.254\sqrt{1+7.94\frac{f_l}{f_c'}} - 2\frac{f_l}{f_c'} - 1.254\right]$$

$= 41.53\,\text{MPa}$

$$\varepsilon_{cc} = \varepsilon_c\left[1+5\left(\frac{f_{cc}}{f_c'}-1\right)\right]$$

$= 0.0078$

$$E_c = 4730\sqrt{f_c'}$$

$= 25777.4$

$$\beta = \frac{5700}{\sqrt{f_c'}} - 500$$

$$= \frac{5700}{\sqrt{29.7}} - 500$$

$= 545.91$

$$E_{cc} = \frac{f_{cc}}{\varepsilon_{cc}}$$

$= 5324.36\,\text{MPa}$

$$E_{sec,u} = \frac{E_c}{1+2\beta\varepsilon_{fu}}$$

$= 1551.64\,\text{MPa}$

$$\varepsilon_{cu} = \varepsilon_{cc}\left[\frac{E_{cc}(E_c - E_{sec,u})}{E_{sec,u}(E_c - E_{cc})}\right]^{1-\frac{E_{cc}}{E_c}}$$

$= 0.0237$

$f_{cu} = \varepsilon_{cu}E_{sec,u} = 36.82\,\text{MPa}$

$P_u = \lambda f_{cu}A_c + f_y A_{st}$

$= (0.8)(36.82)(0.018)\text{x}10^3\ \text{kN}$

$= 536.09\,\text{kN}$

Solving for 42 MPa strength

$f_c' = 42.84\,\text{MPa}$

$D = 152.4\,\text{mm}$

$k_e = 1\,(\text{For full wrap in circular cylinders})$

$E_f = 16215\text{MPa}$

$n = 2$

$t_f = 0.33\text{mm}$

$\frac{b_f}{s} = 1$

$\varepsilon_{fu} = 0.0143$

$\rho_f = \frac{4nt_f}{D}(\frac{b_f}{s})$

$= 0.017$

$f_l = \frac{1}{2}k_e\rho_f E_f \varepsilon_{fu}$

$= \frac{1}{2}(1)(0.017)(16215)(0.0143)$

$= 1.97\,\text{MPa}$

$f_{cc} = f_c'\left[2.254\sqrt{1+7.94\frac{f_l}{f_c'}} - 2\frac{f_l}{f_c'} - 1.254\right]$

$= 54.79\,\text{MPa}$

$\varepsilon_{cc} = \varepsilon_c\left[1+5\left(\frac{f_{cc}}{f_c'}-1\right)\right]$

$= 0.00694$

$E_c = 4730\sqrt{f_c'}$

$= 30958.92\text{MPa}$

$\beta = \frac{5700}{\sqrt{f_c'}} - 500$

$= 370.86$

$E_{cc} = \frac{f_{cc}}{\varepsilon_{cc}}$

$= 7894.81\text{MPa}$

$E_{sec,u} = \frac{E_c}{1+2\beta\varepsilon_{fu}}$

$= 2667.36\text{MPa}$

$\varepsilon_{cu} = \varepsilon_{cc}\left[\frac{E_{cc}(E_c - E_{sec,u})}{E_{sec,u}(E_c - E_{cc})}\right]^{1-\frac{E_{cc}}{E_c}}$

$= 0.0181$

$f_{cu} = \varepsilon_{cu} E_{sec,u} = 48.37\,\text{MPa}$

$P_u = \lambda f_{cu} A_c + f_y A_{st}$

$= (0.8)(48.37)(0.018)\text{x}10^3\ \text{kN}$

$= 704.26\,\text{kN}$

Solving for 64 MPa strength

$f_c' = 64.67\,\text{MPa}$

$D = 152.4\,\text{mm}$

$k_e = 1\,(\text{For full wrap in circular cylinders})$

$E_f = 16215\,\text{MPa}$

$n = 2$

$t_f = 0.33\,\text{mm}$

$\frac{b_f}{s} = 1$

$\varepsilon_{fu} = 0.0143$

$\rho_f = \frac{4nt_f}{D}(\frac{b_f}{s})$

$= 0.017$

$f_l = \frac{1}{2} k_e \rho_f E_f \varepsilon_{fu}$

$= \frac{1}{2}(1)(0.017)(16215)(0.0143)$

$= 1.97\,\text{MPa}$

$f_{cc} = f_c' \left[2.254\sqrt{1 + 7.94\frac{f_l}{f_c'}} - 2\frac{f_l}{f_c'} - 1.254 \right]$

$= 77.4\,\text{MPa}$

$\varepsilon_{cc} = \varepsilon_c \left[1 + 5\left(\frac{f_{cc}}{f_c'} - 1 \right) \right]$

$= 0.00635$

$E_c = 4730\sqrt{f_c'}$

$= 38037.55\text{MPa}$

$\beta = \frac{5700}{\sqrt{f_c'}} - 500$

$= 208.8$

$$E_{cc} = \frac{f_{cc}}{\varepsilon_{cc}}$$

$= 12188.98\text{MPa}$

$$E_{sec,u} = \frac{E_c}{1+2\beta\varepsilon_{fu}}$$

$= 5456\,\text{MPa}$

$$\varepsilon_{cu} = \varepsilon_{cc}\left[\frac{E_{cc}(E_c - E_{sec,u})}{E_{sec,u}(E_c - E_{cc})}\right]^{1-\frac{E_{cc}}{E_c}}$$

$= 0.0128$

$f_{cu} = \varepsilon_{cu}E_{sec,u} = 69.84\,\text{MPa}$

$P_u = \lambda f_{cu}A_c + f_y A_{st}$

$= (0.8)(69.84)(0.018)\text{x}10^3\ \text{kN}$

$= 1016.87\,\text{kN}$